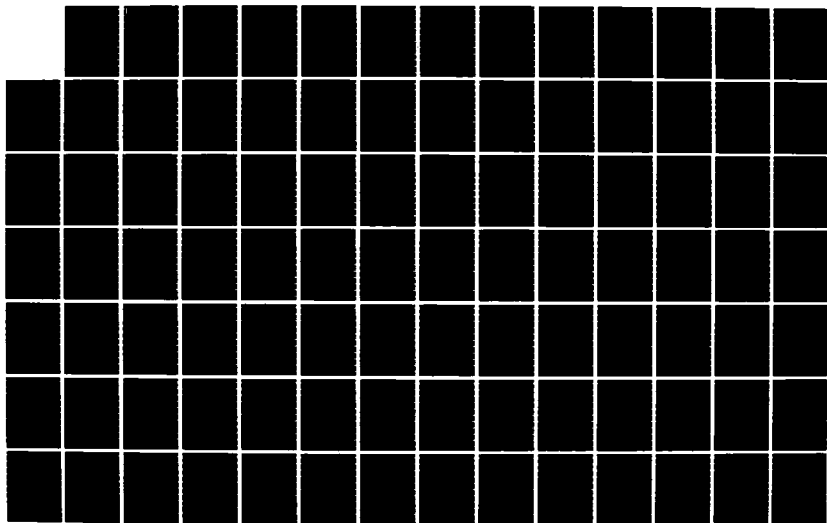


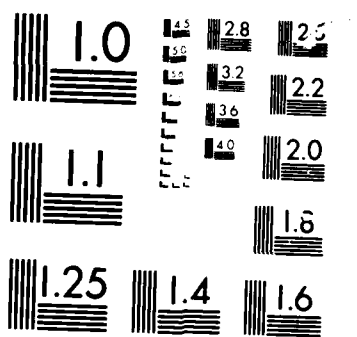
AD-A169 818 EVALUATION OF IMPROVEMENTS TO BRAYTON CYCLE PERFORMANCE 1/2
(U) ARMY MILITARY PERSONNEL CENTER ALEXANDRIA VA
M A SPASYK 29 MAY 86

UNCLASSIFIED

F/G 10/2

NL





MICROFON

AD-A169 018

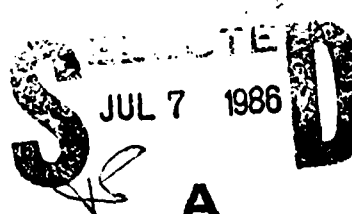
②

EVALUATION OF IMPROVEMENTS TO
BRAYTON CYCLE PERFORMANCE

Major Michael A. Spasyk
HQDA, MILPERCEN (DAPC-OPA-E)
200 Stovall Street
Alexandria, VA 22332

Final Report 29 May 1980

Approved for public release; distribution is unlimited.



A thesis submitted to the faculty of the
University of Utah, Salt Lake City, Utah, 84112,
in partial fulfillment of the requirements for the degree of
Master of Science in Mechanical Engineering.

OTIC FILE COPY

86 7 1 089

7

EVALUATION OF IMPROVEMENTS TO
BRAYTON CYCLE PERFORMANCE

by

Michael A. Spasyk

A thesis submitted to the faculty of
the University of Utah
in partial fulfillment of the requirements for the degree of

Master of Science

in

Mechanical Engineering



Department of Mechanical and Industrial Engineering

The University of Utah

June 1986

This document has been approved
for issue and circulation
within the United States

Unclassified

SECURITY CLASSIFICATION OF THIS PAGE (When Data Entered)

2

READ INSTRUCTIONS
BEFORE COMPLETING FORM

REPORT DOCUMENTATION PAGE		READ INSTRUCTIONS BEFORE COMPLETING FORM
1. REPORT NUMBER	2. GOVT ACCESSION NO.	3. RECIPIENT'S CATALOG NUMBER
		AD-A169 018
4. TITLE (and Subtitle) Evaluation of Improvements to Brayton Cycle Performance		5. TYPE OF REPORT & PERIOD COVERED Final Report 29 May 1986
7. AUTHOR(s) Michael A. Spasyk, MAJ, USA		6. PERFORMING ORG. REPORT NUMBER
9. PERFORMING ORGANIZATION NAME AND ADDRESS Student, HQDA, MILPERCEN (DAPC-OPA-E), 200 Stovall Street, Alexandria, Virginia 22332		10. PROGRAM ELEMENT, PROJECT, TASK AREA & WORK UNIT NUMBERS
11. CONTROLLING OFFICE NAME AND ADDRESS HQDA, MILPERCEN, ATTN: DAPC=OPA-E, 200 Stovall Street, Alexandria, Virginia 22332		12. REPORT DATE 29 May 1986
14. MONITORING AGENCY NAME & ADDRESS (if different from Controlling Office)		13. NUMBER OF PAGES 114
		15. SECURITY CLASS. (of this report) Unclassified
		15a. DECLASSIFICATION/DOWNGRADING SCHEDULE
16. DISTRIBUTION STATEMENT (of this Report) Approved for public release; distribution unlimited.		
17. DISTRIBUTION STATEMENT (of the abstract entered in Block 20, if different from Report)		
H		
18. SUPPLEMENTARY NOTES A thesis submitted to the faculty of the University of Utah, Salt Lake City, Utah, 84112, in partial fulfillment of the requirements for the degree of Master of Science in Mechanical Engineering.		
19. KEY WORDS (Continue on reverse side if necessary and identify by block number) A computer modelling of performance of 5 Brayton gas turbine cycles; simple Brayton cycle, cycle with intercooling, regeneration, and reheat, and cycle with steam injection, for solar power applications. Emphasis on the effect of turbine inlet temperature on efficiency (First & Second Law) and net work.		
20. ABSTRACT (Continue on reverse side if necessary and identify by block number) This study addresses the problem of finding an energy conversion method to take advantage of the high maximum cycle temperatures achieved with solar central receivers. Most current practice is to use steam-based heat engines with solar receivers but these Rankine cycles cannot operate at the higher possible temperatures. Derivatives of gas-based Brayton cycles are considered to take advantage of the expected increased cycle performance of higher temperatures.		

Unclassified

SECURITY CLASSIFICATION OF THIS PAGE(When Data Entered)

Computer modelling was done to examine the effect of maximum temperature on efficiency of two Brayton cycle derivatives and a simple Brayton cycle (GT). The modified Brayton cycles include a combination of intercooling, regeneration, and reheat (IGT) and a Brayton cycle with steam injection (STIG). The turbine inlet temperature, the steam-to-air injection mass ratio (for the STIG), and the compression pressure ratios were treated as parameters in the analysis. Both First Law and Second Law efficiencies were examined.

Efficiencies were highest for the IGT followed by the STIG and GT, respectively. Considerable improvements in specific work output were demonstrated by the STIG over both the IGT and GT systems. First and Second Law analyses show a gradual increase of efficiency with turbine inlet temperature with diminishing returns at higher temperatures.

Quality
Control

Information For	
Project	TEA&I
Task	100
Objectives	1
Personnel	1
By	
Distribution/	
Availability Codes	
Dist	1
<i>[Signature]</i>	

Unclassified

SECURITY CLASSIFICATION OF THIS PAGE(When Data Entered)

Copyright © Michael A. Spasyk 1986

All Rights Reserved

THE UNIVERSITY OF UTAH GRADUATE SCHOOL

SUPERVISORY COMMITTEE APPROVAL

of a thesis submitted by

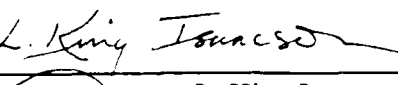
Michael A. Spasyk

This thesis has been read by each member of the following supervisory committee and by majority vote has been found to be satisfactory.

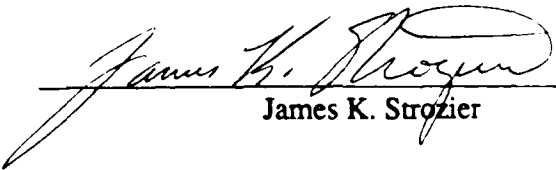
5/13/86


Chairman: Robert F. Boehm

5-14-86


L. King Isaacson

14 May 86


James K. Strozier

THE UNIVERSITY OF UTAH GRADUATE SCHOOL

FINAL READING APPROVAL

To the Graduate Council of The University of Utah:

I have read the thesis of Michael A. Spasyk in its final form and have found that (1) its format, citations, and bibliographic style are consistent and acceptable; (2) its illustrative materials including figures, tables, and charts are in place; and (3) the final manuscript is satisfactory to the Supervisory Committee and is ready for submission to the Graduate School.

5/13/86
Date

Robert F. Boehm

Robert F. Boehm
Member, Supervisory Committee

Approved for the Major Department

David W. Hoeppner
David W. Hoeppner
Chairman Dean

Approved for the Graduate Council

James L. Clayton
James L. Clayton
Dean of The Graduate School

ABSTRACT

This study addresses the problem of finding an energy conversion method to take advantage of the high maximum cycle temperatures achieved with solar central receivers. Most current practice is to use steam-based heat engines with solar receivers. Solar central receiver applications offer maximum cycle temperatures in excess of the operating range of steam-based Rankine cycles. Gas-based Brayton cycles are considered to take advantage of the expected increased cycle performance of higher temperatures.

Simple Brayton cycles have been eliminated from consideration since they do not offer efficiency improvements over the lower temperature Rankine cycles. Derivatives of Brayton engines do offer favorable performance compared to Rankine cycles. Computer modelling was done to examine the effect of maximum temperature on efficiency of two Brayton cycle derivatives and a simple Brayton cycle (denoted as GT). The modified Brayton cycles include a combination of regeneration and one stage each of intercooling and reheat (IGT) and a Brayton cycle with steam injection (STIG). The turbine inlet temperature, the steam-to-air injection mass ratio (for the STIG) and the compression pressure ratios were treated as parameters in the analysis. The compression ratios investigated are 4, 8, 12, 16, and 20. Turbine inlet temperatures ranged from 1000 K (1340°F) to 2500 K (4040°F). For the STIG the steam/air mass ratio varied between 0 and 0.5. Both First Law and Second Law efficiencies were examined as turbine inlet temperature and steam/air mass ratios were varied for each compression ratio.

Results show that efficiencies were highest for the IGT followed by the STIG and GT, respectively. Considerable improvements in specific work output were demonstrated by the STIG over both the IGT and GT systems. First Law and Second

Law analyses of the effect of turbine inlet temperature show a gradual increase of efficiency with turbine inlet temperature with diminishing returns at higher temperatures. These results demonstrate reason for optimism about increased performance for higher temperature air-based systems compared to Rankine systems at presently used temperatures.

This thesis is dedicated to the memory of my father John J. Spasyk and to
my mother Jean F. Spasyk.

TABLE OF CONTENTS

ABSTRACT	iv
LIST OF FIGURES	viii
LIST OF TABLES	x
NOMENCLATURE	xi
ACKNOWLEDGEMENTS	xiv
Chapter	
I. INTRODUCTION	1
II. THEORY	8
Compressor/Turbine.....	8
Heat and Reheat	10
Heat Exchangers.....	11
Pressure Losses	12
Heat Recovery Steam Generator.....	16
Pump	20
Turbine Cooling	20
First Law Efficiency	21
Second Law Efficiency	22
Limits on Cycle Performance	31
III. RESULTS AND DISCUSSION	35
First Law Analysis	35
Second Law Analysis.....	50
IV. CONCLUSIONS AND RECOMMENDATIONS	66
Appendices	
A. FORTRAN PROGRAM GT.....	73
B. FORTRAN PROGRAM CONDEN	96
REFERENCES	99

LIST OF FIGURES

Figure	Page
1. The GT, IGT, and STIG cycle configuration	3
2. Heat exchangers	14
3. Possible heat recovery steam generator (HRSG) pinch point (pp) locations ...	17
4. First Law efficiency versus turbine inlet temperature ($Pr = 4$)	36
5. First Law efficiency versus turbine inlet temperature ($Pr = 8$)	37
6. First Law efficiency versus turbine inlet temperature ($Pr = 12$)	38
7. First Law efficiency versus turbine inlet temperature ($Pr = 16$)	39
8. First Law efficiency versus turbine inlet temperature ($Pr = 20$)	40
9. Specific net work versus turbine inlet temperature ($Pr = 4$)	41
10. Specific net work versus turbine inlet temperature ($Pr = 8$)	42
11. Specific net work versus turbine inlet temperature ($Pr = 12$)	43
12. Specific net work versus turbine inlet temperature ($Pr = 16$)	44
13. Specific net work versus turbine inlet temperature ($Pr = 20$)	45
14. First Law efficiency versus steam/air mass ratio for STIG cycle at five turbine inlet temperature ($Pr = 16$)	49
15. Second Law efficiency versus turbine inlet temperature for GT cycle at three compression pressure ratios	53
16. Second Law efficiency versus turbine inlet temperature for GT cycle at three compression ratios with exit availability not included	54
17. Second Law efficiency versus steam/air mass ratio for STIG cycle at five turbine inlet temperatures ($Pr = 16$)	56
18. First Law efficiency versus steam/air mass ratio for STIG cycle at five turbine inlet temperatures ($Pr = 16$)	58

19. Second Law efficiency versus steam/air mass ratio for STIG cycle at turbine inlet of 1500K (Pr = 16)	59
20. Second Law efficiency versus steam/air mass ratio for STIG cycle at five turbine inlet temperatures (Pr = 16)	60
21. Second Law efficiency versus steam/air mass ratio for GT cycle with HRSG and steam heated to turbine inlet temperature at three turbine inlet temperatures (Pr = 16)	63
22. Second Law efficiency versus steam/air mass ratio for GT cycle with HRSG where steam is not heated beyond the HRSG at five turbine inlet temperatures (Pr = 16)	64

LIST OF TABLES

Table	Page
1. Parameters and Assumptions	9
2. HEX Effectiveness.....	13
3. Second Law Efficiency Definitions	30
4. Comparison of Selected Data with Bhutani et al. [9]	51
5. Comparison of Selected Data with Boyle [11]	52
6. Improvements in Performance by the IGT and STIG Cycles Compared to the GT Cycle	67
7. Pressure Losses Calculated in This Study	70
8. Pressure Loss Schemes Listed in Literature	71

NOMENCLATURE

A	Area
b	Specific availability (kJ/kg)
C	Constant
c_p	Specific heat at constant pressure (kJ/kg K)
d	Diameter
GT	Simple Brayton cycle
h	Specific enthalpy (kJ/kg)
h_i	Equations (7), (8) only -convective heat transfer coefficient
HEX	Heat exchanger
h_f	Specific fluid enthalpy at saturation
h_{fg}	Latent heat of vaporization ($h_g - h_f$)
HRSG	Heat recovery steam generator
IGT	Brayton cycle with intercooler, regeneration, & reheat
m	Mass flow rate
Mr	Steam/air mass ratio
MW	Molecular weight (kg/kmol)
P, p	Pressure (kPa)
Pr	Compression pressure ratio
q, q_h	Specific heat transfer (kJ/Kg)
q_{HEX}	Specific heat transferred in the HRSG
q_{sat}	Specific heat transfer to heat water to saturation from ambient
$q_{superheat}$	Specific heat transfer to heat water to superheat from ambient

\bar{R}	Universal gas constant
R_t	Total heat transfer resistance
s	Specific entropy (kJ/kg K)
s_f	Specific fluid entropy at saturation
s_{fg}	Difference between specific gaseous and fluid entropy at saturation $(s_g - s_f)$
STIG	Brayton cycle with steam injection
T	Temperature (K)
ΔT_{ap}	HRSG approach temperature difference
ΔT_{pp}	HRSG pinch point temperature difference
V	Velocity
w	Specific work (kJ/kg)
w_e	Specific Carnot equivalent work of a heat input (kJ/kg)
x	Quality (mass of vapor at saturation/total mass)
y	Mole fraction

Greek Letters

ϵ	Second Law efficiency
η	First Law efficiency
μ	Dynamic viscosity
ρ	Density

Subscripts

Numbers	State points (see Figure 1)
ap	Approach point
c	Compressor
p	Pump

pp	Pinch point
s	Isentropic
sat	Saturation
t	Turbine

ACKNOWLEDGEMENTS

I wish to thank my committee chairman Dr. Robert F. Boehm for his advice, guidance, and patience throughout the course of my work on this project. Appreciation is extended to my other supervisory committee members, Dr. James K. Strozier, and Dr. L. King Isaacson. I studied under all three professors. They made my stay at the University of Utah a rewarding experience.

CHAPTER I

INTRODUCTION

The current practice for power generation from solar central receivers is to use steam-based heat engines. Even the newer receiver concepts, using molten salt or liquid sodium, are envisioned to use a heat exchanger external to the receiver to generate steam for driving a Rankine cycle system to produce power. In spite of this apparent contentment with steam-based systems, it is well-known that there should be a thermodynamic basis for expecting increasing cycle performance if the cycle maximum temperature is increased. However, any substantial increase in cycle maximum temperature may well preclude the use of steam. Gas-based cycles are therefore considered for this application.

Air cycles have been considered for solar applications over the years. The Stirling cycle and Brayton cycle are both undergoing some development for solar power generation systems based upon dish (distributed) receivers. For larger systems such as might be used for solar central receivers, the development of Brayton-derivative cycles seems to be one of the few alternatives available. Brayton applications have been generally eliminated from serious consideration because they appear to offer too much of an efficiency penalty compared to lower temperature systems. This impression has been drawn because of increased receiver losses as temperatures are increased as well as the seemingly low cycle performance of simple Brayton cycles. However, there are some Brayton engine derivatives that may demonstrate favorable performance compared to Rankine systems. This study will evaluate the performance of two of these derivatives and compare them to the performance of the simple Brayton cycle (denoted as GT).

These include a familiar combination of a Brayton cycle with regeneration and one stage each of intercooling and reheat (denoted as IGT) and a less investigated Brayton cycle with steam injection (STIG). This study determines realistic performance of these cycles operating on air. Special concern is given to the impact of maximum cycle temperature on overall performance.

As explained earlier, current solar power generation systems use a heat exchanger to transfer the heat from the molten salt or liquid sodium fluid to a steam based Rankine cycle. Part of the problem of making full use of higher temperatures afforded by solar systems is transfer of the solar energy to the power generation system. This study will not address the problem of how the exchange of heat from the initial fluid medium of the solar control receiver is made to the air or steam/air mixture working fluid of the cycles evaluated. This problem is a significant one and is not addressed here. In this study this heat exchanger is termed as a heater in the text and Figure 1. It will be assumed that the solar central receiver exists to heat the working fluid to the turbine inlet temperatures investigated in this study.

The configurations of these three systems are illustrated in Figure 1. The advantages the IGT system enjoys compared to the simple GT system include the intercooler to decrease compressor work and the reheat to increase turbine work. Since both of these components incur an efficiency penalty, the IGT system includes a regenerator to increase efficiency by preheating the compressor discharge with the turbine exhaust. The performance characteristics of this Brayton derivative cycle have been well-documented. To serve as an example, several gas turbine texts were reviewed to compare the improvements offered by the IGT cycle over the GT cycle. Boyce [1] reports an 81.4% increase in specific net work and a 53.5% increase in efficiency at a turbine inlet temperature of 1256 K (1800°F) and a pressure ratio of 10.5. At a higher temperature of 1478 K (2200°F) and the same pressure ratio, he reports an increase of

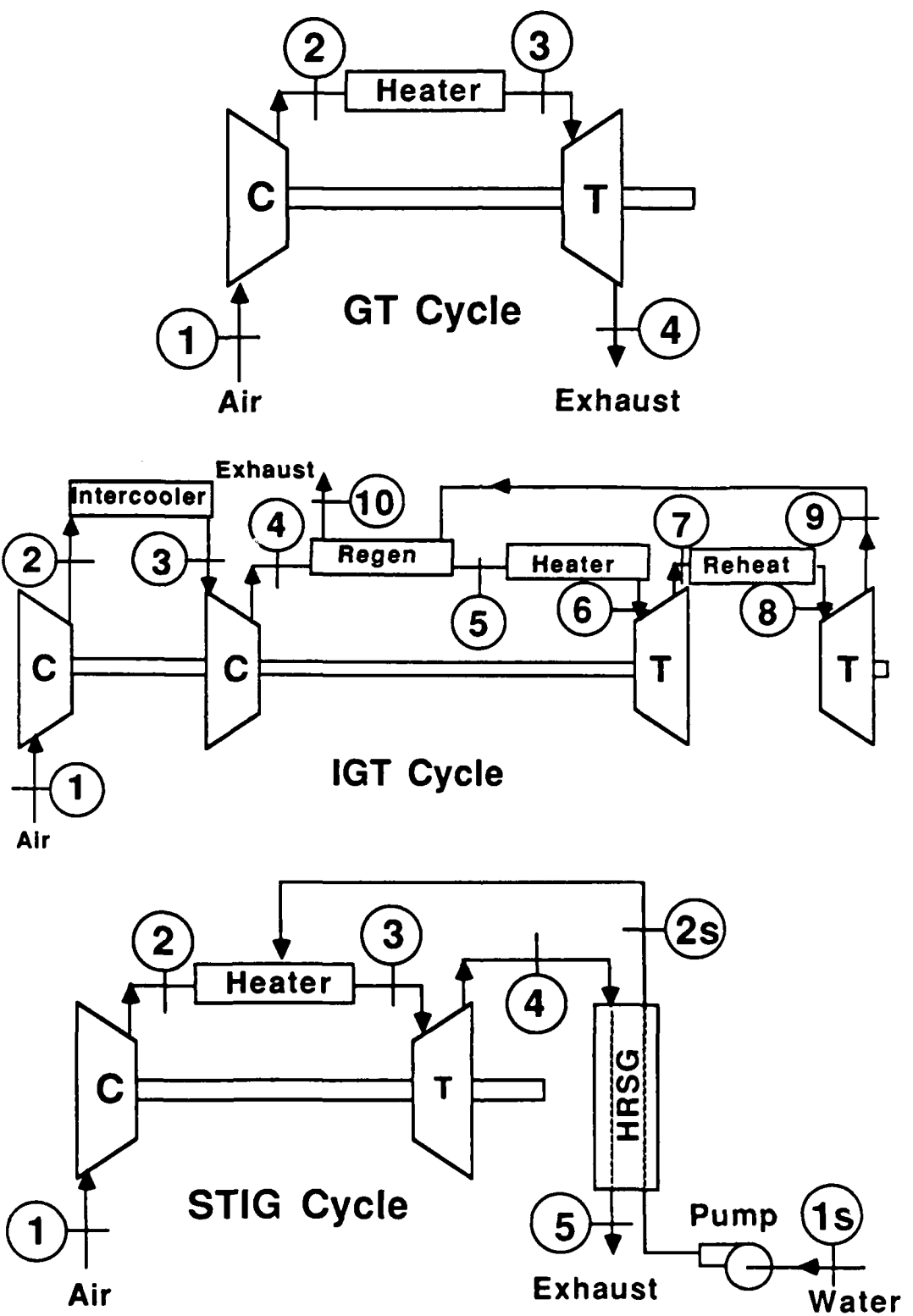


Figure 1. The GT, IGT, and STIG cycle configurations.

52.5% in specific net work and a 56.2% increase in efficiency. Bathie [2] states that the IGT cycle provides a 33.3% increase in specific net work and a 42.2% increase in efficiency over the GT cycle at a turbine inlet temperature of 1400 K (2060°F). Wilson [3] in his recent text lists performance curves for a Brayton cycle with intercooling and regeneration (no reheat). This system offered an increase of 20.1% in specific net work and an increase of 23.1% in efficiency over the GT cycle at a turbine inlet temperature of 1465 K (2177°F) and a pressure ratio of 20. At a higher turbine inlet temperature of 2051 K (3232°F) and the same pressure ratio, he reports an increase of 30.3% in specific net work and 41.4% in efficiency over the GT cycle.

The STIG system also increases cycle efficiency by use of the turbine exhaust to generate steam. This steam is then injected into the working fluid, in this case at the heater, to increase the power output due to increased working fluid mass flow and also by increasing the working fluid's specific heat. The theoretical performance of different variations of the STIG has been evaluated by several authors [4-17]. It has been known for some time that water/steam injection increases efficiency and power output [4]. Renewed interest started during the recent energy crisis period of a decade ago. Some of the earliest work on water/steam injection was performed by the NACA with the objective of augmenting the performance of gas turbine aircraft engines [5]. Early studies included water injection for power increase only, which typically decreased cycle efficiency 2% for each 1% increase in turbine mass flow [6]. The literature referenced here studies various other configurations of steam injection [5, 7-11] to include steam injection after the combustor [7], water injection by an evaporator prior to preheating in a heat exchanger [8], and steam generated by turbine exhaust which is used in both a gas turbine cycle and a steam turbine cycle [9].

The mentioned advantages of the STIG over the GT include the increases in cycle efficiency and power output. Boyce et al. [10] describe a 2-3% increase in efficiency

and a 12% increase in power output for each 5% increase by weight injection of steam in their external combustion steam injected gas turbine. Stochl [4] finds increases in efficiency and power output as high as 30% and 50%, respectively, at a turbine inlet temperature of 1366 K (2000°F). Even more dramatic is Fraize and Kinney's [5] findings of efficiency increases of 8 to 14 points while increases for power output vary as much as 70% to 130% for their coal-fired gas turbine power cycle with steam injection. This also demonstrates that STIG applications may be possible for a variety of fuels and not just "clean" fuels. STIG systems have the advantage of simplicity when compared to the IGT or conventional combined cycles of gas and steam turbines. Existing gas turbine cycles have been modified for steam injection to handle higher loads with no increase in rotating machinery [12]. The STIG's simplicity also means smaller capital costs in comparison to more complex systems. Steam injection is known to reduce the level of pollutants when fuel is combusted. Field tests have found that a 5% by weight injection of steam will reduce the amount of NO_x emissions to acceptable levels [10]. The STIG cycle has the disadvantages of corrosion and water consumption which all steam-based systems must cope with. Currently, two U.S. commercial firms offer STIG cogeneration systems. They are International Power Technology (IPT), Palo Alto, California and Mechanical Technology, Inc. (MTI), Latham, New York [13]. IPT has two operational installations of their Cheng-Cycle cogeneration STIG systems at San Jose State University and a Sunkist Growers installation in Ontario, California [13,14]. There are no utilities currently operating steam injected gas turbines, but Pacific Gas and Electric Co. is interested in seeing the technology developed [13]. Actual testing of a STIG system in an electrical power generation configuration, with steam injected into a Westinghouse 191-6 gas turbine (compression ratio at 6.5, steam/air mass ratio at .05), yielded a 20% increase of generated electricity [15]. After 3000 hours of operation, there was no ill effect on the turbine blades.

This study will vary turbine inlet temperature and steam/air mass ratio (for the STIG) for constant values of compression pressure ratio to evaluate their effect on cycle efficiency and power output. The compression ratios (denoted as Pr) investigated are 4, 8, 12, 16, 20. This range is common to the studies in the literature. Brown and Cohn [16] state that the highest pressure ratio currently foreseen for single-shaft industrial gas turbines is 16. Although a pressure ratio of 20 would provide the highest efficiency, a pressure ratio of 16 was selected as the superior economic candidate for the basic STIG cycle. The turbine inlet temperature range investigated is 1000-2500 K (1340-4040°F). The temperatures examined in the literature were commonly in the range of 1073-1700 K (1471-2600°F) with Day and Kidd [6] examining the range of 1228-2450 K (1750-3950°F). The investigated range is admitted to be high. The high end of which may not be technically possible without exotic materials and elaborate turbine cooling schemes, but an examination of the effect of high temperatures on performance is the purpose of this study. The range of steam/mass air ratios (denoted as Mr) investigated is 0 to 0.5. It will be shown here that maximum First Law efficiency is achieved within this range. This is confirmed by the literature.

The Second Law efficiency will also be investigated for the configurations shown in Figure 1 plus two GT cogeneration applications where all the steam produced by turbine exhaust goes to process applications and is not injected in the gas turbine cycle. Second Law efficiency will be defined here as the ratio of the net work output determined by the First Law analysis and the maximum reversible work determined with the thermodynamic states calculated in the First Law analysis. This definition draws on the work of Boehm [18], Moran [19], and Kotas [20]. Each of the systems to be investigated here, the GT, IGT, and STIG cycles, do not have combustion processes. These systems have heat addition processes from an external heat source. This source can be the solar central receiver and its initial working fluid. This study utilizes

definitions from Boehm [18] and Moran [19] to express the heat addition processes over varying temperatures as reversible Carnot equivalent work. In addition it is necessary to complete the expression for reversible work by adding the availabilities of the inlet streams and subtracting the availabilities of the exit streams. The work of all three of these authors was referred to in expressing these availabilities.

CHAPTER II

THEORY

Computer modelling of a First Law analysis is the basis of this study. The model determines the thermodynamic states at each point in the three configurations. (The FORTRAN program GT developed for this study is in Appendix A). Given all the necessary states, the program calculates the performance characteristics of each configuration: specific work output, First Law efficiency, and Second Law efficiency. This chapter will detail the modelling techniques used in the computer program to determine the end states of various processes and phenomena. The assumed values used in the program are listed in Table 1.

Compressor/Turbine

The compression or expansion ratios and the assumed values of the component isentropic efficiencies are the basis of the calculation of the process (temperature change) through these components. They are assumed adiabatic. The assumed isentropic efficiencies are on the high side of those listed in the literature. For the IGT, the two stages of compression and expansion have the same pressure ratio which was determined by the square root of the total pressure ratio. The final turbine expands the working fluid to atmospheric pressure. The calculation for end temperature is shown below.

Compressor

$$T_{2s} = T_1 (Pr)^{k-1/k} \quad (1)$$

Table 1
Parameters and Assumptions

Parameter	Assumed Value
Ambient temperature, T_1	300 K
Ambient pressure, P_1	101.325 kPa
Air specific heat (initial iteration value), c_{p_a}	1.0035 kJ/kg K [21]
Air ratio of specific heats (initial iteration value), k_{a_o}	1.397 [9]
Air molecular weight, MW_a	28.97 kg/kmol [21]
Air ideal gas constant, R_a	.28700 kJ/kg K [21]
Steam specific heat (initial iteration value), c_{p_s}	1.8723 kJ/kg k [21]
Steam ratio of specific heats (initial iteration value), k_{s_o}	1.327 [21]
Steam molecular weight, MW_s	18.015 kg/kmol [21]
Steam ideal gas constant, R_s	.46152 kJ/kg K [21]
Water density, ρ_{H_2O}	977.0 kg/m ³ [24]
Universal gas constant, \bar{R}	8.31434 kJ/kmol K [21]
Compressor efficiency, η_c	0.87
Turbine efficiency, η_t	0.89
Pump efficiency, η_p	0.70
Compressor pressure ratios, Pr	4, 8, 12, 16, 20
Pressure lost constant, k_{plost}	12.128 (kPa) ² /K

$$T_{2\text{actual}} = \frac{T_1 + T_{2s} - T_1}{\eta_c} \quad (2)$$

Turbine

$$T_{2s} = T_1 / (\Pr)^{k-1/k} \quad (3)$$

$$T_{2\text{actual}} = T_1 - \eta_t (T_1 - T_{2s}). \quad (4)$$

The specific work required and produced by the compressor and turbine processes, respectively, is calculated as

$$w = c_p (T_{2\text{actual}} - T_1). \quad (5)$$

The program does the calculations in SI units. The specific work is in terms of kilojoules per kilogram of compressor air flow. The calculation of the turbine specific work as shown above is additionally multiplied by $(0.95 + Mr)$. The 0.95 designates the 95% of the air flow not lost from the working fluid for the turbine cooling (more on this topic later). The steam/air mass ratio, Mr , is added to the working fluid for the STIG configuration. A variable specific heat for air or a steam/air mixture working fluid is determined using a variable air specific heat relationship [22] and a variable steam specific heat relationship [23]. These relationships use an average temperature of the start and end points. For the STIG cycle the mixture specific heat is determined using the steam/air mass ratio, Mr .

Heat and Reheat

The turbine inlet temperature is an independent parameter in this study so the end temperature of the heating process is known. The specific heat input required is calculated in similar fashion as the work calculation using an energy balance as shown

below.

$$q_h = (0.95 + Mr) c_p (T_{\text{turbine inlet}} - T_1) \quad . \quad (6)$$

Heat Exchangers

The heat exchangers to be modelled in this study are the intercooler, the regenerator, and the heat recovery steam generator (HRSG). A simple but appropriate way was sought to express their efficiencies without setting any values for the heat exchanger's particular dimensions. A similar, analogous relationship was determined and applied to each heat exchanger. This was accomplished by expressing heat exchanger effectiveness in terms of the ratio of the minimum temperature difference between the two streams and the total convective heat resistance of the two streams. The conductive heat resistance of the heat exchanger is neglected. This ratio for each heat exchanger is set equal to the ratio of one representative heat exchanger. This is shown below.

$$\left. \frac{\Delta T_{\min}}{R_t} \right|_{\text{each HEX}} = \left. \frac{\Delta T_{\min}}{R_t} \right|_{\text{representative HEX}} \quad . \quad (7)$$

This can be further expressed as

$$\left. \frac{\Delta T_{\min}}{R_t} \right|_{\text{each HEX}} = R_t_{\text{HEX}} \cdot \left. \frac{\Delta T_{\min}}{R_t} \right|_{\text{representative HEX}}$$

$$= \Delta T_{\min} \frac{\frac{1}{h_1 A_1} + \frac{1}{h_2 A_1}}{\frac{1}{h_3 A_2} + \frac{1}{h_4 A_2}} . \quad (8)$$

For an assumption of equal heat transfer areas, the equation becomes

$$\Delta T_{\min} \underset{\text{each HEX}}{=} \Delta T_{\min} \underset{\text{representative}}{=} \frac{\frac{1}{h_1} + \frac{1}{h_2}}{\frac{1}{h_3} + \frac{1}{h_4}} . \quad (9)$$

The representative minimum temperature difference selected was 50°C for the regenerator. A value of 51.1°C was determined from a regenerator efficiency of 0.81 [16] for a turbine inlet temperature of 1700 K and compression pressure ratio of 16. The representative values of the applicable convective heat transfer coefficients (Table 2) were selected [24, 25]. The minimum temperature difference between the streams of the other two heat exchangers was calculated and is shown in Table 2.

The locations of these ΔT_{\min} points are shown in Figure 2. The location is determined by the relative values of mass flow and specific heat between the two streams. These parameters determine the slope of the two streams (shown as linear on a T-length (x) diagram) and will determine where the two streams are closest. The locations of the intercooler and regenerator are pointed out but the location of the "pinch point" in the HRSG can be at various locations due to varying turbine exhaust temperature and steam/air mass ratio. This will be discussed later in this chapter.

Pressure Losses

A method to express pressure losses without using any apparatus parameters and which was applicable at any location was sought. For steady flow through the components, the fluid velocity and geometry of the apparatus is generally constant. There-

Table 2
HEX Effectiveness

Medium	Convective Heat Transfer Coefficient (W/m ² ·K)
Forced convection of air	200
Forced convection of water	2000
Convection of boiling water	5000

Heat Exchanger	Minimum Temperature Difference (°C)
Regenerator (Air-Air)	50
Intercooler (Air-Water)	27.5
HRSG (Air-Boiling Water)	26.0

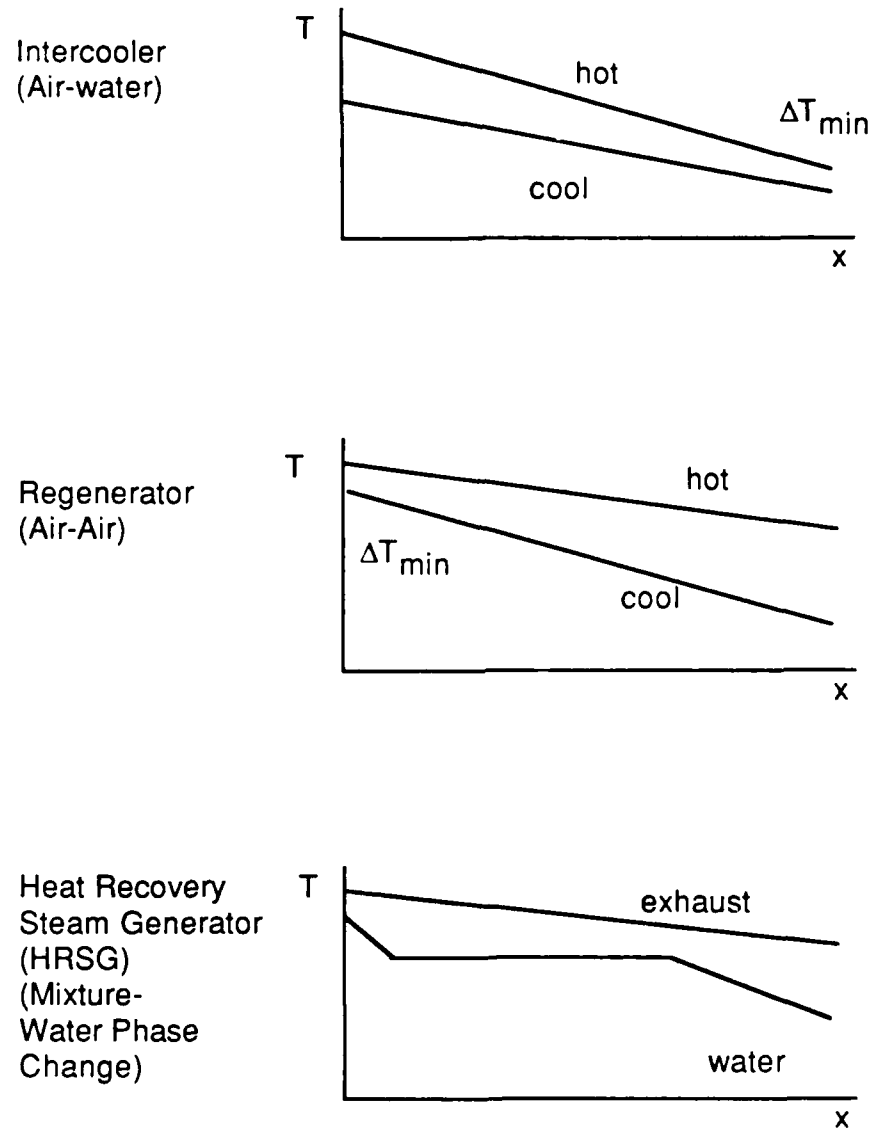


Figure 2. Heat exchangers.

fore, the Reynold's number is constant.

$$Re = \frac{\rho V d}{\mu} = \text{constant} . \quad (10)$$

For a constant Reynold's number and dimensions, the friction factor will be constant. The relationship for friction of internal turbulent flow is modified using an expression for mass flow rate and constant area. The following equation for mass flow rate is used.

$$m = \rho A V . \quad (11)$$

The equation for the friction factor of internal turbulent flow is expressed as

$$\text{friction} = f(Re) = \frac{\Delta p}{\rho V^2} = \text{constant}. \quad (12)$$

Applying Equation (11), Equation (12) becomes

$$\frac{\Delta p \rho}{m^2} = C_1 . \quad (13)$$

The ideal gas relation is used.

$$\frac{\Delta p \frac{p}{RT}}{m^2} = C_1 . \quad (14)$$

Since m and R are constant, the equation can be expressed as

$$\frac{(\Delta p) p}{T} = C_2 . \quad (15)$$

This yields an expression for pressure drop in terms of pressure, temperature, and a

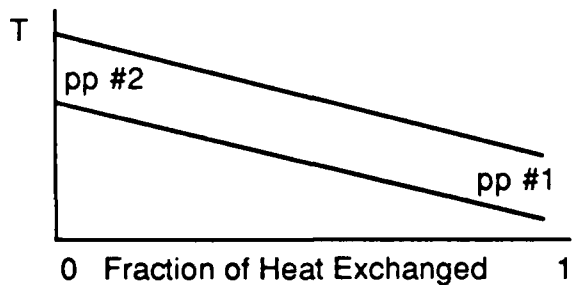
constant. A representative value of a pressure drop of 5 psi at atmospheric conditions was used to determine the constant, C_2 . The pressure drop through the intercooler, regenerator, heaters, and HRSG can now be determined using entry pressure and an average temperature.

The literature used a number of techniques to model pressure losses in one or more of the major heat transfer components. Fraize and Kinney [5] set the pressure drop across both the combustor and steam generator at 2% of the initial pressure. Bhutani et al. [9] applied a pressure drop of 4% across only the heater. Boyle [11] accounted for a 4% pressure drop across the combustor, a 4% drop in the turbine exhaust steam in the HRSG, and a 12% drop in the steam flow in the HRSG. He assigned generally larger values to account for parasitic pipe losses also.

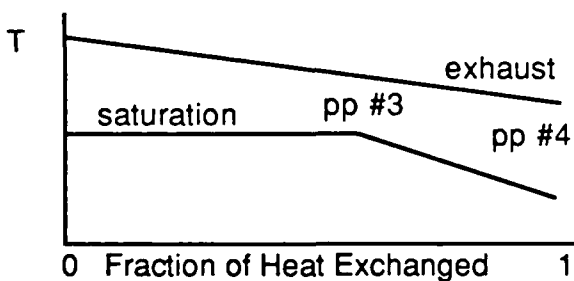
The method selected for this study to account for pressure losses has the advantages of determining the losses by use of flow parameters alone. This method is applicable to any of the mentioned components.

Heat Recovery Steam Generator (HRSG)

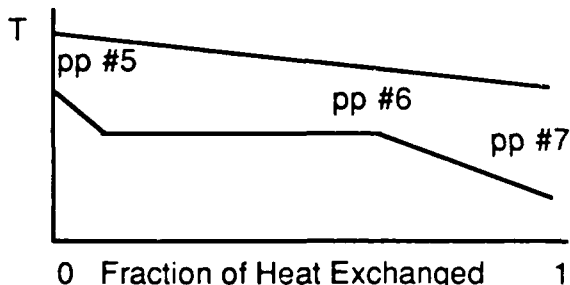
The effect of varying steam/air mass ratio and turbine exhaust temperature on the performance of the HRSG is constrained by a minimum pinch point limit (ΔT_{pp}) between the two streams. The amount of heat to be recovered effectively by the incoming water requires that the temperatures of the exhaust gas stream must be higher than the water/steam stream temperature by a minimum amount at all points in the heat exchanger. Another temperature difference to be defined is the approach temperature difference (ΔT_{ap}). This is the temperature difference between the entering hot exhaust stream and the exiting cooler water/steam stream. The location of the approach temperature difference as well as the possible locations of the pinch point temperature difference are shown in Figure 3. The literature describes the efficiency of the HRSG by setting ΔT_{ap} at a certain value and then checks to see if the ΔT_{pp} minimum limit has not



Turbine inlet temperature is not hot enough to boil water in HRSG.



Turbine inlet temperature is hot enough to start water to boil. Steam exits HRSG in saturation.



Turbine inlet temperature is high enough for steam to reach superheat.

Figure 3. Possible heat recovery steam generator (HRSG) pinch point (pp) locations.

been violated at the point where boiling of the water begins (point 6 in Figure 3). This sets the value of the exiting steam to the temperature of the turbine exhaust minus ΔT_{ap} . Once the temperature difference at the beginning of boiling approaches ΔT_{pp} , the temperature of the exhaust stream at the pinch point is set at the water's saturation temperature plus ΔT_{pp} . The temperature of exiting steam is then allowed to vary.

The range of values of ΔT_{pp} in the literature is 16.7 - 27.8°C (30 - 50°F) [4, 5, 7, 9, 11, 21, 26]. Stochl [4] considers the value of 27.8°C (50°F) as a reasonable value for both ΔT_{ap} and ΔT_{pp} . In his study he examined four values for each. Other authors have set ΔT_{ap} at a different value than ΔT_{pp} including 41.7°C (75°F) [16] and 55.5°C (100°F) [9]. The value of 26°C developed in this study for ΔT_{pp} is certainly in line with the literature. In terms of the literature this study places both ΔT_{ap} and ΔT_{pp} at 26°C. Figure 3 shows that the steam exiting the HRSG can be superheated, saturated, or can still be liquid depending on the turbine exhaust temperature and the steam/air mass ratio. The modelling of the HRSG in this study can handle each possibility. The modelling done in the literature commonly describes the performance of the HRSG only when ΔT_{ap} is set for exiting superheated steam and when the ΔT_{pp} value is applied at the first point of boiling for steam exiting as superheated steam and saturated steam. In Figure 3 these three situations are designated as pinch points 5, 6, and 3, respectively. It will be shown in the results of this study that the steam/air mass ratio which achieves the maximum First Law efficiency is the ratio which causes the pinch point (minimum temperature difference between the two streams) to move from the approach temperature location to the first point of boiling. This point of maximum First Law efficiency is confirmed by the literature. To describe the STIG performance over the entire range of turbine inlet temperatures and steam/air mass ratios the modelling of the HRSG was developed to handle all seven possible pinch point locations.

The known conditions within the HRSG before calculations are made include the

turbine exhaust temperature, the ratio of steam to air in the turbine exhaust, inlet water temperature, and the water saturation temperature. The water is pumped to compressor discharge pressure plus the calculated pressure loss through the HRSG and combustor. The saturation temperature for that pressure at each of the selected compression ratios and the other saturation properties of latent heat of vaporization (h_{fg}) and s_{fg} (for the Second Law analysis) were interpolated from Keenan et al. [27]. Additionally, a liquid water specific heat value for each compression ratio was determined by selecting the corresponding value of c_p for an average temperature (between ambient and saturation conditions) from the curve in Figure 2 in Keenan et al. [27]. The two unknown temperatures are the exiting steam temperature and the exiting hot stream exhaust temperature (denoted as T_{stack}). These unknown temperatures are found by an iterative process. First the pinch point temperature difference (ΔT_{pp}) of 26°C is set at first two possible locations (points 1 and 2 in Figure 3) and the unknown temperatures are found by equating the heat given up by the hot stream to the heat added to the cold stream. This assumes no heat loss from the HRSG. In both cases the temperature difference at the other possible pinch point location is checked to see if it is more applicable. If the heat transferred is sufficient to heat the water, for that stream/air mass ratio, to saturation then the next two possible pinch point locations (points 3 and 4 in Figure 3) for exiting saturated steam are checked. If the heat transferred in both of those situations is enough to heat the steam to superheat then the last three possible pinch point locations for this case (points 5, 6, and 7, Figure 3) are investigated to see which is applicable. In general the specific heat (kJ/kg air) given up by the hot stream, which is equated to the total heat transferred, is calculated as shown below.

$$q_{HEX} = (0.95 + Mr) \cdot c_{p,mixture} \cdot (T_{turbine\ exit} - T_{stack}) \quad . \quad (16)$$

The specific heat added to the cold stream is determined as shown below (in the case of

superheat steam exiting).

$$q = Mr \cdot [c_{p_{\text{water}}} \cdot (T_{\text{sat}} - T_1) + h_{fg} + c_{p_{\text{steam}}} \cdot (T_{\text{exiting}} - T_{\text{sat}})] \quad \text{.} \quad (17)$$

The HRSG modelling subroutine also finds the required heat input to raise the exiting steam to the desired turbine inlet temperature. This quantity is found by subtracting the heat transferred in the HRSG from the total heat required to raise the water from ambient conditions to the turbine inlet temperature. This is shown below.

$$q_{h_{\text{steam}}} = Mr \cdot [c_{p_{\text{water}}} \cdot (T_{\text{sat}} - T_1) + h_{fg} + c_{p_{\text{steam}}} \cdot (T_{\text{turbine}} - T_{\text{sat}})] - q_{\text{HEX}} \cdot \text{inlet} \quad (18)$$

As mentioned earlier the values of specific heat at constant pressure (c_p) for the air, steam, and steam/air mixture streams are determined at average temperatures from temperature dependent relations for air and steam specific heat ($c_p(T)$) [22, 23].

Pump

The required work to pump the water to the desired compressor discharge pressure is calculated as

$$\text{Specific Work} = \frac{Mr \cdot (Pr \cdot P_1 + \Delta P_{\text{HRSG}})}{\rho_{\text{water}} \cdot \eta_p} \quad . \quad (19)$$

This quantity is negligible for the range of parameters of this study.

Turbine Cooling

For higher temperature applications in gas turbines a certain amount of compressor air is bled off from the working stream to cool the turbine blades to keep them within their materials' operating temperature limits. There are several modelling techniques listed in the literature. Fraize and Kinney [5] state that the amount of air bled from the

compressor is 1.5% of the total compressor flow for each 100°F above a turbine inlet temperature of 1750°F (1228 K). Day and Kidd [6] set a schedule of 4% flow loss for a turbine inlet temperature of 1500°F (1089 K), a 8.5% loss for a temperature of 1750°F (1228 K), and a 16% loss for a temperature of 2000°F (1367 K). For this study the technique of Bhutani et al. [9] was used. This is a straight 5% air flow loss to turbine cooling. This was reflected in earlier listed equations. This is an admittedly simple calculation. The authors of this technique applied it to their study which had a 1700 K (2600°F) turbine inlet temperatue. They make a good point that in reality the initial quantity of bleed flow would be larger but certain portions of the air coolant are regained to the working fluid at all subsequent turbine blade stages to the stage at which that air stream is applied for cooling. In keeping with the desire not to be locked in specifying any particular component parameters or dimensions than is necessary this technique of determining turbine cooling bleed off was used.

First Law Efficiency

The calculation of the First Law efficiency is a straightforward calculation of the ratio of net work output to heat input. For the IGT cycle there are two stages of compression and expansion as well as two heating components. The STIG cycle has a work requirement for the water pump and a heat input requirement to heat the steam exiting the HRSG to the turbine inlet temperature. The First Law efficiency calculation is

$$\eta = \frac{\sum_{i=1}^2 w_{\text{turbine}_i} - \sum_{i=1}^2 w_{\text{compressor}_i} - w_{\text{pump}}}{\sum_{i=1}^2 q_{\text{air}_i} + q_{\text{steam}}} . \quad (20)$$

Second Law Efficiency

At present there are no universally accepted definitions for Second Law efficiency. This study will follow the concepts of Boehm [18], Moran [19], and Kotas [20]. Second Law efficiency will be defined here as the ratio of the net work and the reversible work. The reversible work is further defined as the sum of the inlet stream availabilities and Carnot equivalent work of each of heat inputs minus the sum of the exit stream availabilities.

$$w_{rev} = \sum_{\text{inlets}} b + \sum_{\substack{\text{heat} \\ \text{inputs}}} w_e - \sum_{\text{exits}} b \quad (21)$$

The results to be shown later will show the reversible work with and without accounting for the exit stream availabilities as a negative term in the reversible work. It may be argued that the exit streams that are vented to the stack are not available and need not be assessed as a loss or penalty. Some further definitions need to be made. First, thermodynamic availability is defined as the amount of work that can be produced when a substance at a given state reverts to the "dead" state while producing work with a Carnot cycle [18]. Here the dead state is usually defined as atmospheric conditions and the hypothetical Carnot cycle is assumed to be rejecting heat to the ambient temperature, T_1 . For this study the availability of a stream is expressed as shown below.

$$b = h - h_1 - T_1(s - s_1) \quad (22)$$

The kinetic, chemical, and potential components of the availability are considered negligible. For a mixture of n ideal gases, the availability becomes (in molal basis) [19, 20]

$$\bar{b} = \sum_{k=1}^n y_k \left[\int_{T_1}^T \left(1 - \frac{T_1}{T}\right) c_{pk} dT \right] + \bar{R} T_1 \ln \left(\frac{P}{P_1} \right) \quad (23)$$

The Carnot equivalent work of the heat inputs is calculated as

$$w = \left(1 - \frac{T_1}{T}\right) q_h . \quad (24)$$

In comparison to this study's definition of Second Law efficiency, the definitions provided in the literature are provided here. Moran [19] provides an example of a heat engine where work is produced by drawing heat from a high temperature reservoir, at temperature T_H , and rejecting heat to a low temperature reservoir, at temperature T_L . The Second Law efficiency can be expressed as follows (T_o is ambient temperature):

$$\epsilon = \frac{W_{net}}{\left(1 - \frac{T_o}{T_H}\right) \delta Q_H - \left(1 - \frac{T_o}{T_L}\right) \delta Q_L} . \quad (25)$$

He states that this expression does not charge as a loss the availability exiting in the heat interaction at T_L . This study follows more closely this alternate definition, which as he describes charges the availability exiting in the heat interaction at T_L as a loss. This is expressed as

$$\epsilon = \frac{W_{net}}{\left(1 - \frac{T_o}{T_H}\right) \delta Q_H} . \quad (26)$$

This study used this approach and assesses availabilities entering and leaving the control volume of the system. Kotas [20] provides a Second Law efficiency definition for a gas turbine plant. This plant burns fuel internal to the cycle. His Second Law efficiency is expressed below.

$$\epsilon = \frac{\text{Rated plant net output}}{\text{Total availability of all input fuel components}} . \quad (27)$$

Kotas and El-Masri [28] provide details of the use of finding stream availability at each of the cycle state points to locate the cause and magnitude of losses within the system. This study uses a control volume approach to evaluate overall cycle performance, so finding the location and magnitude of the system's irreversibilities is not a goal of this study. This approach of a Second Law analysis is still quite new, but has a promising future.

Simple Brayton Cycle (GT)

For the GT and IGT cycles the referenced dead state is air at ambient temperature and pressure. The availability of the air inlet stream is then zero. The Second Law efficiency (ϵ) for the GT cycle is defined as shown.

$$\epsilon = \frac{w_{\text{net}}}{w_{e_{\text{air}}} - b_{\text{exhaust}}} . \quad (28)$$

The Carnot equivalent work of the heat input is calculated as shown below.

$$w_{e_{\text{air}}} = 0.95 \int_{T_2}^{T_3^*} \left(1 - \frac{T_1}{T}\right) \delta q = 0.95 \int_{T_2}^{T_3} \left(1 - \frac{T_1}{T}\right) c_{\text{pair}} dT \quad (29)$$

$$w_{e_{\text{air}}} = 0.95 c_{\text{pair}} \left[(T_3 - T_2) - T_1 \ln \left(\frac{T_3}{T_2} \right) \right] . \quad (30)$$

The exhaust availability is calculated as

$$b_{\text{exhaust}} = 0.95 [\Delta h - T_1 (\Delta s)] . \quad (31)$$

*Refer to Figure 1 to find the locations of referenced state points.

Since $P_4 = P_1$, then this term can be expressed as

$$b_{\text{exhaust}} = 0.95 c_{\text{pair}} [(T_4 - T_1) - T_1 \ln (\frac{T_4}{T_1})] . \quad (32)$$

Improved Brayton Cycle (IGT)

As mentioned above, the availability of the inlet air stream is zero. In the IGT cycle there are two heating processes and the cooling of the air stream in the intercooler. These are expressed as three Carnot equivalent heat inputs. Each is calculated as shown above for the GT cycle. The exhaust gas availability is determined using the exhaust temperature from the regenerator. The cycle Second Law efficiency is defined as

$$\epsilon = \frac{w_{\text{net}}}{\sum_{i=1}^2 w_{e_{\text{heating},i}} - w_{e_{\text{intercooling}}} - b_{\text{exhaust}}} \quad (33)$$

Brayton Cycle with Steam Injection (STIG)

A Second Law efficiency for the STIG cycle is computed in an analogous manner to the approach covered for the GT and IGT cycles. In addition, two other Second Law efficiencies will be developed for comparison in which all the steam produced in the HRSG goes to process work elsewhere and is not injected into the gas turbine. In these second two cases, one will heat the exiting steam to the turbine inlet temperature and the other will not heat the steam beyond its HRSG exit temperature.

In evaluating the Second Law efficiencies for these three systems, it will allow a comparison of a steam injection system and a cogeneration system. These systems are alike except the STIG system injects the steam produced. An evaluation of the level of irreversibilities of the steam injection can be made.

For the first definition of the Second Law efficiency, the reference state is the

steam/air mixture at ambient temperature and pressure. In this case, the inlet air and water streams are at ambient pressure which is greater than their corresponding partial pressure in the exhaust mixture stream. The inlet stream availabilities are then nonzero. Using the earlier definition of availability (Equation (23)), the availability of the air inlet stream (on a mass basis) can be expressed as

$$b_{\text{air inlet}} = \frac{T_1 \cdot \bar{R} \cdot \ln(1/y_{\text{air}})}{MW_{\text{air}}} . \quad (34)$$

The water inlet stream is expressed in a similar fashion. The availability of the mixture exhaust is expressed as

$$b_{\text{mix exhaust}} = (Mr + 0.95) \cdot c_{p_{\text{mix}}} \cdot [T_{\text{stack}} - T_1 - T_1 \cdot \ln(\frac{T_{\text{stack}}}{T_1})] . \quad (35)$$

The heat input requirements for the STIG cycle are to the air and the steam. Depending on the turbine exhaust temperature and the steam/air mass ratio, the steam can exit the HRSG at superheat or in saturation. The Carnot work equivalent for the air heat input is

$$w_{e_{\text{air}}} = 0.95 \cdot c_{p_{\text{air}}} \cdot (T_3 - T_2 - T_1 \ln(\frac{T_3}{T_2})) . \quad (36)$$

The heat supplied to saturated steam to heat it to superheated vapor is done at constant temperature. This equivalent Carnot work is

$$w_{e_{\text{sat steam}}} = Mr \int_{T_1}^T (1 - \frac{T_1}{T}) \delta q = Mr (1 - \frac{T_1}{T_{\text{sat}}}) dh \quad (37)$$

$$w_{e_{\text{sat steam}}} = Mr (1 - \frac{T_1}{T_{\text{sat}}}) (q_{\text{superheat}} - q_{\text{HEX}}) . \quad (38)$$

The equivalent work for the heat input to take the steam through superheat to the desired turbine inlet temperature is calculated as

$$w_{e_{\text{superheat}}} = M_r \cdot c_{p_{\text{steam}}} \cdot [(T_3 - T_{\text{sat}}) - T_1 \ln \left(\frac{T_3}{T_{\text{sat}}} \right)] . \quad (39)$$

The Second Law efficiency for this application is defined as

$$\epsilon_1 = \frac{w_{\text{net}}}{b_{\text{air}_{\text{inlet}}} + b_{\text{water}_{\text{inlet}}} + w_{e_{\text{air}}} + w_{e_{\text{sat steam}}} + w_{e_{\text{superheat steam}}} - b_{\text{mix}_{\text{exhaust}}}} . \quad (40)$$

In the last two Second Law efficiencies to be described for the GT cycle with stream production, the air and water streams never mix. The reference states are separate air and water streams at ambient conditions. The availability of these inlet streams is zero. The exit stream of steam is produced to do process work. Its availability will be added to w_{net} in the numerator of the efficiency ratio. For this cycle, it was found that the steam could exit as liquid water, saturated steam, or superheated steam. This is due to the loss of increased turbine exhaust specific heat when steam is not injected into the working fluid. With only air in the hot stream of the HRSG, the HRSG modelling subroutine must be able to handle all 7 possible pinch points as described earlier. The availability of the HRSG exhaust stream is done as shown before except it is for only air. If the steam exits as liquid water its availability is described as

$$b_{\text{water}} = M_r \cdot c_{R_{\text{water}}} \left[(T_{\text{water}_{\text{exit}}} - T_1) - T_1 \ln \left(\frac{T_{\text{water}_{\text{exit}}}}{T_1} \right) \right] . \quad (41)$$

If the steam exists as saturated steam, the quality of the steam is found to properly ac-

count for the $(h - h_f)$ and $(s - s_f)$ contributions to the availability by expressing them as $x \cdot h_{fg}$ and $x \cdot s_{fg}$. The quality is found as

$$x = \frac{h - h_f}{h_{fg}} = \frac{(h - h_1) - (h_f - h_1)}{h_{fg}} = \frac{q_{\text{HEX}} - q_{\text{sat}}}{h_{fg}} . \quad (42)$$

The availability is then expressed as

$$b_{\text{sat steam}} = Mr \left\{ c_{P\text{water}} \cdot [(T_{\text{sat}} - T_1) - T_1 \ln \left(\frac{T_{\text{sat}}}{T_1} \right)] + x \cdot h_{fg} - T_1 \cdot x \cdot s_{fg} \right\} . \quad (43)$$

For steam that exits as superheated steam (and similarly the case where the steam is heated to the turbine inlet temperature) the availability becomes the following relation.

$$\begin{aligned} b_{\text{superheat}} &= Mr \left\{ c_{P\text{water}} \cdot [(T_{\text{sat}} - T_1) - T_1 \ln \left(\frac{T_{\text{sat}}}{T_1} \right)] + h_{fg} - T_1 s_{fg} \right. \\ &\quad \left. + c_{P\text{steam}} \cdot [(T_{\text{exit}} - T_{\text{sat}}) - T_1 \ln \left(\frac{T_{\text{exit}}}{T_{\text{sat}}} \right)] \right\} . \end{aligned} \quad (44)$$

Additionally for the case where the steam is heated to turbine inlet temperature, the calculation of equivalent work of heat input must also handle the three possibilities of exiting steam (water, saturated steam, and superheated steam). The calculation for the case when the steam exits as liquid water will show how each case is done.

$$\begin{aligned} w_{e\text{steam}} &= Mr \left\{ c_{P\text{water}} \cdot [(T_{\text{sat}} - T_{\text{exit}}) - T_1 \ln \left(\frac{T_{\text{sat}}}{T_{\text{exit}}} \right)] + \left(1 - \frac{T_1}{T_{\text{sat}}} \right) h_{fg} \right. \\ &\quad \left. + c_{P\text{steam}} \cdot \left[(T_{\text{turbine}} - T_{\text{sat}}) - T_1 \ln \left(\frac{T_{\text{turbine}}}{T_{\text{sat}}} \right) \right] \right\} . \end{aligned} \quad (45)$$

The Second Law efficiency for the case of no steam injection and where the steam is heated to turbine inlet temperature is expressed as

$$\epsilon_2 = \frac{w_{net} + b_{steam(turbine\ inlet\ temp)}}{w_{e_{air}} + w_{e_{steam}} - b_{air\ exhaust}} . \quad (46)$$

The Second Law efficiency for the case of no steam injection and where the steam is not heated beyond HRSG exit temperature is expressed as

$$\epsilon_3 = \frac{w_{net} + b_{steam(HRSG\ exit\ temp)}}{w_{e_{air}} - b_{air\ exhaust}} . \quad (47)$$

This method of expressing the Second Law efficiency for these GT cycles with steam production closely follows the Second Law efficiency definition provided by El-Masri [28]. His definition is

$$\epsilon = \frac{W_{net} + \sum_{\text{exits}} b}{Q_{\text{added}}} . \quad (48)$$

Additionally he provides an interesting expression of the Second Law efficiency in terms of the Carnot efficiency and irreversibilities at each stage of the cycle.

$$\epsilon = \eta_{\text{Carnot}} - \sum_{\text{components}} L \quad (49)$$

He expresses L as the ratio of the stream availability loss in a process to the total heat added to the cycle.

This study presents several variations of the definition of Second Law efficiency. As a summary, these definitions are recapped in Table 3. Generally, each definition is a ratio of net work to reversible work. Depending on how the reference state is defined, the reversible work may include inlet stream availabilities. It will be shown in the next

Table 3
Second Law Efficiency Definitions

Cycle	Second Law Efficiency (ϵ) ^a
GT	$\epsilon = \frac{\text{Work Out}}{\text{Reversible Work}} = \frac{\text{Net Work}}{\text{Carnot Equivalent Work of Heat Input}} = \frac{w_{\text{net}}}{w_{e_{\text{air}}}}$
IGT	$\epsilon = \frac{\text{Net Work}}{\text{Carnot Equivalent Work of Heat Inputs & Outputs}} = \frac{w_{\text{net}}}{\sum_{i=1}^2 w_{e_{\text{heating}}} - w_{e_{\text{intercooling}}}}$
STIG	$\epsilon = \frac{\text{Net Work}}{\frac{\text{Availability of Inlet Streams and}}{\text{Equivalent Work of Heat Inputted}} + \frac{w_{\text{net}}}{b_{\text{air}} + b_{\text{water}} + w_{e_{\text{air}}} + w_{e_{\text{saturated steam}}} + w_{e_{\text{superheat steam}}}}} = \frac{w_{\text{net}}}{b_{\text{air}} + b_{\text{water}} + w_{e_{\text{air}}} + w_{e_{\text{saturated steam}}} + w_{e_{\text{superheat steam}}}}$
GT with HRSG (Steam at Turbine Inlet Temp)	$\epsilon = \frac{\text{Net Work and Steam Availability}}{\text{Equivalent Work of Heat Inputted to Steam and Air}} = \frac{w_{\text{net}} + b_{\text{steam}} (\text{turbine inlet temp})}{w_{e_{\text{air}}} + w_{e_{\text{liquid}}} + w_{e_{\text{saturated water}}} + w_{e_{\text{superheated steam}}}}$
GT with HRSG (Steam at HRSG Exit Temp)	$\epsilon = \frac{\text{Net Work and Steam Availability}}{\text{Equivalent Work of Heat Inputted to Air}} = \frac{w_{\text{net}} + b_{\text{steam}} (\text{HRSG exit temp})}{w_{e_{\text{air}}}}$

^aDefinitions do not include exhaust stream availability which will be shown to be not useful to this study.

chapter that including the exit stream availability in the reversible work is not useful to this study. The major components of the reversible work are the Carnot equivalent work of the heat added to the air and, depending on the cycle, added to the liquid water, saturated steam, and superheated steam. For the GT cycle with the HRSG to produce steam, the availability of the steam at either turbine inlet temperature or HRSG exit temperature is added to the net work.

Limits on Cycle Performance

The limits to cycle performance are a result of maximum limits to the parameters of steam/air mass ratio and maximum cycle temperature. Both of these parameters are influenced by several variables.

Condensation

The appearance of condensation in the exhaust gas from the HRSG of the STIG cycle places a maximum limit on the steam/air mass ratio. If the stack temperature at the HRSG exit is below the dew point temperature at ambient pressure then possibly corrosive condensation will occur within the HRSG. Although not the case in this study, when fuel containing sulfur is burned, any condensation in the exhaust flow will be acidic. The literature has selected a number of safe minimum stack temperature limits to preclude the formation of acidic condensation. Stochl [4] places a minimum T_{stack} limit in the range of 250-300°F (394-417 K) while Bhutani et al. [9] placed the minimum limit at 275°F (408 K) and Day and Kidd [6] selected 310°F (428 K) as the limit. Depending on the degree of water treatment of the feedwater for the STIG cycle, the condensation of the steam in the HRSG can have a corrosive potential for long term operation. The effect on overall cycle performance to preclude any condensation within the STIG cycle will be shown later.

Visible Plume

Depending on the ambient conditions, a visible exhaust plume from condensing steam can form at a stack temperature above the prevailing dewpoint temperature. Although the plume is only steam, a visible plume is a sign of possible pollution. To preclude a visible plume, a lower limit than design conditions would be placed on the maximum steam/air mass ratio. In areas where large fluctuations of ambient conditions occur, it may be necessary to install sensing equipment to monitor ambient temperature and relative humidity so that the steam/air mass ratio can be adjusted to eliminate a visible plume.

Compressor Surge Limit

In fixed-geometry machines not specifically designed for steam injection the relative increase in mass flow through the turbine with steam injection can result in an increase in compressor back pressure and therefore an increase in the compressor pressure ratio. As the steam injection increases, the compressor pressure ratio increases toward its surge limit. The maximum increase in performance obtainable with steam injection then depends on the surge margin available to the particular compressor [4]. This study did not place any limits on steam/air mass ratio as no particular compressor surge limits were specified.

Complete Oxygen Combustion

This limit pertains to cases when fuel is burned in the combustor and is included here for information only. Complete oxygen combustion serves as a limit to both maximum cycle temperature and steam/air mass ratio. For a certain steam/air mass ratio there is no longer any excess oxygen to burn additional fuel to heat an increase in steam injection to the desired temperature. Further additions to steam are not possible if the turbine inlet temperature is not reduced [6, 11].

Materials' Temperature Limit

As discussed earlier, turbine cooling is necessary for higher temperature applications in gas turbine cycles. Although over a billion dollars has been spent since World War II on metallurgical research in developing new alloys to extend jet engine and gas turbine temperature limits, there has only been an advance of approximately 100°C [29]. The maximum permissible metal temperature in gas turbine blades has been extended from ~700 to ~ 800°C (~1292 to ~1472°F). Boyle [11] sets a maximum temperature limit at 1089 K (1500°F). This temperature limit is based on the fact that in 40 years of research the same type of alloys of Fe - Cr - Ni are still primarily used. These alloys have a melting point around 1643 K (2550°F) giving a sintering temperature (local welding at 75% melting temperature) of ~ 1230 K (~ 1750°F). Fraize and Kinney [5] state that at the time of their writing DOE programs were ongoing to extend ceramic technology to applications for gas turbines. This will be a difficult task. Ceramics have excellent resistance to thermal stresses but are very brittle. The addition of aluminum to ceramic compounds is being tried to improve ductility [1]. Successful ceramic compounds could possibly extend maximum temperatures to 1561 K (2350°F) [3]. Application of coated carbon-carbon materials may extend temperatures to 1700 K (2600°F) [3]. At this point in time, turbine inlet temperatures can be extended as far as the cooling schemes can keep the turbine blades within the permissible temperature limits. Fraas [29] states that with air cooling there is a point of diminishing returns where efficiency decreases due to increasing compressor air bleed off requirements to cool the turbine. Boyce [1] reports that this point of diminishing returns is 1533 K (2500°F). Fraas [29] does place hope in water cooling of gas turbine blades which may allow turbine inlet temperatures as high as 2273 K (2600°F). The water cooling will require pumping which in terms of cycle efficiency will be a much smaller cost than bleed off from the working fluid. It is therefore unlikely that the higher temperature

limits of this study (range is 1000-2500 K) will be applicable for some time yet.

Steam Dissociation

Another limit to the maximum cycle temperature is the degree of dissociation of steam at the increasing turbine inlet temperatures. Bhutani et al. [9] placed a limit of 1100°F (1000°F as a practical limit) on the superheat of steam in Rankine systems due to the decomposition of the steam. Fraas [29] describes the primary hazard is that steam increasingly dissociates at temperatures above ~ 315°C (600°F) which allows the hydrogen to diffuse through the metal walls and frees the oxygen to attack the metal walls. The literature referenced [4-17] has not placed any temperature or steam/air mass ratio limits for the STIG cycle due to this phenomenon. In some application of gas turbines dissociation can be valuable from the standpoint of increasing the turbine volume flow relative to the compressor volume flow [29].

CHAPTER III

RESULTS AND DISCUSSION

This chapter will describe the results of the First Law and Second Law Analyses of the performance of the three Brayton cycle systems.

First Law Analysis

Figures 4 through 8 show plots of First Law cycle efficiency versus turbine inlet temperature for the three systems at each of the compressor ratios. Figures 9 through 13 show the plots of specific net work versus turbine inlet temperature for each pressure ratio. A fourth curve (dash line) is shown on Figures 4 through 13 to depict the effect of limiting the steam/air mass ratio so that no condensation occurs in the STIG cycle. Each of the plots for the STIG cycle uses the steam/air mass ratios which achieve the maximum First Law efficiency. This includes the plots of specific net work which reflect the net work at the steam/air mass ratio which achieve the maximum efficiency. Each of the plots does not cover the entire turbine inlet temperature of 1000-2500 K. The plots were cut off just before the temperature where a steam/air mass ratio of 0.500 no longer provided a maximum efficiency for the STIG cycle. Performance curves for the IGT cycle were not provided at the smallest pressure ratio, $Pr = 4$, since at lower turbine inlet temperatures, the 2 turbines cannot provide enough work to run the 2 compressors.

On comparing the 3 cycles in Figures 4 through 13 it can be seen that both the Brayton derivative cycles (IGT and STIG) provide improvements in both efficiency and net work output over the simple Brayton cycle (GT). The IGT cycle is superior than the other two cycles in efficiency over the entire temperature range. The STIG cycle

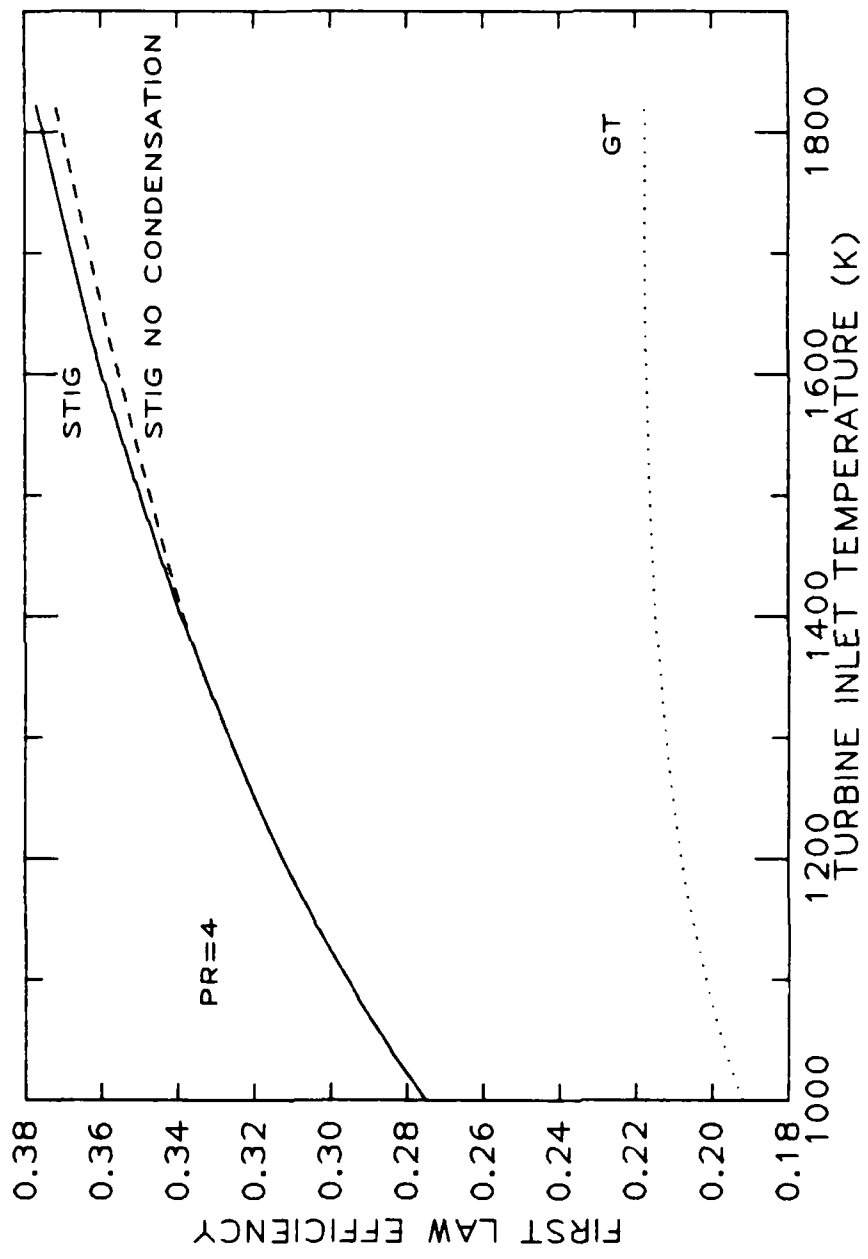


Figure 4. First Law efficiency versus turbine inlet temperature ($\text{Pr} = 4$).

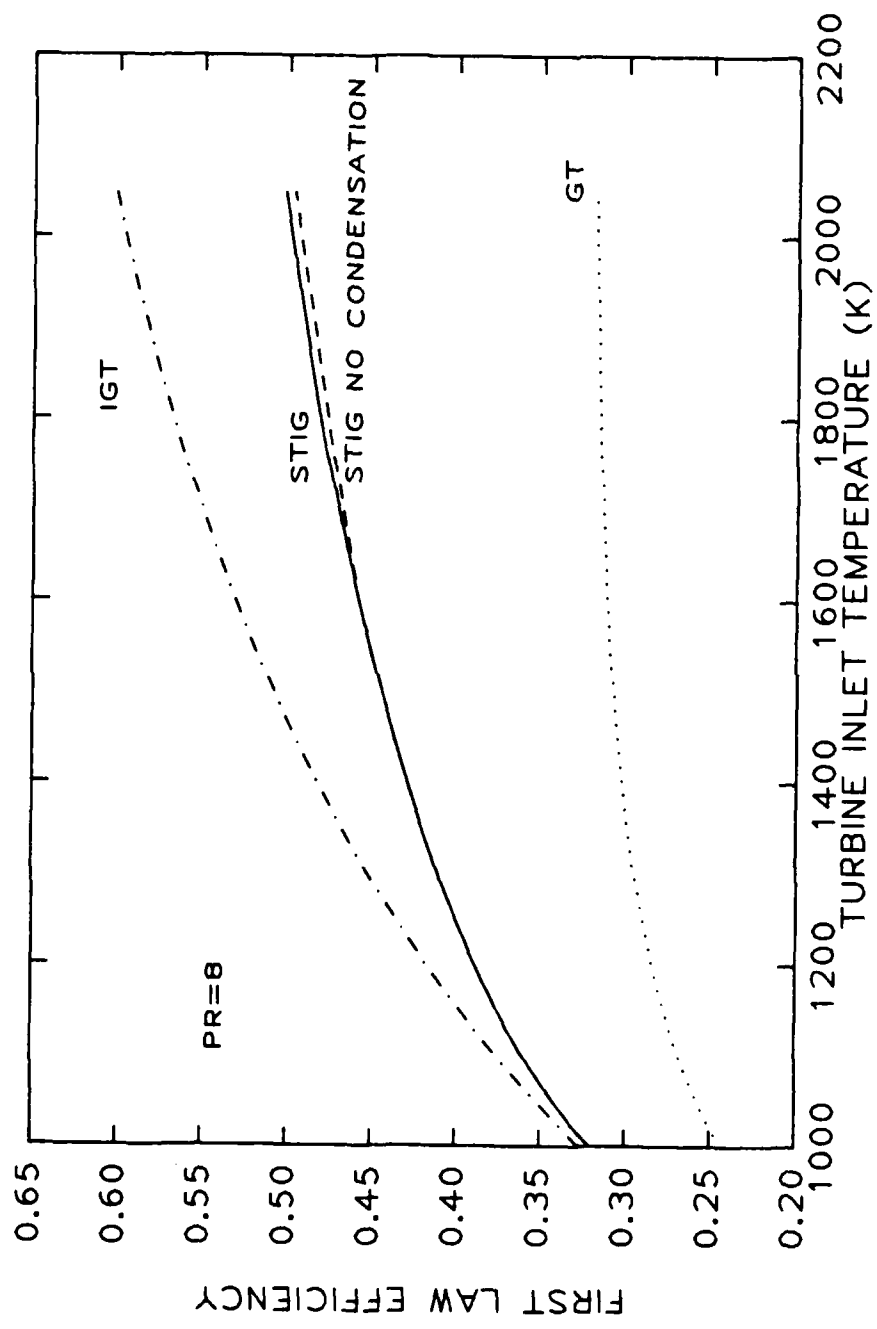


Figure 5. First Law efficiency versus turbine inlet temperature ($\text{Pr} = 8$).

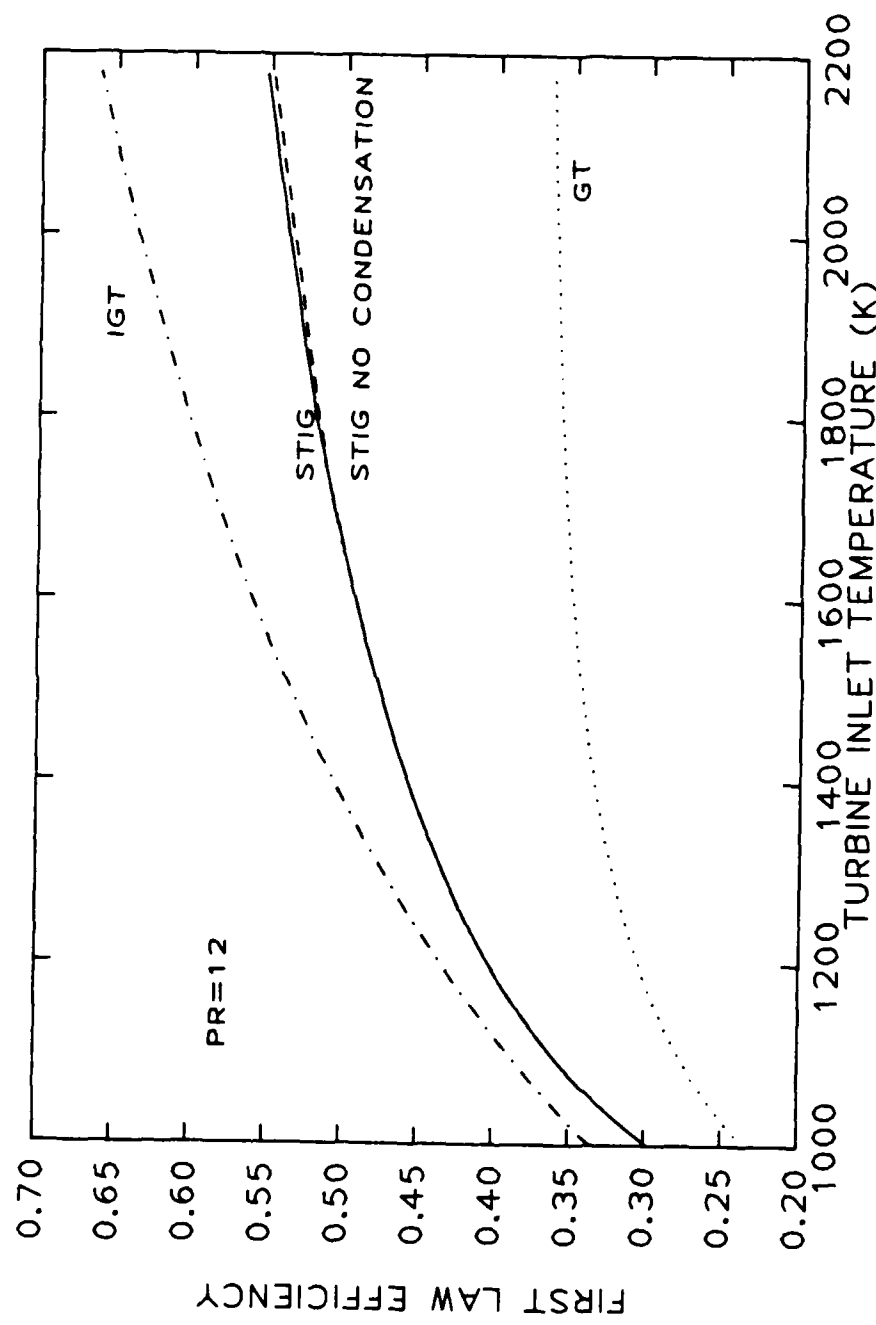


Figure 6. First Law efficiency versus turbine inlet temperature ($P_f = 12$).

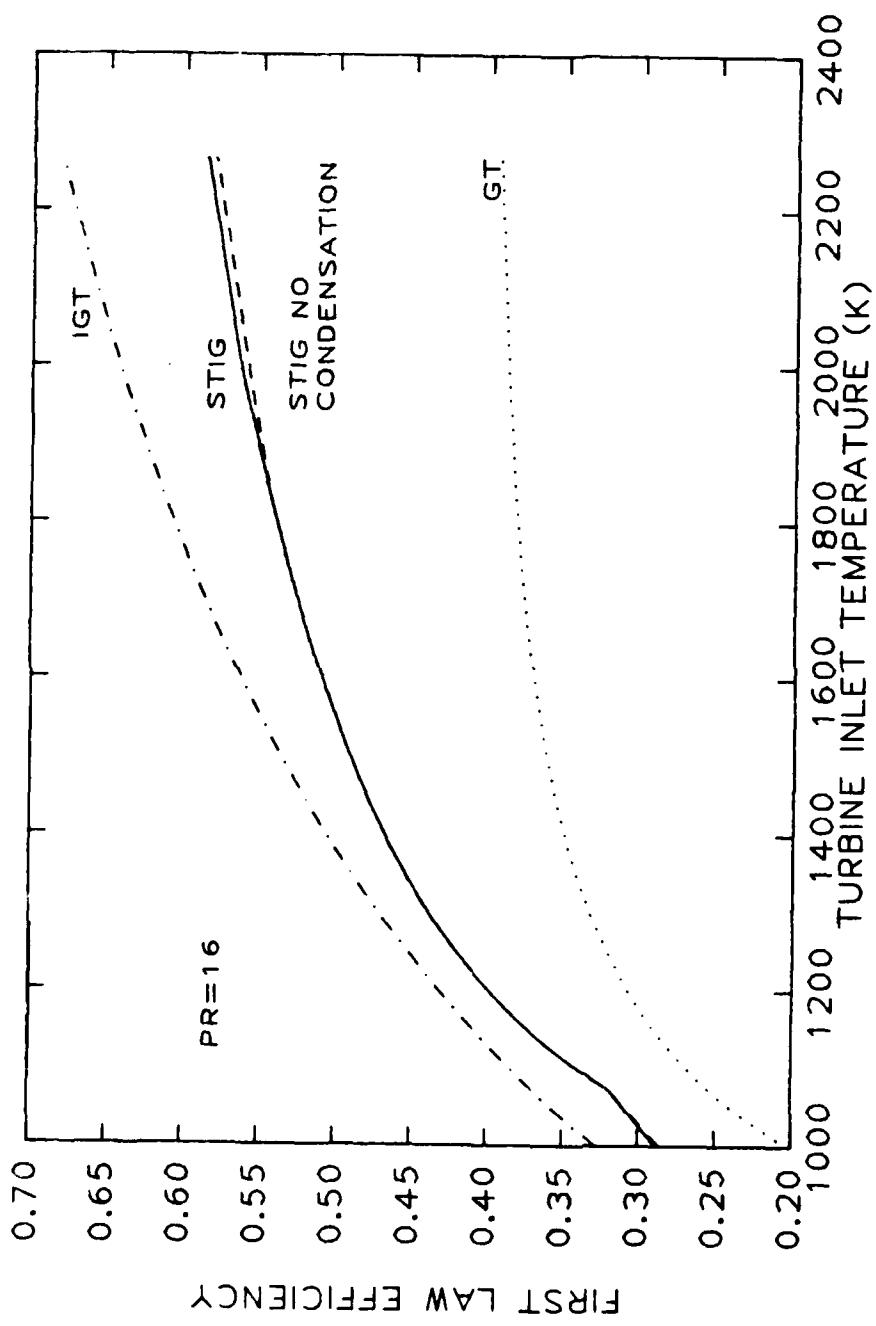


Figure 7. First Law efficiency versus turbine inlet temperature ($\text{Pr} = 16$).

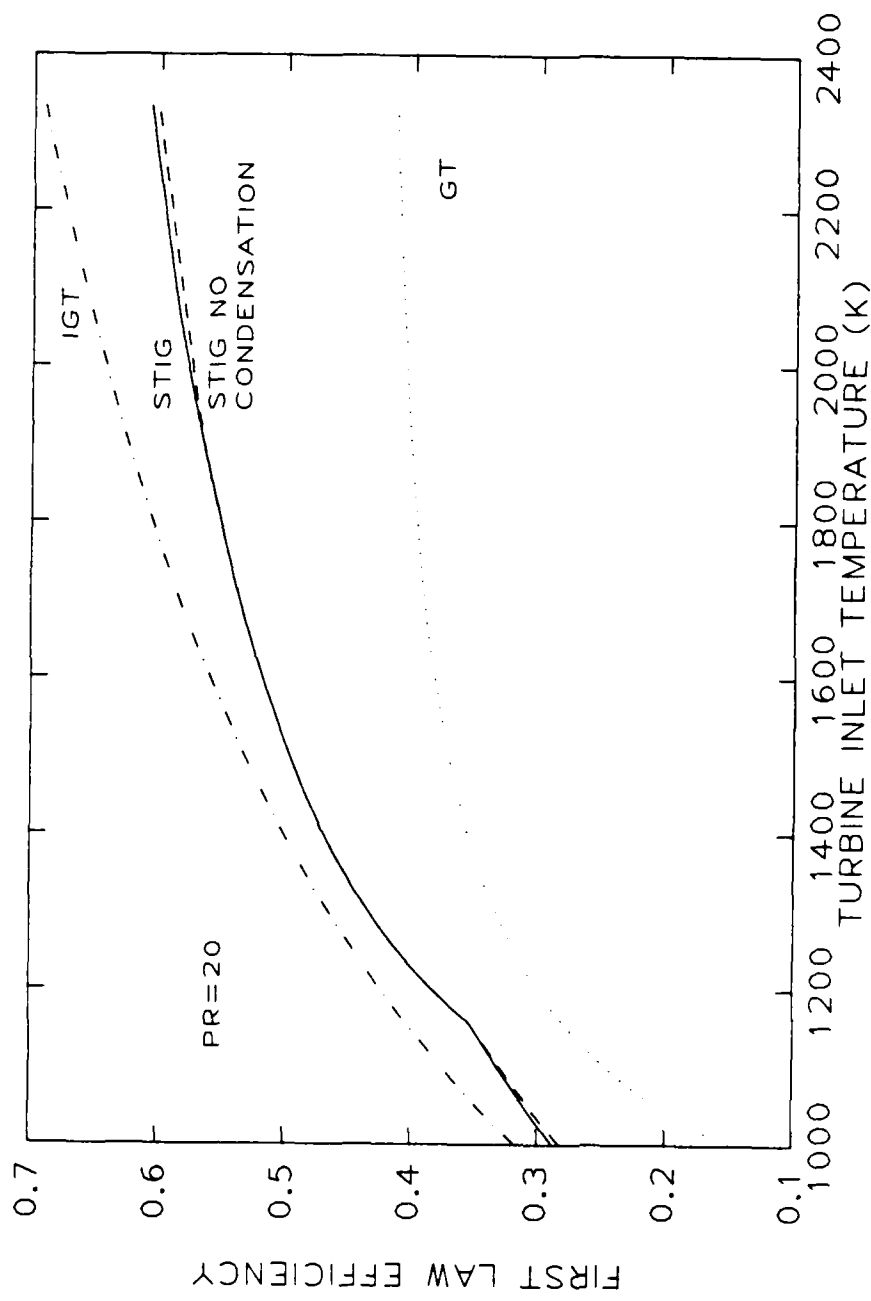


Figure 8. First Law efficiency versus turbine inlet temperature ($\text{Pr} = 20$).

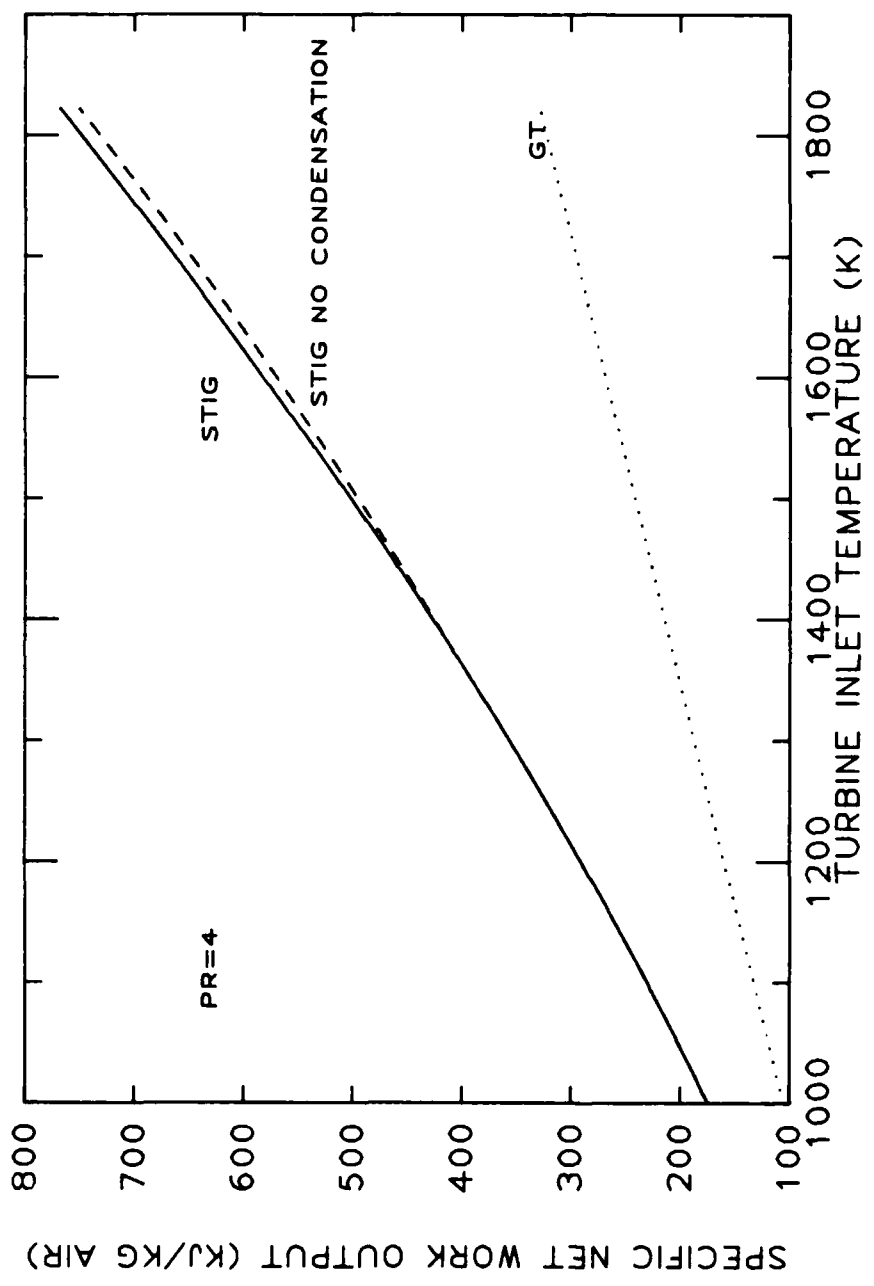


Figure 9. Specific net work versus turbine inlet temperature ($\text{Pr} = 4$).

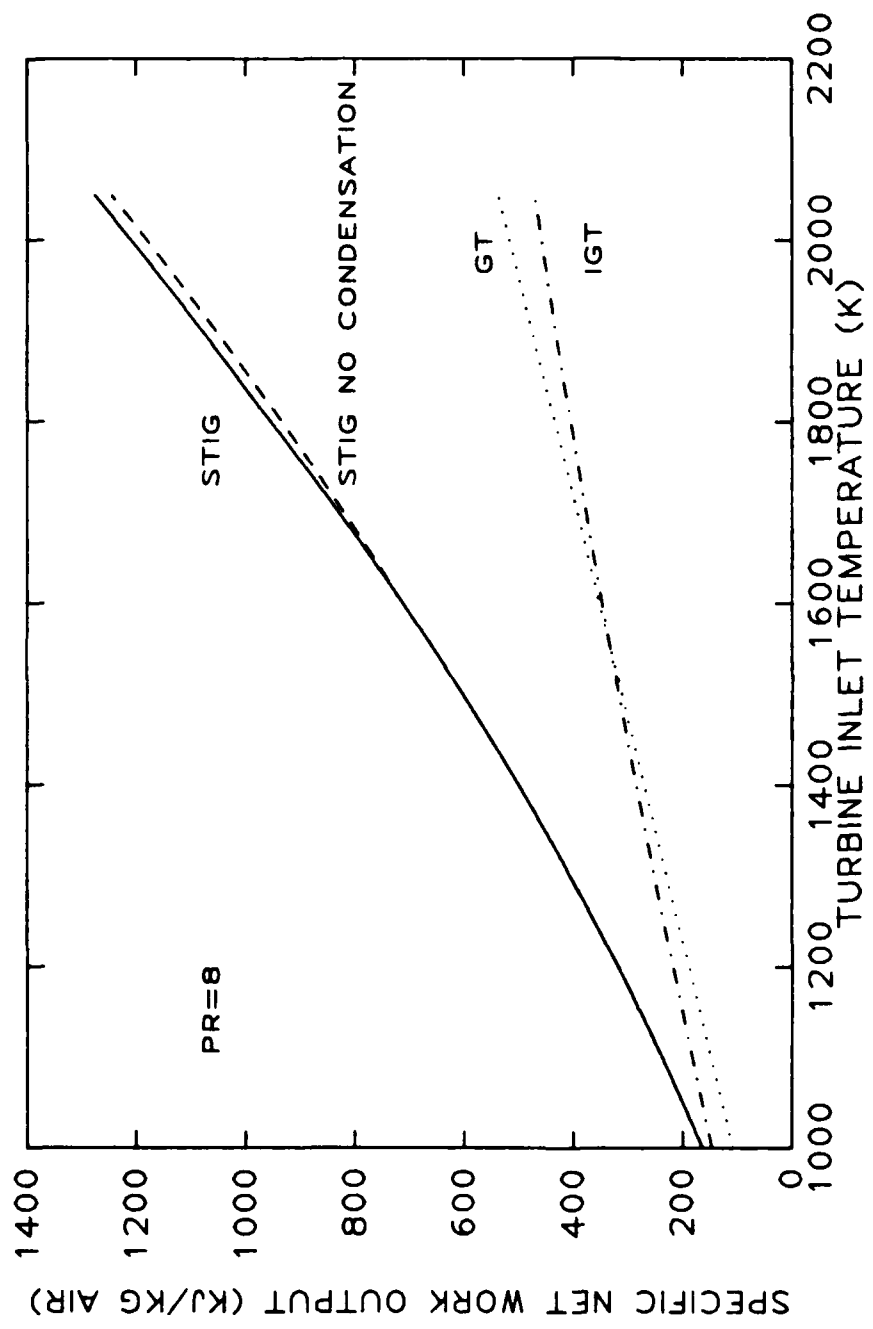


Figure 10. Specific net work versus turbine inlet temperature ($\text{Pr} = 8$).

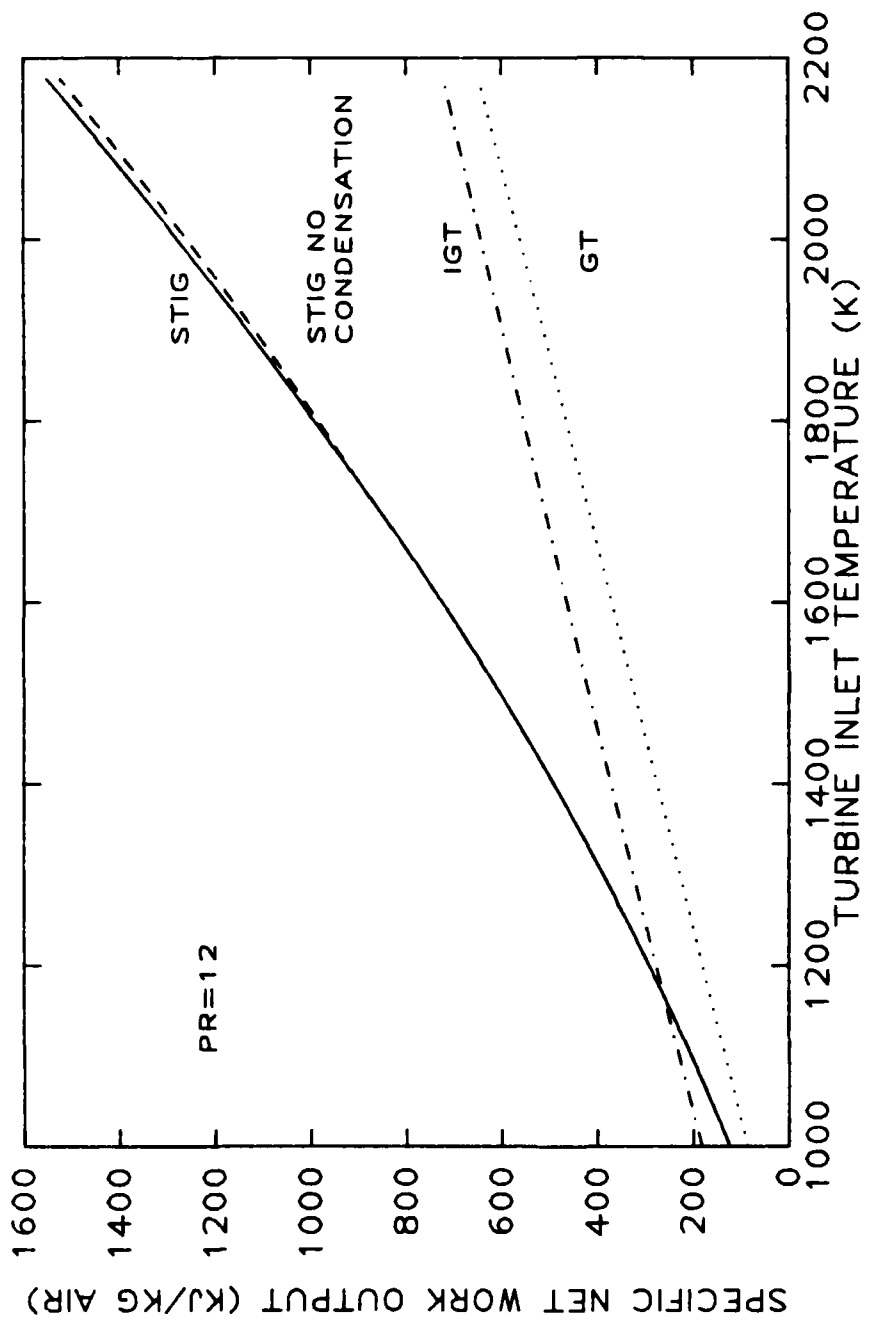


Figure 11. Specific net work versus turbine inlet temperature ($\text{Pr} = 12$).

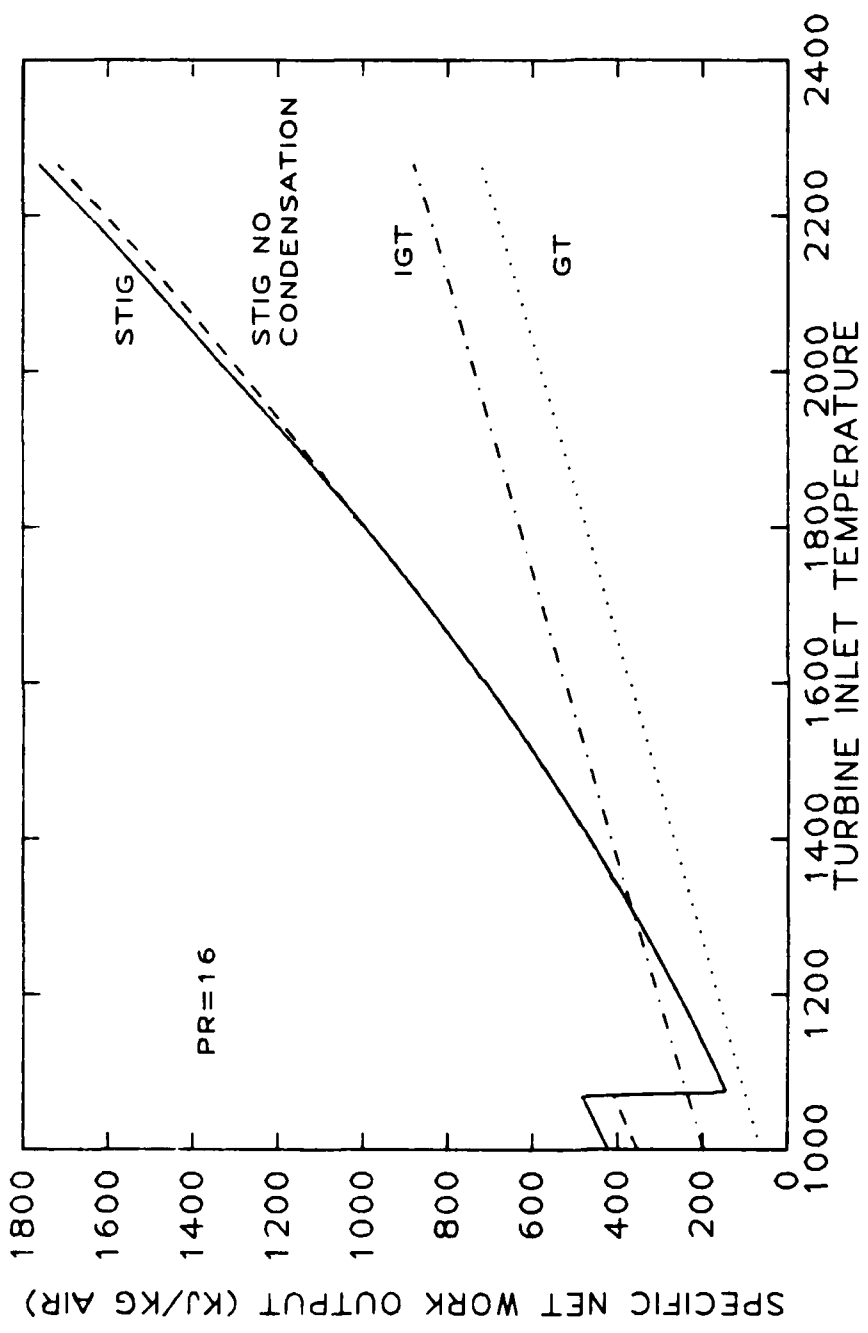


Figure 12. Specific net work versus turbine inlet temperature ($\text{Pr} = 16$).

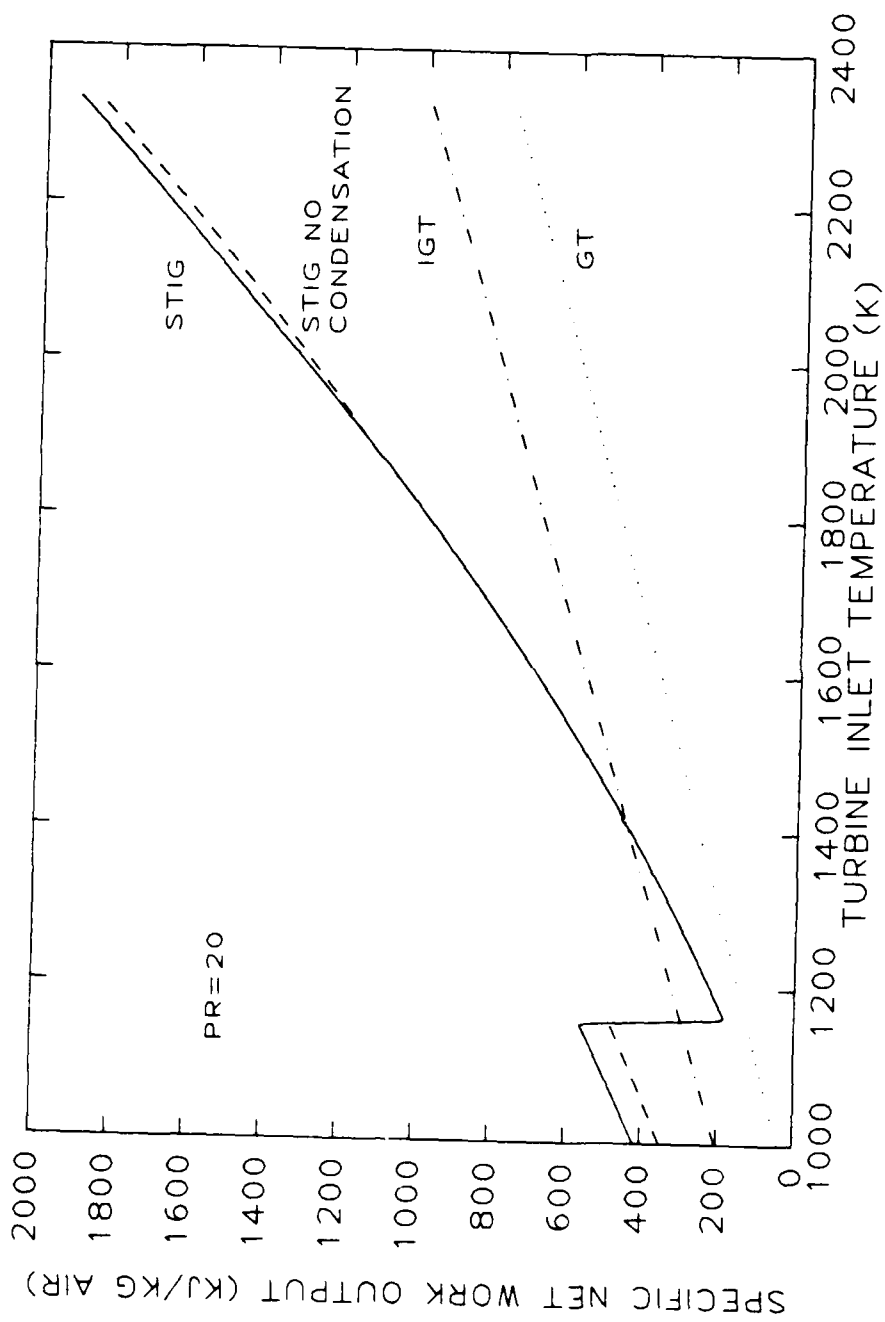


Figure 13. Specific net work versus turbine inlet temperature ($\text{Pr} = 20$).

provides a considerably greater improvement in net work output than the IGT cycle over much of the temperature range. As the pressure ratio increases the STIG cycle achieves a maximum efficiency at lower steam/air mass ratios. At the highest two pressure ratios, 16 and 20, there appears to be a discontinuity in the specific net work plots for the STIG cycle. In this area of higher pressure ratio and lower turbine inlet temperature the maximum efficiency is achieved at a different HRSG pinch point location than the rest of the studied regime. This pinch point location occurs at higher steam/air mass ratios. The higher steam/air mass ratios yield higher net work outputs. This phenomenon will be covered later.

The GT and IGT efficiencies continue to increase with temperature but do so with a much diminished return. The STIG cycle as mentioned achieves a maximum efficiency. The performance of the STIG cycle is dictated by the performance of its heat recovery steam generator (HRSG). For the temperature range studied here, as steam is introduced in the HRSG at small mass ratios the turbine exhaust stream is hot enough to heat the smaller quantities of steam relative to air, to a superheated vapor. The streams are closest at pinch point #5 as shown in Figure 3. The relative specific heat values (c_p) and mass flow ratios of the two flow streams are such that the slope of hot stream as seen in Figure 3 is quite shallow. Pinch point 5 is the appropriate location for the small mass ratios and the high temperatures covered in this study. As the mass flow rate increases the turbine exit temperature increases due to the increase in the turbine working fluid's specific heat. The exit temperature of the steam leaving the HRSG also increases since its temperature is fixed to the increasing turbine exit temperature by the minimum pinch point difference (ΔT_{pp}). With the pinch point at this location, the efficiency increases with the mass ratio. In other words, the gain in the turbine work is greater than the penalty of heating more steam to the desired turbine inlet temperature.

The phenomenon of increasing efficiency with steam/air mass ratio does not go on

indefinitely. The specific heat of the turbine exhaust increases with the mass ratio. The slope of the hot exhaust in the HRSG, as shown in Figure 3, decreases as the steam/air mass ratios increases. The difference in the temperature of the two streams finally reaches the ΔT_{pp} value at the first point of boiling. This location was noted as pinch point location #6 in Figure 3. With further increases in the steam/air mass ratio the minimum temperature difference remains fixed at this location and the exiting steam temperature will then decrease as the mass ratio increases. From now on increases in the turbine work are less than the penalty of heating increasing amounts of steam to the desired turbine inlet temperature. After the pinch point location transition occurs the cycle efficiency decreases as mass ratio increases. Throughout much of the studied regime the mass ratio, which causes this transition to occur, provides the maximum efficiency plotted in Figures 4 through 8. This is verified by similiar plots in the literature [4, 6, 9, 19, 11, 16, 26].

If the steam/air mass ratio is still increased at lower turbine inlet temperatures the exiting steam transitions from superheated vapor to saturated steam. This is denoted as pinch point location #3 in Figure 3. With further increases in mass ratio the pinch point location makes one last transition to location #4. Throughout the temperature range investigated the steam always exits as a saturated or superheated vapor. At higher turbine inlet temperatures the pinch point location will change from #6 to #7 before moving to position #4.

At higher pressure ratios (16 and 20) and lower turbine inlet temperatures the maximum efficiency is not achieved at transition from pinch point location #5 to #6, but at the transition from #3 to #4. Efficiency increases in this regime when the pinch point is at the point of first boiling. In this area increases in turbine work with increasing mass ratio are greater than the penalties of heating the air and steam to the turbine inlet temperature. The penalty of heating the air was decreased by the higher compressor exit

temperatures at higher compressor pressure ratios. Figure 14 shows plots of efficiency versus steam/air mass ratio for increasing turbine inlet temperatures at constant pressure ratio ($Pr = 16$). It can be seen here that the maximum efficiency is reached at higher mass ratios (the transition of pinch point from location 3 to 4) at the lower temperatures. As the temperature increases, less and less gain is made in efficiency as mass ratio increases. The plots of efficiency versus mass ratio get very flat until the maximum efficiency is achieved at a much lower mass ratio (the transition from pinch point location #5 to #6). The result of this quick transition from a high mass ratio to a lower mass ratio is seen in Figures 12 and 13 where the steep drop in specific net work occurs.

The effect of limiting the steam/air mass ratio to preclude any condensation in the STIG cycle is also shown in Figures 4 through 13. The steam/air mass ratio is allowed to increase until the HRSG stack temperature is just above the water dewpoint temperature for the steam's partial pressure. In general, the dewpoint temperature increases as the steam/air mass ratio increases or as the steam partial pressure increases. The performance curves of the STIG cycle are affected when a high steam/air mass ratio yields the maximum efficiency. This occurs at the higher temperatures for the lower pressure ratio curves and at the high and low temperature regions of the higher pressure ratios, 16 and 20. The STIG performance curves with the dewpoint temperature constraint were calculated by the FORTRAN program called CONDEN found in Appendix B. This program checks the STIG performance data files calculated by the main program GT. If the stack temperature at the maximum efficiency is below the dewpoint temperature, the steam/air mass ratio is decreased until the a stack temperature is achieved which is above the dewpoint temperature. Program CONDEN uses a relation for steam saturation temperature as a function of saturation pressure given by Irvine and Liley [23].

Selected performance data calculated by this study's program are compared to

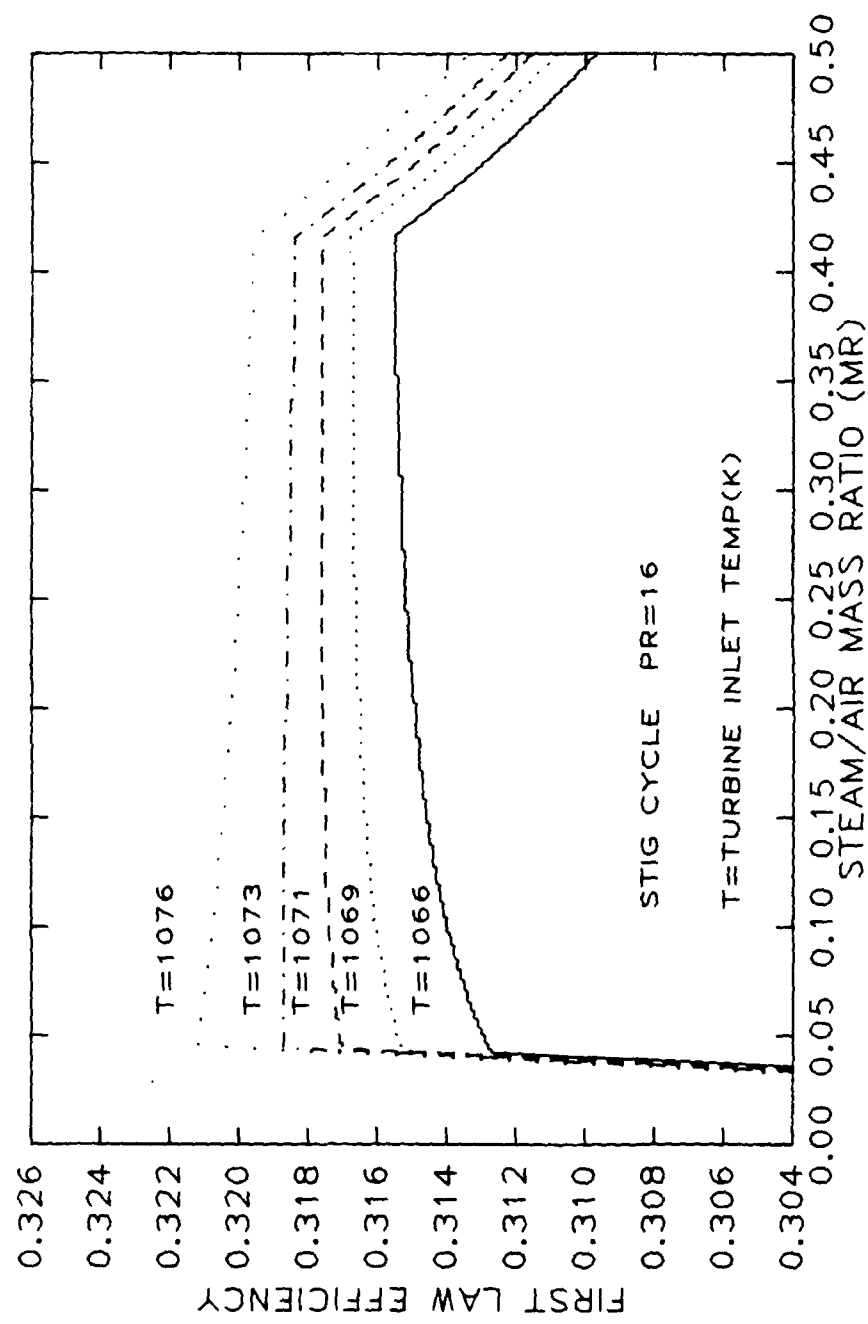


Figure 14. First Law efficiency versus steam/air mass ratio for STIG cycle at five turbine inlet temperatures ($\text{Pr} = 16$).

data at the same parameters presented in Bhutani et al. [9] and Boyle [11]. Parameters of temperature inlet temperature, steam/air mass ratio, compression pressure ratio, isentropic component efficiencies, ambient conditions, and HRSG pinch point temperature difference, were matched to those of the literature and the performance characteristics were computed. Table 4 shows comparison of data with that of Bhutani et al. [9]. Table 5 shows comparison of data with that of Boyle [11]. As can be seen there is close agreement between the study's efficiency data and that of the literature. There is more difference in the results of net specific work. These are due to different methods in pressure loss modeling and how the working fluid specific heat (c_p) is found.

Second Law Analysis

By conducting a Second Law analysis of the performance of the Brayton cycles further insight was sought into the performance characteristics of these cycles. Second Law efficiency expresses heat inputs as Carnot equivalent work requirements. This means that for a certain amount of heat, one could, at best, only utilize the Carnot equivalent of that heat input. This assesses smaller heat input penalties in calculating the Second Law efficiency. A Second Law analysis also accounts for the availability of inlet and exit streams. This can assess further penalty. In general, Second Law efficiencies are higher than First Law efficiencies. But the Second Law efficiencies do not mirror First Law efficiency in most of the cases studied here.

Figure 15 shows Second Law efficiency versus turbine inlet temperature plots for the GT simple Brayton cycle at the three highest pressure ratios (12, 16, 20). Figure 16 plots the relation of the same parameters for the GT cycle but this time the Second Law efficiency is calculated without the availability of the exit stream. As was mentioned in Chapter II, accounting for the availability of this stream may not have useful purpose as it is exhausted out the stack and is not really available. For the case of the GT cycle there is a noticeable difference in whether it is accounted for in the denominator or not. When

Table 4
Comparison of Selected Data with Bhutani et al. [9]^a

Pr	Mr	W_{net}^b	η^b	W_{net}^c	η^c	$\Delta\%W_{net}^d$	$\Delta\%\eta^d$
8	0.0	169.086	.3142	151.4	.303	11.7	3.7
8	0.1	221.329	.3654	202.0	.357	9.6	2.4
8	0.1	273.409	.4078	252.8	.410	8.2	0.5
8	0.3	325.387	.4437	303.8	.440	7.1	0.8
8	0.4	377.299	.4600	354.6	.462	6.4	0.4
12	0.0	179.480	.3542	158.8	.342	13.0	3.6
12	0.1	240.104	.4117	217.2	.402	10.5	2.4
12	0.2	300.525	.4577	275.6	.450	9.0	1.7
12	0.3	360.820	.4956	334.2	.490	8.0	1.1
12	0.4	421.030	.4883	392.4	.487	7.3	0.3
16	0.0	181.697	.3766	159.5	.363	13.9	3.7
16	0.1	247.776	.4389	222.9	.429	11.2	2.3
16	0.2	313.627	.4874	286.3	.480	9.5	1.5
16	0.3	379.334	.5186	349.8	.520	8.4	0.3
16	0.4	444.945	.5034	413.4	.504	7.6	0.1
20	0.0	180.650	.3908	157.4	.378	14.8	3.4
20	0.1	250.711	.4571	224.3	.448	11.8	2.0
20	0.2	320.528	.5076	291.3	.500	10.0	1.5
20	0.3	390.189	.5259	358.1	.533	9.0	1.3
20	0.4	459.746	.5130	425.6	.512	8.0	0.2

a - Turbine inlet temperature is 1700 K.

b - This study's data (W_{net} - BTU/1bm air)

c - Bhutani et al.'s data

d - Percent difference from Bhutani et al.

Table 5
Comparision of Selected Data with Boyle [11]^a

Mr	W_{net}^b	η^b	W_{net}^c	η^c	$\Delta\%W_{net}^d$	$\Delta\%\eta^d$
0.0	109.00	.3338	121	.333	9.9	0.2
0.157	187.654	.4472	180	.412	4.3	8.5
0.170	194.518	.4442	203	.430	4.2	3.3

^aPressure ratio is 16. Turbine inlet temperature is 2000°F.

^bThis study's data (W_{net} - BTU/lbm air).

^cBoyle's data.

^dPercent difference from Boyle.

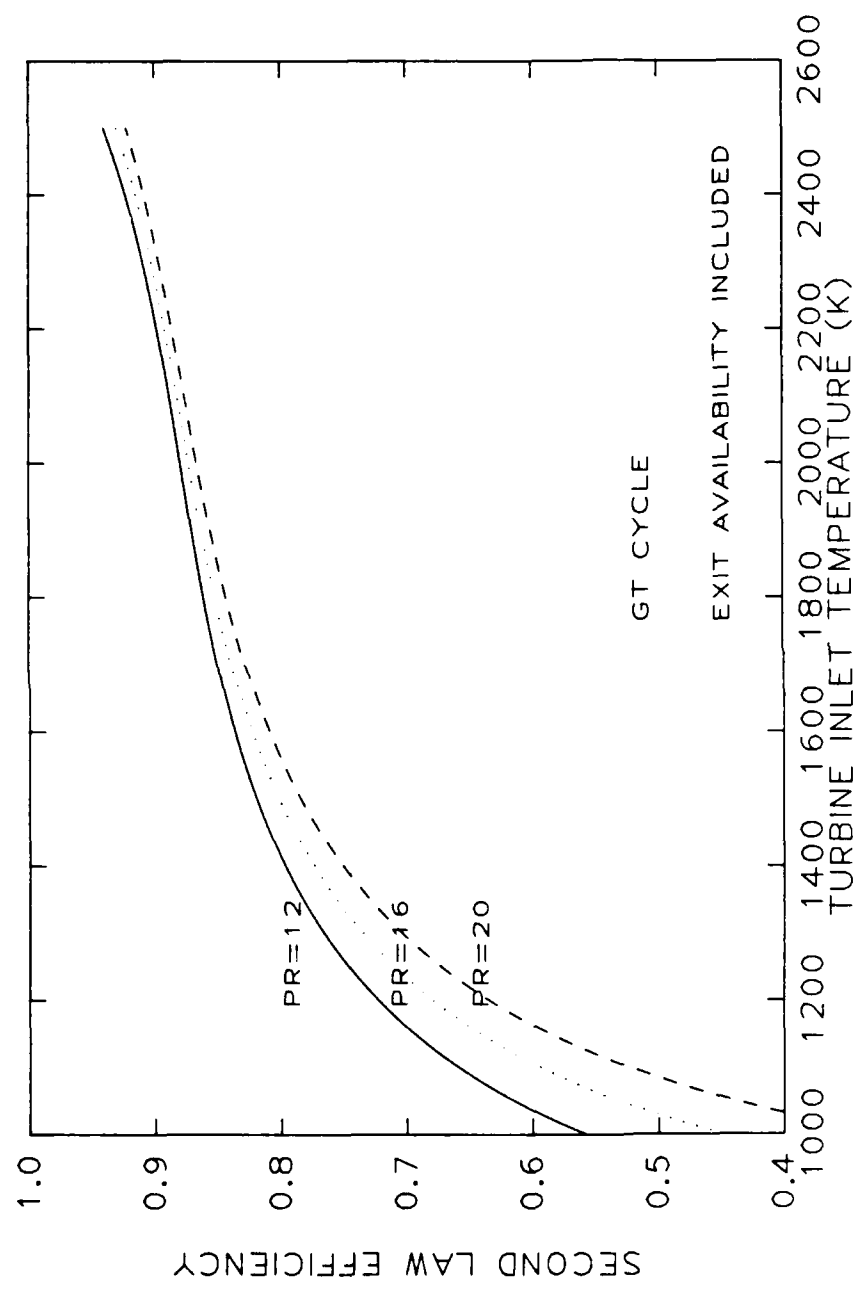


Figure 15. Second Law efficiency versus turbine inlet temperature for GT cycle at three compression pressure ratios.

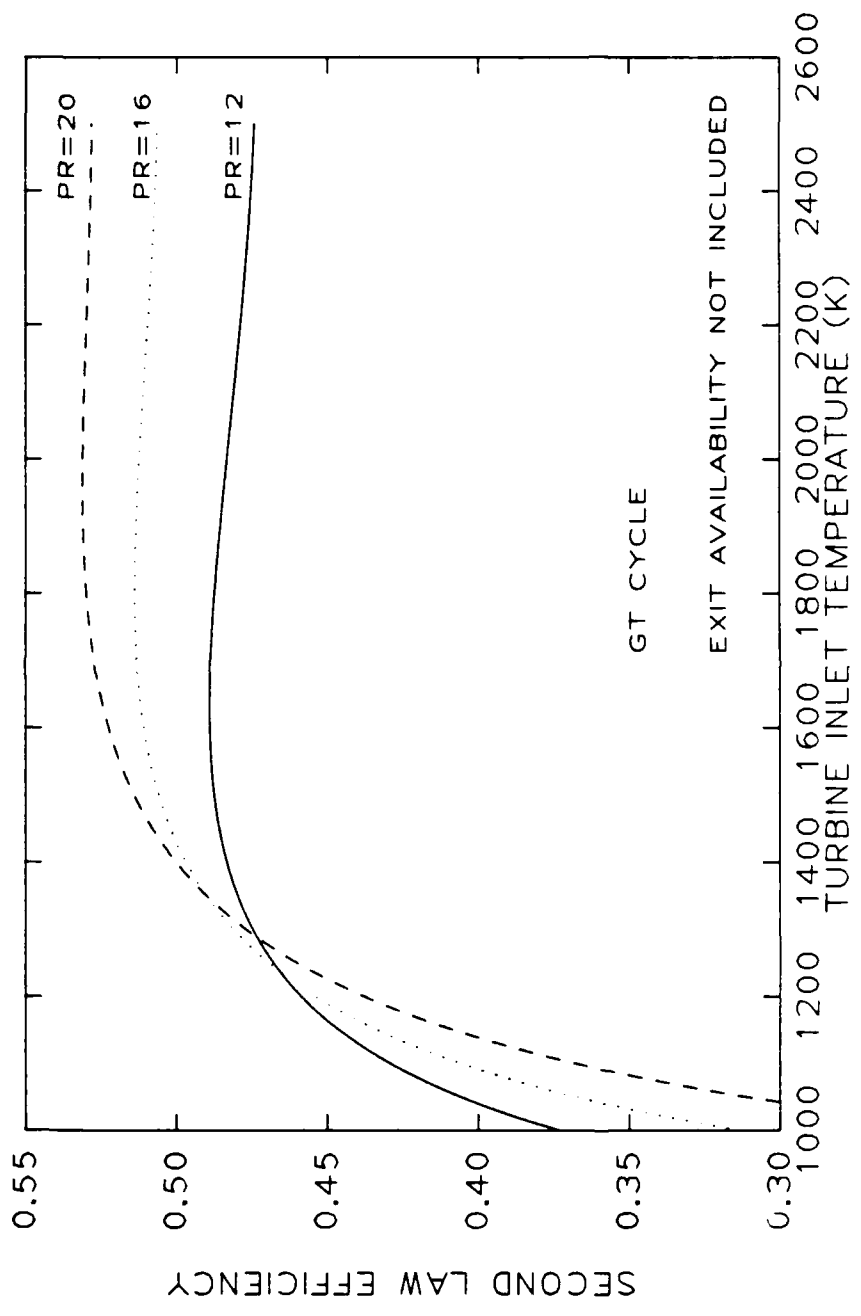


Figure 16. Second Law efficiency versus turbine inlet temperature for GT cycle at three compression ratios with exit availability not included.

the exhaust stream availability is deducted from the penalty side of the Second Law efficiency, the efficiency continues to increase with turbine inlet temperature. When the exhaust stream availability is not accounted for there is a maximum Second Law efficiency within the studied temperature range. This is due to the effect of converting the heat input to a Carnot equivalent work term which asymptotically approaches a limit as temperature increases. This provides the insight that when expressing heat penalties as Carnot equivalent energy values, the GT cycle has a temperature limit for maximum efficiency.

Figure 17 shows the same set of plots for the IGT cycle. Here the dashed lines are the Second Law efficiency plots calculated without accounting for the exhaust stream availability. There is not much difference between these plots, whether this availability is considered or not. This is due to the small quantity this availability represents. Because this system has a regenerator which takes advantage of the hot turbine exhaust to increase efficiency, the cycle's final exhaust temperature is much lower than the GT cycle at comparable conditions. The exhaust stream availability is then much lower for the IGT cycle. It is also seen that there is no maximum Second Law efficiency achieved for the IGT cycle over the studied temperature range. The effect of two heating stages does not provide the limiting effect of Carnot energy representation that was seen for one heating stage. For this cycle the Second Law efficiency continues to increase as temperature increases.

The results of the STIG cycle are again more complex than the other two systems. It is also a matter of the performance of the heat recovery steam generator. Three definitions of the Second Law efficiency for steam producing cycles were calculated for comparison. The first efficiency represents the STIG cycle as depicted in Figure 1. The second two efficiencies represent steam produced in a HRSG without injection into the gas turbine. These two cases represent steam produced for cogeneration purposes. On

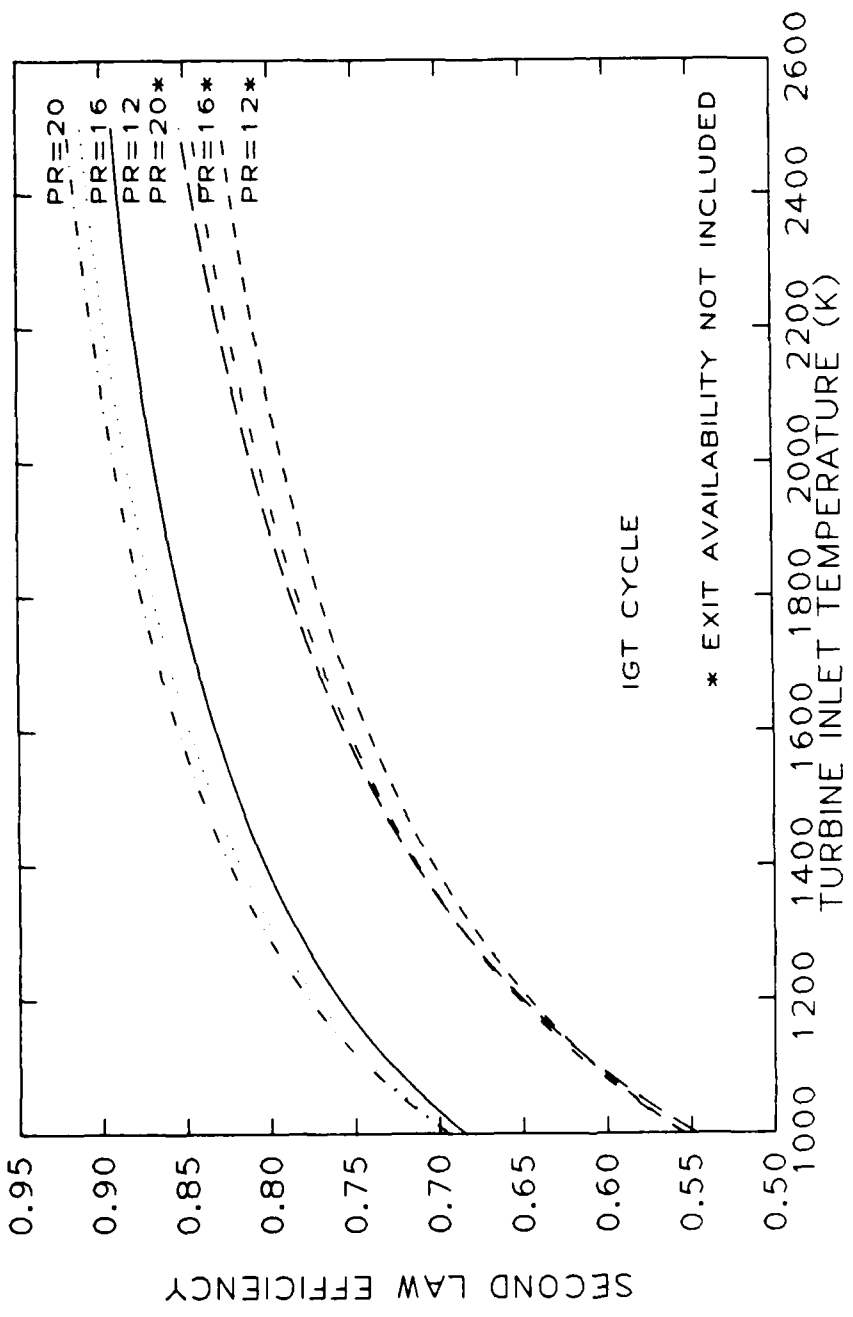


Figure 17. Second Law efficiency versus turbine inlet temperature for IGT cycle at three compression ratios.

the first of these two cases, the steam is heated to the turbine inlet temperature. In the second case the steam is not heated after it leaves the HRSG. To handle these last two cases, the study's program must calculate the turbine and HRSG processes with only air as the working fluid.

To more easily represent what the Second Law analysis predicts about the STIG cycle performance, efficiency plots are calculated versus steam/air mass ratio at a number of turbine inlet temperatures. This shows the effect of mass ratio and turbine inlet temperature on performance. The effect of pressure ratio is not as significant as these other two parameters but will be discussed. First Figure 18 shows the effect of mass ratio on First Law efficiency for a range of temperatures at a pressure ratio of 16. It has been explained in detail earlier how the maximum efficiency is achieved.

For the plots of Second Law efficiency for the STIG cycle it was determined to calculate the efficiency without accounting for the availability of the exit stream. Figure 19 shows the difference between the two calculations. The dashed line is the efficiency without the exit stream availability accounted for. At low mass ratios it is such a large term compared to the heat penalties that it shows that it is better not to use any steam.

Figure 20 shows the effect of mass ratio on the first definition of Second Law efficiency. This represents the Second Law efficiency for the STIG system depicted in Figure 1. It can be seen that a maximum efficiency is not achieved at lower temperatures. A maximum efficiency is later achieved as the turbine inlet temperature is increased. At lower turbine inlet temperatures the Second Law efficiency continues to increase when the pinch point is at locations 6, 3, or 4. The difference in the Second Law efficiency and the First Law efficiency in this regime is that for the Second Law analysis the heat penalty side is not increasing as fast as the net work side of the efficiency calculation. For the First Law calculation the opposite is true in this regime. The reason for the dropping off of the heat penalty for the Second Law efficiency can be

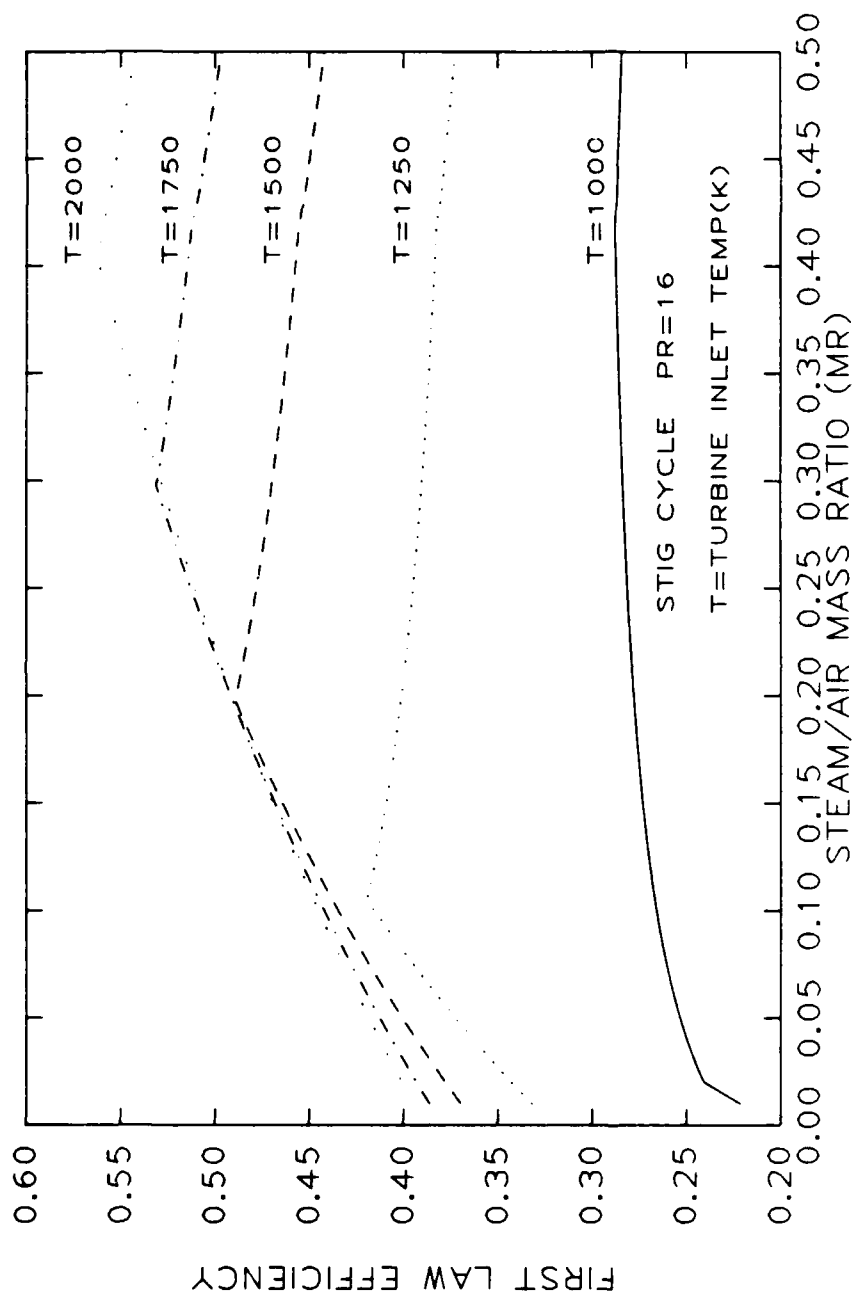


Figure 18. First Law efficiency versus steam/air mass ratio for STIG cycle at five turbine inlet temperatures (Pr = 16).

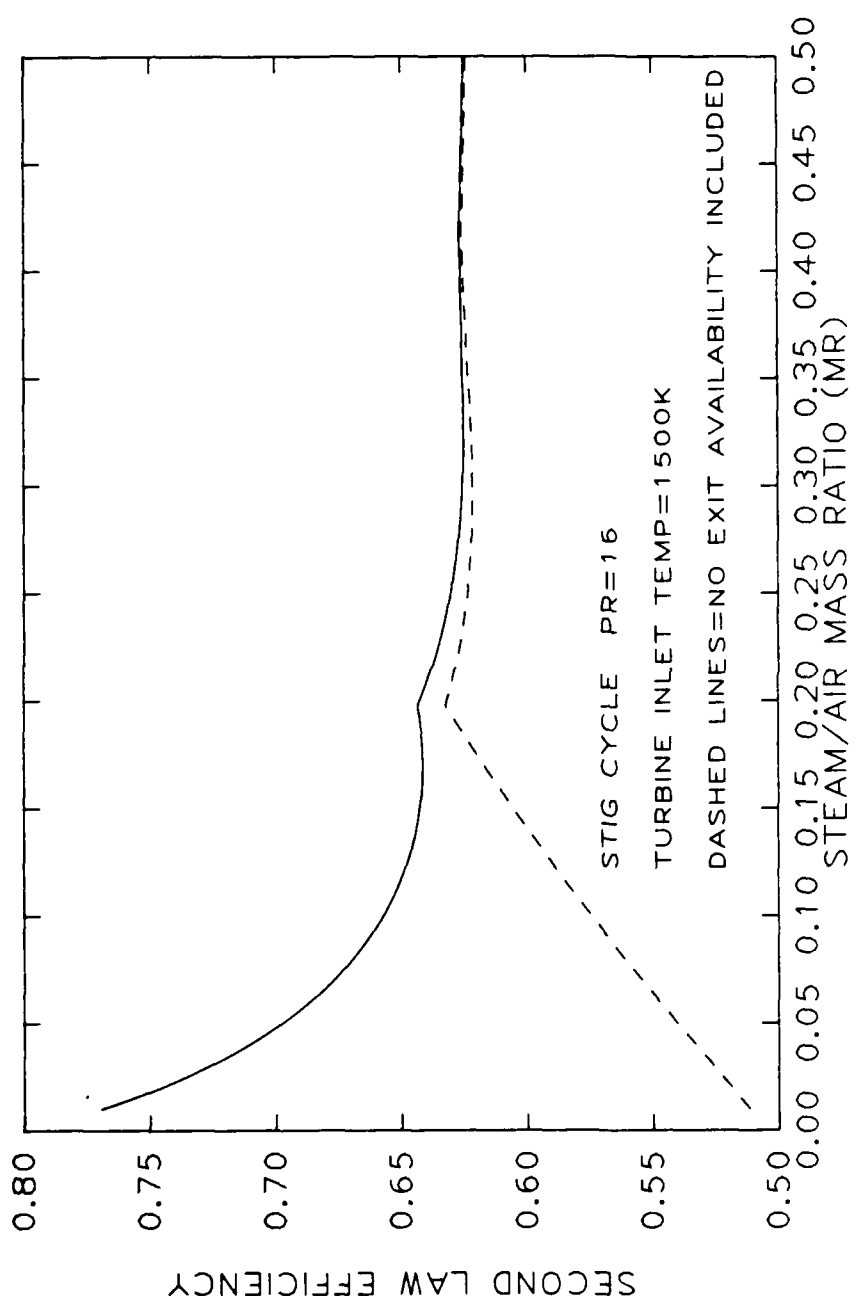


Figure 19. Second Law efficiency versus steam/air mass ratio for STIG cycle at turbine inlet temperature of 1500 K ($\text{Pr} = 16$).

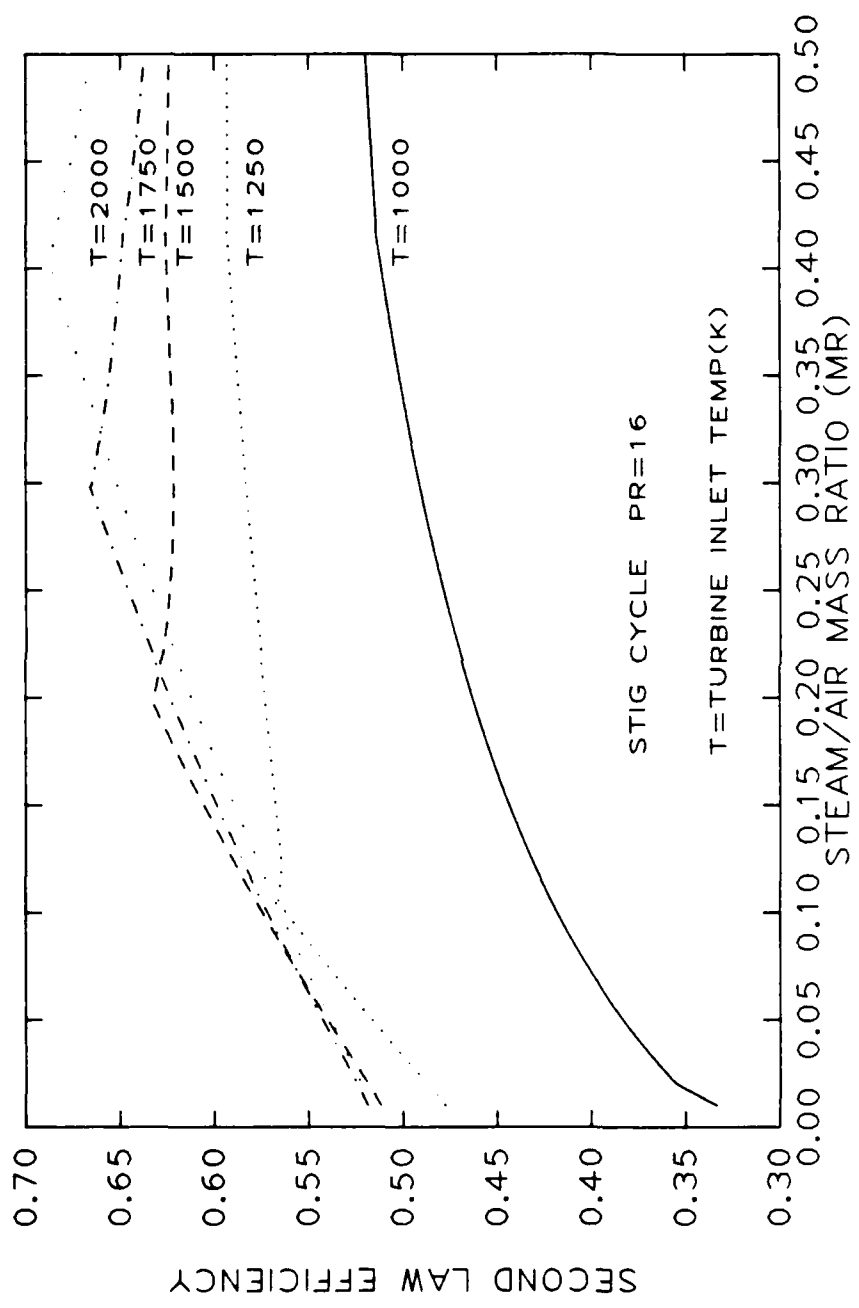


Figure 20. Second Law efficiency versus steam/air mass ratio for STIG cycle at five turbine inlet temperatures ($\text{Pr} = 16$).

found in its method of calculation. The effect of increasing turbine inlet temperature is to decrease the heat penalty for heating the steam to superheat, when the steam exits the HRSG as saturated vapor, with pinch point locations at #3 and #4. Increasing turbine inlet temperature also decreases the heat penalty to heat the steam to the desired turbine inlet temperature, when the steam exits the HRSG as superheated vapor, with pinch point location at #6. This results in a wider temperature range than the First Law analysis, where the efficiency increased for pinch point locations at points 6 and 3. There is a limit to the effect of decreasing these heat penalties by increasing turbine inlet temperature. With increasing turbine inlet temperature, the transition to pinch point locations 6 and 3 happens at higher mass ratios. With a higher mass ratio, the effect previously mentioned is reversed by the higher quantity of steam.

Increases in pressure ratio have a similar effect in increasing the temperature range where Second Law efficiency continues to increase as steam/air mass ratio. For increasing pressure ratio, the heat penalty to heat the exiting steam through superheat to the desired turbine inlet temperature decreases, plus the heating penalty of heating superheat steam decreases. In the case of pinch point #6, the exiting superheat steam increases in temperature as the pressure ratio increases. For pinch point locations #3 and #4, the saturation temperature at which the steam exits increases as the pressure ratio increases. These increases in exit temperature decrease the required steam heat inputs as mentioned above.

In total, the analysis of the Second Law efficiency shows that at lower turbine inlet temperatures the efficiency increases throughout the steam/air mass ratio range. At progressively higher temperatures, as pressure ratio increases, a maximum Second Law efficiency is finally achieved at the same steam/air mass ratio as the maximum First Law efficiency.

For comparison purposes, a Second Law analysis is done on a GT cycle which

produces steam for cogeneration purposes but has no steam injection. Figure 21 shows similar Second Law efficiency versus steam/air mass ratio plots at various turbine inlet temperatures for the system which heats the steam to the turbine inlet temperatures. This figure shows that the Second Law efficiency continues to increase throughout the mass ratio range for all the selected temperature plots. A maximum efficiency is reached at a higher turbine inlet temperature (not shown in Figure 21) than any of the other systems evaluated.

This system experiences the same decreases in some of the heat penalties at pinch point locations #6 and #3 as explained for the previous systems. In addition, this system accounts for the availability of the steam at the turbine inlet temperature on the net work side of the efficiency ratio. This has a positive effect on the Second Law efficiency as turbine inlet temperature increases. By accounting for the steam in this manner, the Second Law efficiency continues to increase with mass ratio over a wider temperature range than the STIG cycle and the system to be shown next.

Figure 22 shows the Second Law efficiency versus steam/air mass ratio plots for various temperatures at $Pr = 16$ for the system in which the steam is not heated after exiting the HRSG. For this system there is always a maximum Second Law efficiency achieved within the mass ratio and temperature ranges of this study. At lower turbine inlet temperatures, the maximum efficiency occurs at the transition from pinch point #3 to #4. At this point the availability of the steam exiting the HRSG decreases with the pinch point located at position #4. At higher turbine inlet temperatures the maximum efficiency occurs at lower mass ratios where the pinch point location transitions from #5 to #6. The system previous to this showed that higher efficiencies can be achieved by further heating the steam from the point left off at by this system.

As a note, in calculating the performance of a HRSG with only air in the hot stream, the exiting steam can leave the HRSG as liquid water, saturated steam, or

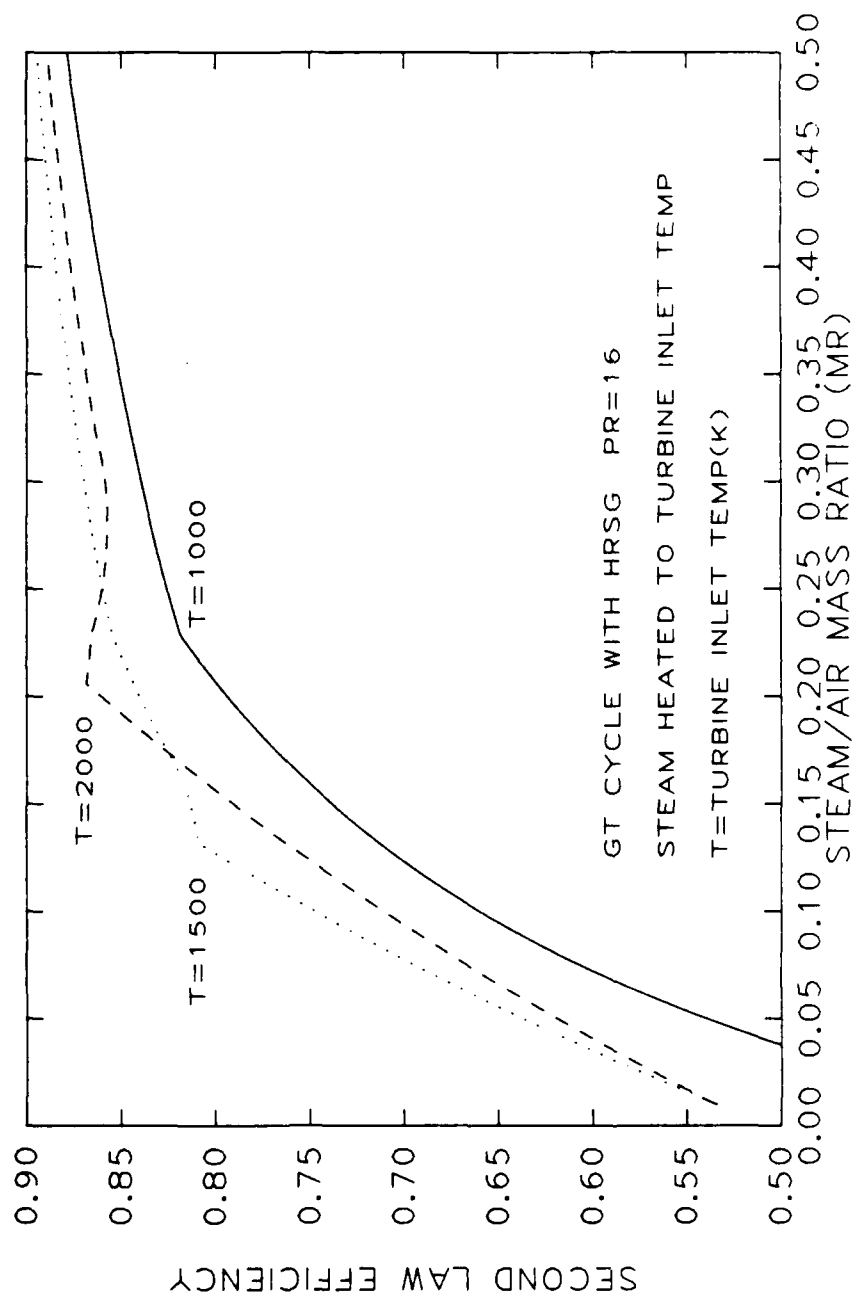


Figure 21. Second Law efficiency versus steam/air mass ratio for GT cycle with HRSG and steam heated to turbine inlet temperature at three turbine inlet temperatures ($Pr = 16$).

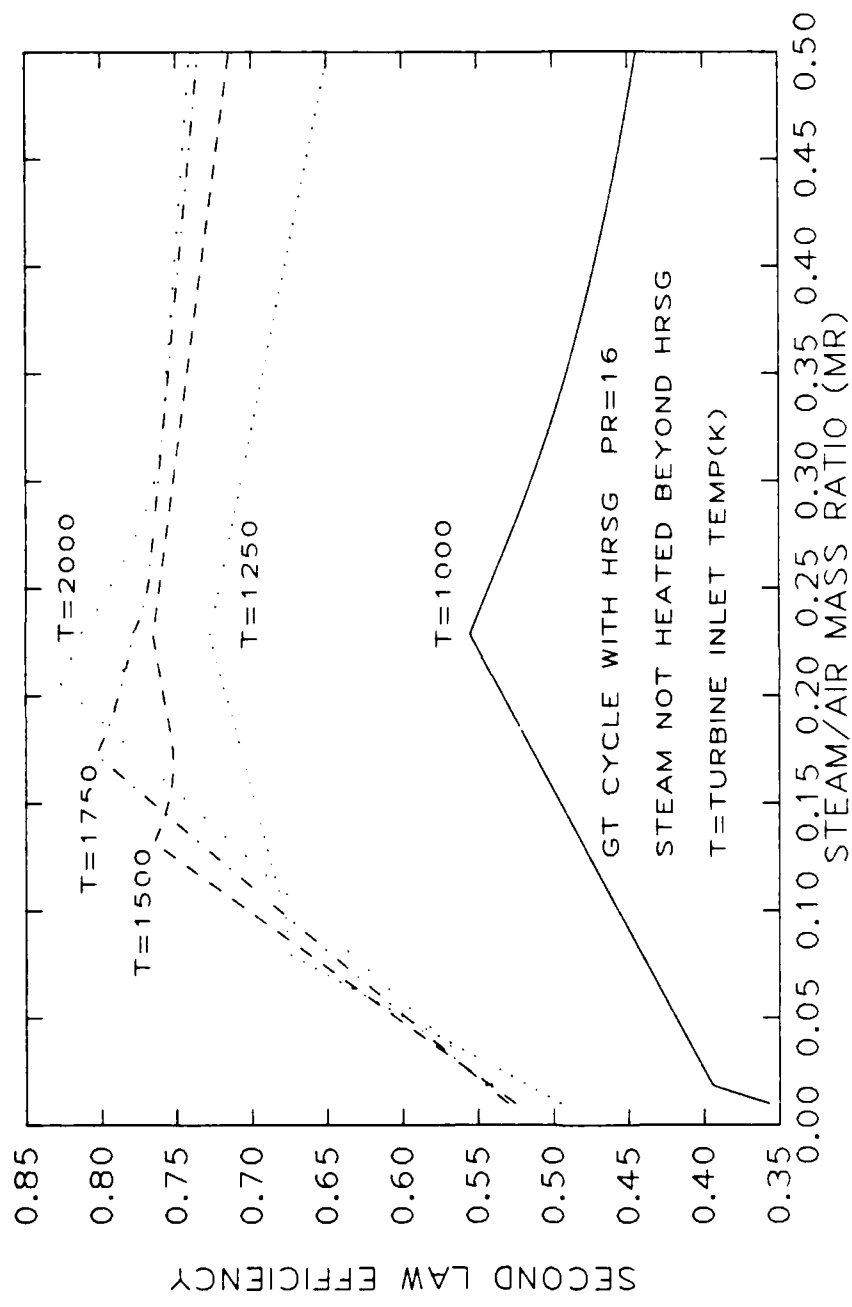


Figure 22. Second Law efficiency versus steam/air mass ratio for GT cycle with HRSG where steam is not heated beyond the HRSG at five turbine inlet temperatures ($\text{Pr} = 16$).

superheated steam. The computer subroutine modelling the HRSG had to handle all three situations.

CHAPTER IV

CONCLUSIONS AND RECOMMENDATIONS

From the First Law analysis it can be concluded that both of the Brayton derivative cycles, IGT and STIG, offer significant improvements over the simple GT Brayton cycle. In this study a major emphasis has been placed on examining cycle performance as a function of cycle maximum temperature. No attempts are made to define equipment concepts for the heat addition process. As turbine inlet temperature is increased, all three cycles demonstrate a diminishing increase of efficiency as temperature increases but the IGT and STIG are quite superior to the GT cycle. The IGT cycle is the clear winner in First Law efficiency with the STIG in second. The STIG cycle shows a most dramatic increase in net work output. It demonstrates an increasing relation with temperature. The STIG work output can be more easily controlled by the steam injection rate, which need not require fluctuations in rotating machinery speed. The STIG cycle represents a much simpler system. This equates to smaller capital costs. The STIG cycle results shown here and the other advantages mentioned in Chapter I demonstrate that the STIG cycle is the most promising candidate for higher temperature applications. Table 6 shows the improvement in the net work output and efficiency that the IGT and STIG cycles have over the GT cycle at selected maximum temperatures and a constant pressure ratio.

As pointed out in Chapter II the limits on turbine inlet temperature due, to the effectiveness of turbine cooling schemes and the turbine material's temperature limit, do not allow application of the whole range of the temperatures investigated here. Further technological advances will have to be made before the application of the higher

Table 6
Improvements in Performance by the IGT and STIG
Cycles Compared to the GT Cycle^a

Cycle	Mr ^b	T ^c	Increase in Net Work	Increase in Efficiency
IGT	0.0	1000	210.3%	63.1%
STIG	0.2	1000	271.8%	38.2%
	0.3	1000	407.4%	41.2%
IGT	0.0	1500	47.2%	48.3%
STIG	0.2	1500	83.9%	35.2%
	0.3	1500	125.7%	29.9%
IGT	0.0	2000	27.3%	65.5%
STIG	0.2	2000	63.1%	26.4%
	0.3	2000	94.6%	36.2%

^aPressure ratio of 16 used for all examples.

^bMr represents the steam/air mass ratio for the STIG cycle.

^cT represents the turbine inlet temperature (K).

temperatures studied here can be realized. Within current temperature limits the STIG cycle still exhibits a greater net work capacity although its greatest improvements over the IGT cycle in net work are achieved at higher temperatures. The STIG is not as efficient as the IGT in this range but offers several other improvements of simplicity, lower capital costs, and flexibility in the control of the steam injection to vary work output or turbine inlet temperature. These advantages are deemed more valuable overall than the IGT's improvement in efficiency. And with further advances in maximum turbine inlet temperature, the STIG cycle will offer greater improvements in net work.

The Second Law analysis provided some further insights in the performance of these cycles. When the efficiency is represented as the ratio of net work output to reversible work the GT cycle experienced maximum efficiencies at intermediate turbine inlet temperatures. The Second Law efficiencies calculated for the IGT cycle was similar to its First Law efficiencies. Its Second Law efficiency continued to increase with turbine inlet temperature. Like the First Law efficiency, the increase in the Second Law efficiency diminished in the higher temperature range. The maximum Second Law efficiency for the STIG cycle was achieved at a higher steam/air mass ratio than the First Law efficiency at the lower temperature ranges for each pressure ratio. At the higher pressure ratios no maximum efficiency was achieved within the steam/air mass ratio range at these lower temperatures. This demonstrates that for the STIG cycle, less irreversibilities are experienced at higher mass ratios than those which achieved the maximum First Law efficiencies at these lower temperatures. Location of the higher irreversibilities within the cycle was not included in the scope of this study.

Both First and Second Law efficiencies have been provided for each cycle and for a GT cycle with a HRSG. Comparisons are made of when maximum efficiencies are achieved as the parameters of turbine inlet temperature, steam/air mass ratio, and compressor pressure ratio are varied. But for solar power generation applications which

is more applicable, First or Second Law efficiency? The utility of the long used First Law efficiency is its value of measuring what you are getting for your money. The First Law efficiency tells the plant manager what amount of power is generated for the associated fuel costs. For a solar powered system there are no fuel costs. The Second Law efficiency makes more sense in telling the designer how close a given design is to a completely reversible system. And with a more detailed Second Law analysis of each system component the designer can locate where the major irreversibilities are.

Where the parameters of this study provide a maximum in First Law efficiency but not in Second Law efficiency, it would be more useful to solar power applications to seek the parameters which provide the maximum Second Law efficiency as shown in this study.

Each of the simplifying assumptions of this study represents recommended areas of further study in this area. There are two recommendations which should be among a more detailed study of these power cycles. First, a turbine cooling scheme should be used that varies the amount of compressor air bleed off with the turbine inlet temperature. Bhutani et al. [9] made a good case for the straight 5% bleed off of compressor air at a turbine inlet temperature of 1700 K. This study used this method. To provide a conservative performance analysis for higher temperatures, a cooling system which tasks more air for turbine cooling may be better.

A second recommendation for further study is to adopt a set pressure loss figure for each applicable process from among the literature. Table 7 lists the pressure losses calculated for the STIG and IGT cycles at various parameters. The method developed in this study for calculating the pressure loss in terms of average temperature and initial pressure is applicable for only selective ranges of these two parameters. This judgement is made by comparing the results in Table 7 to selected pressure loss figures from the literature listed in Table 8.

Table 7
Pressure Losses Calculated in This Study^a

Cycle	Component	Pr	%Δp ^b
STIG ^c	Heater	12	0.9
		16	0.5
	HRSG	12	0.7
		16	0.4
IGT	Intercooler	12	3.6
		16	2.8
	Regenerator	12	0.7
		16	0.4
	First Heating	12	1.2
		16	0.6
	Second Heating	12	13.9
		16	10.1

^aTurbine inlet temperature for each example is 1500 K.

^b%ΔP represents percent pressure drop (%ΔP = ΔP(100)/P_{initial}).

^cMr for STIG cycle examples is 0.250.

Table 8
Pressure Loss Schemes Listed in Literature

Reference	$\% \Delta P^a$	Comments
Fraize and Kinney [5]	2.0	Assessed at each heating process and HEX.
Bhutani et al. [9]	4.0	Assessed at combustor only.
Boyle [11] ^b	4.0	Assessed at burner
	4.0	Assesed to turbine exhaust flow in HRSG
	12.0	Assessed to steam flow in HRSG

^a $\% \Delta p$ represents percent pressure loss.

^bBoyle [11] selected large values to account for pipe losses also.

There are numerous further adaptations and more detailed modeling schemes which are applicable to more advanced study in this area. Studying the effect of changes in ambient conditions would not require any adaptation to the existing program. A further change to the STIG cycle without an addition of rotating machinery is intercooling to reduce compressor work. Where this study left off in its Second Law analysis, further studies can analyze individual component irreversibilities. There is certainly more to be done in this area. A goal of this study is to present its findings in a manner to give further work in this area several possible stepping off points.

APPENDIX A

FORTRAN PROGRAM GT

PROGRAM GT

C
C
C
C
C

Program finds 1st and 2d law cycle efficiency and net work versus turbine inlet temp for simple Brayton cycle (GT); Brayton cycle with intercooling , reheat, and regeneration (IGT); and Brayton cycle with steam injection (STIG).

CHARACTER*1 CYCLE,OUTPUT

INTEGER C,I,J,K,K1,L,LAW,II,JJ,R
REAL T6,T(9),P(9),Te(9),Pe(9),T5s,T5se,ETA,EPS(6),Wc(2),Wct,
+Wt(2),Wtt,Wp,Wce,Wte,Pro(5),PL,Mr,Cpmix,Cph,Cpsc,Qha(2),Qhs,
+Qh,Qhex,Qhat,Qhe,Qhse,Qhexe,Qhate,Cpmixe,Cphe,Cpsce,Ke,Tstack,
+Tstace,MAX(1334,5),MAX1(491,4),Wnet,Wnete,Be,We(3),Wt1,Bs1,Bs2,
+Be1,Wes(3),T5s1,Tstak1,Qhexa,T9a

C
DATA Pro(1)/4.0/,Ke/.4299/,SL41/4.2857142E-04/,SL42/4.3103448E-04/,
+SL81/4.1121495E-04/,SL82/3.960396E-04/,SL121/3.8709677E-04/,
+SL122/3.7719298E-04/,SL161/3.5251798E-04/,SL162/3.6885245E-04/,
+SL201/3.8E-04/,SL202/3.8636363E-04/

C
C Make choice of which cycle to be analyzed.
C

WRITE(*,10)

10 FORMAT('0','Enter code below for desired cycle analysis:'/' ',T5,
+'G-For simple Brayton cycle'/' ',T5,'I-For improved Brayton cycle'
+', with intercooling,regeneration,&reheat'/' ',T5,'S-For Brayton
+', 'cycle with steam injection')

READ(*,20) CYCLE

FORMAT(A1)

C
C Make choice of which compression pressure ratio to be analyzed.
C

WRITE(*,30)

30 FORMAT('0','Enter integer below for desired compressor pressure ',
+'ratio (Pr):'/' ',T5,'1-Pr=4'/' ',T5,'2-Pr=8'/' ',T5,'3-Pr=12'/
+' ',T5,'4-Pr=16'/' ',T5,'5-Pr=20')

READ(*,40) L

FORMAT(I1)

C
C Make choice of which type of output is desired.
C

WRITE(*,50)

50 FORMAT('0','Enter responce for desired output below:'/' ',T5,
+'T-Tabular data output'/' ',T5,'1-Plot of turbine inlet ',
+'temperature vs efficiency'/' ',T5,'2-Plot of steam/air mass ',
+'ratio vs efficiency'/' ',T5,'3-Plot of First Law efficiency ',
+'and corresponding mass ratio'/' ',T7,'versus turbine inlet ',
+'temperature')

READ(*,60) OUTPUT

FORMAT(A1)

C
C Make choice of which type of efficiency to be outputted.
C

```

IF(OUTPUT.EQ.'1'.OR.OUTPUT.EQ.'2') THEN
  WRITE(*,61)
  FORMAT('0','For efficiency plots specify which type of ',
+'analysis below: / ',T5,'1-First Law efficiency'/' ',T5,'2-',
+'Second Law efficiency')
  READ(*,62) LAW
  FORMAT(I1)
ENDIF
C
C Choose which turbine inlet temperature.
C
IF(OUTPUT.NE.'1'.AND.OUTPUT.NE.'3') THEN
  WRITE(*,63)
  FORMAT('0','Enter value of turbine inlet temperature(K)',,
+'(F6.1).')
  READ(*,65) T6
  FORMAT(F6.1)
ENDIF
C
C Choose which steam/air mass ratio (Mr), (for STIG cycle).
IF(CYCLE.EQ.'S') THEN
  IF(OUTPUT.EQ.'T'.OR.OUTPUT.EQ.'1') THEN
    WRITE(*,70)
    FORMAT('0','Enter value of steam/air mass ratio (Mr)',,
+'(F5.3).')
    READ(*,80) Mr
    FORMAT(F5.3)
  ENDIF
ENDIF
IF(CYCLE.NE.'S') Mr=0.0
C
IF(OUTPUT.NE.'T') GO TO 230
C
C For tabular data output for specified turbine inlet temperature
C and specified Mr.
C
CALL CYCLE2(T6,L,Mr,CYCLE,T,P,PL,ETA,EPS,Wc,Wt,Wp,Wnet,Cph,Cpsc,
+Cpmix,Qha,Qhs,Qhex,Tstack,T5s,K,Be,We,Wt1,Bia,Biw,Be1,Wes,K1,
+T5s1,Tstak1,Qhexa,T9a Bs1,Bs2)
C
DO 90 I=1,9
  Te(I)=1.8*T(I)
  Pe(I)=0.14504*P(I)
90 CONTINUE
Wct=Wc(1)+Wc(2)
Wtt=Wt(1)+Wt(2)
Qhat=Qha(1)+Qha(2)
Qh=Qha(1)+Qha(2)+Qhs
Wce=Ke*Wct
Wpe=Ke*Wp
Wte=Ke*Wtt
Wneta=Ke*Wnet
Qhate=Ke*Qhat
Qhse=Ke*Qhs

```

```

Qhe=Ke*Qh
Qhexe=Ke*Qhex
Cpsce=.2388*Cpsc
Cpmixe=.2388*Cpmix
Cphe=.2388*Cph
T5se=1.8*T5s
Tstace=1.8*Tstack
C
100 IF(CYCLE.NE.'I') THEN
    IF(CYCLE.EQ.'G') THEN
        WRITE(15,100) PL
        FORMAT('0','SIMPLE BRAYTON CYCLE WITH OVERALL Pr= ',F4.1)
        GO TO 120
    ENDIF
    WRITE(15,110) PL,Mr
110    FORMAT('0','BRAYTON CYCLE WITH STEAM INJECTION, Pr= ',F4.1,
+2X,'Mr= ',F5.3)
120    WRITE(15,130)
130    FORMAT('0','STAGE', 4X,'T(K)',6X,'T(R)',5X,'P(kPa)',3X,
+'P(psi)''0')
    I=1
    WRITE(15,140) I,T(1),Te(1),P(1),Pe(1)
140    FORMAT(' ',2X,I1,4X,F8.3,2X,F8.3,2X,F8.3,2X,F8.3)
    I=2
    WRITE(15,140) I,T(5),Te(5),P(5),Pe(5)
    IF(CYCLE.EQ.'S') THEN
        WRITE(15,150) T5s,T5se
150    FORMAT(' ','STEAM IS INJECTED INTO COMBUSTOR AT ',F6.1,
+'K(',F6.1,'R)')
        ENDIF
    I=3
    WRITE(15,140) I,T(6),Te(6),P(6),Pe(6)
    I=4
    WRITE(15,140) I,T(9),Te(9),P(9),Pe(9)
    IF(CYCLE.EQ.'S') THEN
        WRITE(15,160) Tstack,Tstace,K,K1,T5s1,Tstak1,Qhexa,T9a
160    FORMAT(' ','EXHAUST STACK TEMPERATURE IS ',F6.1,'K(',
+F6.1,'R)'' ','HRSG mode is ',I1/' ','Air HRSG Results are:',
+' Mode is ',I1/' ','22X,'Water leaves at temp ',F6.1/' ','22X,
+'Tstack is ',F6.1/' ','22X,'Qhex is ',F8.3/' ','22X,'Exhaust ',
+'enters HRSG at ',F6.1)
        ENDIF
        WRITE(15,170)
170    FORMAT('0'/'0','10X,(kJ/kg)',1X,'(BTU/lbm)')
        WRITE(15,180) Wct,Wce,Wp,Wpe,Wtt,Wte,Wnet,Wnete,Qhat,Qhate,
+Qhs,Qhse,Qh,Qhe,Qhexe,Be,We(1),We(2),We(3)
180    FORMAT(' ','Wc',8X,F7.3,2X,F7.3/' ','Wp',8X,F7.3,2X,F7.3/' ',
+'Wt',7X,F8.3,2X,F7.3/' ','Wnet',5X,F8.3,2X,F7.3/' ','QHair',
+4X,F8.3,2X,F7.3/' ','QHsteam',2X,F8.3,2X,F7.3/' ','QHtotal',
+2X,F8.3,1X,F8.3/' ','Qhrsg',4X,F8.3,2X,F7.3/' ','Bexhaust',
+1X,F8.3/' ','We(1)',4X,F8.3/' ','We(2)',4X,F8.3/' ','We(3)',4X,
+F8.3/' 0')
        IF(CYCLE.EQ.'S') THEN
            WRITE(15,185) Wt1,Bia,Biw,Be1,Wes(1),es(2),Wes(3),Bs1,Bs2

```

```

185      FORMAT(' ', 'Wtair', 5X, F7.3/' ', 'Bia', 7X, F7.3/' ', 'Biw', 7X,
+F7.3/' ', 'Be1', 7X, F7.3/' ', 'Wes(1)', 4X, F7.3/' ', 'Wes(2)', 4X,
+F7.3/' ', 'Wes(3)', 4X, F7.3/' ', 'Bs1', 6X, F8.3/' ', 'Bs2', 7X, F7.3/' ')
      ENDIF
      WRITE(15,190) Cpsc,Cpsce,Cpmix,Cpmixe,Cph,Cphe
190      FORMAT('O',10X,'(kJ/kg-K)',2X,'(BTU/lb-F)''','Cp-steam'
+/' ','COMBUSTOR',2X,F6.4,6X,F6.4/'O','Cp-mix'/' ','TURBINE',4X,
+F6.4,6X,F6.4/'O','Cp-mix'/' ','HRSG',7X,F6.4,6X,F6.4)
      WRITE(15,200) ETA
200      FORMAT('O','1st LAW EFFICIENCY IS ',F7.4)
      WRITE(15,205) EPS(1),EPS(2)
205      FORMAT('O','2D LAW EFFICIENCY (EPS1) IS ',F7.4/' ',18X,
+'(EPS2) IS ',F7.4)
      IF(CYCLE.EQ.'S') THEN
        DO 208 I=2,6
        WRITE(15,207) I,EPS(I)
207      FORMAT(' ',18X,'(EPS',I1,',') IS ',F7.4)
208      CONTINUE
      ENDIF
      GO TO 320
    ENDIF
C
210      WRITE(15,210) PL
      FORMAT('O','BRAYTON CYCLE WITH INTERCOOLING,REGENERATION,& REHEAT'
+/' ','OVERALL Pr= ',F4.1)
      WRITE(15,130)
      DO 220 I=1,9
      WRITE(15,140) I,T(I),Te(I),P(I),Pe(I)
220      CONTINUE
      WRITE(15,170)
      WRITE(15,180) Wct,Wce,Wp,Wpe,Wtt,Wte,Wnet,Wneta,Qhat,Qhate,Qhs,
+Qhse,Qh,Qhe,Qhexa,Bc,We(1),We(2),We(3)
      WRITE(15,190) Cpsc,Cpsce,Cpmix,Cpmixe,Cph,Cphe
      WRITE(15,200) ETA
      WRITE(15,205) EPS(1),EPS(2)
      GO TO 320
C
C      For data output of cycle efficiency and specific net work
C      versus turbine inlet temperature (1000-2500K).
C
230      IF(OUTPUT.EQ.'1') THEN
        T6=1000.0
        DO 250 II=1,1501
          CALL CYCLE2(T6,L,Mr,CYCLE,T,P,PL,ETA,EPS,Wc,Wt,Wp,Wnet,Cph,
+Cpsc,Cpmix,Qha,Qns,Qhexa,Tstack,T5s,K,Bc,We,Wt1,Bia,Biw,Be1,
+We1,K1,T5s1,Tstack1,Qhexa,T9a,Bs1,Bs2)
          IF(LAW.EQ.1) WRITE(16,235) T(6),ETA,Wnet,K
235        FORMAT(' ',F8.3,2X,F6.4,2X,F8.3,2X,I1)
          IF(LAW.EQ.2) WRITE(16,240) T(6),(EPS(I), I=1,6),K,K1
240        FORMAT(' ',F8.3,2X,6(F6.4,2X),I1,2X,I1)
          T6=T6+1.0
250        CONTINUE
      ENDIF
C

```

```

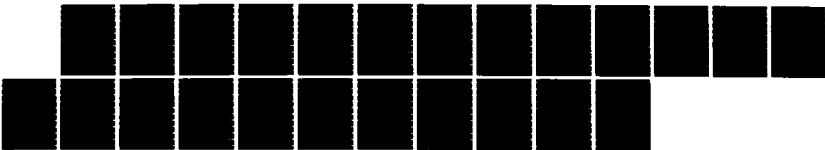
C For data output of cycle efficiency and specific net work
C versus steam/air mass ratio (0.01-0.50), (STIG cycle).
C
C IF(OUTPUT.EQ.'2') THEN
  Mr=0.01
  DO 270 JJ=1,491
    CALL CYCLE2(T6,L,Mr,CYCLE,T,P,PL,ETA,EPS,Wc,Wt,Wp,Wnet,Cph,
+Cpsc,Cpmix,Qha,Qhs,Qhex,Tstack,T5s,K,Be,We,Wt1,Bia,Biw,Bel,
+Wes,K1,T5s1,Tstak1,Qhexa,T9a Bs1,Bs2)
      IF(LAW.EQ.1) WRITE(17,255) Mr,ETA,Wnet,K
255      FORMAT(' ',F5.3,2X,F6.4,2X,F8.3,2X,I1)
      IF(LAW.EQ.2) WRITE(17,260) Mr,(EPS(I), I=1,6),K,K1
260      FORMAT(' ',F5.3,2X,6(F6.4,2X),I1,2X,I1)
      Mr=Mr+0.001
270      CONTINUE
      ENDIF
C
C For output of maximum First Law efficiency and corresponding mass
C ratio & specific net work versus turbine inlet temperature (STIG
C cycle).
C
C IF(OUTPUT.EQ.'3') THEN
  T6=1000.0
  IF(L.EQ.1) R=823
  IF(L.EQ.2) R=1050
  IF(L.EQ.3) R=1178
  IF(L.EQ.4) R=1266
  IF(L.EQ.5) R=1334
  DO 310 II=1,R
    IF(T6.LT.1073..AND.L.EQ.4) THEN
      Mr=0.010
      C=491
      GO TO 275
    ENDIF
    -IF(T6.LT.1160..AND.L.EQ.5) THEN
      IF(T6.LT.1066.) THEN
        Mr=0.414
        CALL CYCLE2(T6,L,Mr,CYCLE,T,P,PL,ETA,EPS,Wc,Wt,Wp,
+Wnet,Cph,Cpsc,Cpmix,Qha,Qhs,Qhex,Tstack,T5s,K,Be,We,Wt1,Bia,Biw,
+Bel,Wes,K1,T5s1,Tstak1,Qhexa,T9a Bs1,Bs2)
        MAX(II,1)=T6
        MAX(II,2)=Mr
        MAX(II,3)=ETA
        MAX(II,4)=Wnet
        MAX(II,5)=Tstack
        GO TO 295
      ENDIF
      Mr=0.010
      C=491
      GO TO 275
    ENDIF
    IF(L.EQ.1) THEN
      Mr=SL41*(T6-1000.)+0.13
      C=(SL42*(T6-1000.)+0.16-Mr)/.001+1.0
    ENDIF
  ENDIF

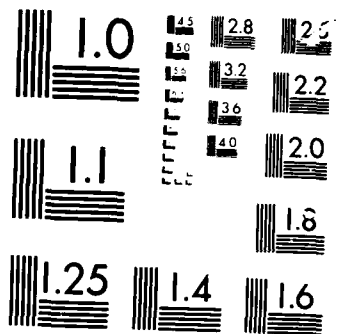
```

RD-A169 018 EVALUATION OF IMPROVEMENTS TO BRAYTON CYCLE PERFORMANCE 2/2
(U) ARMY MILITARY PERSONNEL CENTER ALEXANDRIA VA
M A SPASYK 29 MAY 86

UNCLASSIFIED

F/G 10/2 NL





MICROONE

```

ENDIF
IF(L.EQ.2) THEN
  Mr=SL81*(T6-1000.)+0.06
  C=(SL82*(T6-1000.))+0.10-Mr)/.001+1.0
ENDIF
IF(L.EQ.3) THEN
  Mr=SL121*(T6-1000.)+0.02
  C=(SL122*(T6-1000.))+0.05-Mr)/.001+1.0
ENDIF
IF(L.EQ.4) THEN
  Mr=SL161*(T6-1000.)+0.01
  C=(SL162*(T6-1000.))+0.05-Mr)/.001+1.0
ENDIF
IF(L.EQ.5) THEN
  Mr=SL201*(T6-1150.)+0.025
  C=(SL202*(T6-1150.))+0.075-Mr)/.001+1.0
ENDIF
275  DO 280 JJ=1,C
      CALL CYCLE2(T6,L,Mr,CYCLE,T,P,PL,ETA,EPS,Wc,Wt,Wp,Wnet,
+Cph,Cpsc,Cpmix,Qha,Qhs,Qhex,Tstack,T5s,K,Be,We,Wt1,Bia,Biw,Be1,
+Wes,K1,T5s1,Tstak1,Qhexa,T9a Bs1,Bs2)
      MAX1(JJ,1)=Mr
      MAX1(JJ,2)=ETA
      MAX1(JJ,3)=Wnet
      MAX1(JJ,4)=Tstack
      Mr=Mr+0.001
280  CONTINUE
      MAX(II,3)=MAX1(1,2)
      DO 290 I=2,C
        IF(MAX1(I,2).GT.MAX(II,3)) THEN
          MAX(II,1)=T6
          MAX(II,2)=MAX1(I,1)
          MAX(II,3)=MAX1(I,2)
          MAX(II,4)=MAX1(I,3)
          MAX(II,5)=MAX1(I,4)
        ENDIF
290  CONTINUE
295  WRITE(18,300) (MAX(II,J), J=1,5),L
300  FORMAT(' ',F6.1,2X,F5.3,2X,F6.4,2X,F8.3,2X,F9.5,2X,I1)
      T6=T6+1.0
310  CONTINUE
      ENDIF
C
320  STOP
      END
C
C-----SUBROUTINES-----
C

```

SUBROUTINE CYCLE2(T6,L,Mr,CYCLE,T,P,PL,ETA,EPS,Wc,Wt,Wp,Wnet,Cph,
+Cpsc,Cpmix,Qha,Qhs,Qhex,Tstack,T5s,K,Be,We,Wt1,Bia,Biw,Be1,Wes,
+K1,T5s1,Tstak1,Qhexa,T9a,Bs1,Bs2)

C
C This subroutine calculates the state points for the desired cycle

C using First Law energy balances. The work outputs/inputs and the
 C heat inputs are calculated. From these values, the First and
 C Second Law efficiencies are calculated.

```

C CHARACTER*1 CYCLE,CYCLE1
C INTEGER I,J,K,K1,L
C REAL T6,T(9),P(9),To5,Tn5,T5s,ETAc,ETAT,ETAp,ETA,Wc(2),Wt(2),Wp,
+Kplost,Plost,Pr,Pro(5),PL,Mr,Cpa,Cps,Cpmix,Cph,Cpsc,Qha(2),Qhs,
+Qh,Qhex,RHOs,Tstack,Wnet,Cpa1,Cpa2,Cpa3,Cpa4,Cpm1,Tsat1,EPS(6),
+Bia,Biw,Be,We(3),Ya,Ys,Te1,Te2,Cpm2,Cpm3,Cpm4,T9a,Wt1,Bs1,Bs2,Mr1,
+Wes(3),T5s1,Tstak1,Qsat
C
C DATA Pro(1)/4.0/,To5/0.0/,ETAc/0.87/,ETAt/0.89/,ETAp/0.70/,
+RHOs/997.0/,Kplost/12.128/,MWa/28.97/,MWs/18.015/,Ru/8.31434/,
+Te/0.0/
C
C T(1)=300.0
C P(1)=101.325
C T(6)=T6
C DO 10 I=2,5
C   Pro(I)=Pro(I-1)+4.0
10 CONTINUE
C
C P(9)=P(1)
C Pr=Pro(L)
C PL=Pro(L)
C
C IF(CYCLE.EQ.'I') Pr=SQRT(Pr)
C
C Determine required compressor specific work (Wc).
C
C CALL CWORK(T(1),P(1),Pr,ETAc,P(2),T(2),Wc(1))
C
C IF(CYCLE.NE.'I') THEN
C
C   T(5)=T(2)
C   P(5)=P(2)
C ENDIF
C
C If IGT cycle is called for, find results of intercooler
C and 2d compressor.
C
C IF(CYCLE.EQ.'I') THEN
C
C   Determine temp drop and pressure lost in intercooler.
C   T(3)=327.5
C   Plost=((T(1)+T(2))/(2.0*P(2)))*Kplost
C   P(3)=P(2)-Plost
C
C   Determine required work in 2d compressor.
C   CALL CWORK(T(3),P(3),Pr,ETAc,P(4),T(4),Wc(2))
C ENDIF
C
C Set an initial guess for regenerator outlet temp, T(5).
C

```

```

IF(CYCLE.EQ.'I') T(5)=T(4)+100.0
C
C If analyzing IGT cycle, the program returns here to
C iterate the effect of the regenerator.
C
C Determine pressure lost across the regenerator.
C
20 IF(CYCLE.EQ.'I') THEN
    Plost=((T(4)+T(5))/(2.0*P(4)))*Kplost
    P(5)=P(4)-Plost
ENDIF
C
C Determine pressure loss across combustor.
C
    Plost=((T(5)+T(6))/(2.0*P(5)))*Kplost
    P(6)=P(5)-Plost
C
    IF(CYCLE.EQ.'I') P(7)=P(6)/SQRT(P(6)/P(9))
C
    IF(CYCLE.NE.'I') P(7)=P(9)
C
    Determine turbine specific work (Wt).
C
    CALL TWORK(CYCLE,T(6),P(6),P(7),Mr,ETAt,T(7),Cpmix,Wt(1))
C
    IF(CYCLE.NE.'I') T(9)=T(7)
C
    If IGT cycle is called for, find results of reheat
    C and 2d turbine.
C
    IF(CYCLE.EQ.'I') THEN
        T(8)=T(6)
C
    Determine pressure loss in reheat.
        Plost=((T(7)+T(8))/(2.0*P(7)))*Kplost
        P(8)=P(7)-Plost
C
    Determine 2d turbine work.
        CALL TWORK(CYCLE,T(8),P(8),P(9),Mr,ETAt,T(9),Cpmix,Wt(2))
ENDIF
C
C Determine steam exit temperature from HRSG, required heat input
C to raise exiting steam to turbine inlet temperature, and pump
C work.
C
    IF(CYCLE.EQ.'S') THEN
        CALL HRSG1(T(1),T(6),T(9),Mr,L,Cph,Qhex,T5s,Cpsc,Qhs,Tstack,K,
+Tsat1,Qsat)
        Plost=((T(6)+T(1))/(2.0*P(5)))*Kplost
        Wp=Mr*(P(5)-P(1)+Plost)/(RHOs*ETAp)
ENDIF
C
C Determine heat input to air in combustor.
C
    CALL CPAIR1(T(5),T(6),Cpa)

```

```

C          Qha(1)=0.95*Cpa*(T(6)-T(5))
C          If IGT cycle is called for, add in heat input
C          for the reheat.
C
C          IF(CYCLE.EQ.'I') THEN
C              CALL CPAIR1(T(7),T(8),Cpa)
C              Qha(2)=0.95*Cpa*(T(8)-T(7))
C          ENDIF
C
C          Iteration to account for regenerator is done here.
C
C          IF(CYCLE.EQ.'I') THEN
C              Tn5=T(5)
C              IF(ABS(Tn5-To5).LT.0.1) GO TO 30
C              To5=Tn5
C              T(5)=T(9)-50.0
C              GO TO 20
C          ENDIF
C
C          Iteration to determine Texhaust from regenerator.
C
30         IF(CYCLE.EQ.'I') THEN
C             CALL CPAIR1(T(4),T(5),Cpa1)
C             Te2=T(4)+100.0
C             CALL CPAIR1(Te2,T(9),Cpa2)
C             Te2=T(9)-Cpa1*(T(5)-T(4))/Cpa2
C             IF(ABS(Te2-Te1).GE.0.1) THEN
C                 Te1=Te2
C                 GO TO 35
C             ENDIF
C         ENDIF
C
C         IF(CYCLE.NE.'I') THEN
C             Wc(2)=0.0
C             Wt(2)=0.0
C             Qha(2)=0.0
C             DO 40 J=2,4
C                 P(J)=0.0
C                 T(J)=0.0
C
40         CONTINUE
C             DO 50 I=7,8
C                 P(I)=0.0
C                 T(I)=0.0
C
50         CONTINUE
C         ENDIF
C
C         IF(CYCLE.NE.'S') THEN
C             Wp=0.0
C             Qhs=0.0
C             Qhex=0.0
C             Cph=0.0
C             Cpsc=0.0
C             Tstack=0.0

```

```

K=0
ENDIF
C
C Determine First Law cycle efficiency (ETA).
C
C Wnet=Wt(1)+Wt(2)-Wc(1)-Wc(2)-Wp
C ETA=Wnet/(Qha(1)+Qha(2)+Qhs)
C
C Determine Second Law efficiency for desired cycle.
C
IF(CYCLE.EQ.'G') THEN
  CALL CPAIR1(T(1),T(9),Cpa1)
  CALL CPAIR1(T(5),T(6),Cpa2)
  Be=0.95*Cpa1*(T(9)-T(1)*(1.0+LOG(T(9)/T(1))))
  We(1)=0.95*Cpa2*(T(6)-T(5)-T(1)*LOG(T(6)/T(5)))
  EPS(1)=Wnet/(We(1)-Be)
  EPS(2)=Wnet/We(1)
ENDIF
C
IF(CYCLE.EQ.'I') THEN
  CALL CPAIR1(T(1),T(9),Cpa1)
  CALL CPAIR1(T(5),T(6),Cpa2)
  CALL CPAIR1(T(7),T(8),Cpa3)
  CALL CPAIR1(T(3),T(8),Cpa4)
  Be=0.95*Cpa1*(Te2-T(1)*(1.0+LOG(Te2/T(1))))
  We(1)=0.95*Cpa2*(T(6)-T(5)-T(1)*LOG(T(6)/T(5)))
  We(2)=0.95*Cpa3*(T(8)-T(7)-T(1)*LOG(T(8)/T(7)))
  We(3)=0.95*Cpa4*(T(3)-T(2)-T(1)*LOG(T(3)/T(2)))
  EPS(1)=Wnet/(We(1)+We(2)+We(3)-Be)
  EPS(2)=Wnet/(We(1)+We(2)+We(3))
ENDIF
C
IF(CYCLE.EQ.'S') THEN
  CALL CPM(T(1),Tstack,Mr,Cpm1)
  CALL CPH20(T(1),T(6),Cps1)
  CALL CPH20(T(1),T5s,Cps2)
  CALL CPAIR1(T(5),T(6),Cpa)
  Ya=(0.95*MWs)/(0.95*MWs+Mr*MWa)
  Ys=(Mr*MWa)/(0.95*MWs+Mr*MWa)
  Bia=T(1)*Ru*LOG(1.0/Ya)/MWa
  Biw=Mr*T(1)*Ru*LOG(1.0/Ys)/MWs
  Be=(Mr+0.95)*Cpm1*(Tstack-T(1)*(1.0+LOG(Tstack/T(1))))
  CYCLE1='G'
  Mr1=0.0
  CALL TWORK(CYCLE1,T(6),P(6),P(9),Mr1,ETAt,T9a,Cpm2,Wt1)
  We(1)=0.95*Cpa*(T(6)-T(5)-T(1)*LOG(T(6)/T(5)))
  IF(K.EQ.3.OR.K.EQ.4) THEN
    We(2)=(1.0-T(1)/Tsat1)*Qsat
  ENDIF
  We(3)=Mr*Cpsc*(T(6)-T5s-T(1)*LOG(T(6)/T5s))
  CALL HRSG2(T(1),T(6),T9a,Mr,L,T5s1,Tstak1,Wes,K1,Qhexa,Bs1,Bs2)
  CALL CPAIR1(T(1),Tstak1,Cpa1)
  Be1=0.95*Cpa1*(Tstak1-T(1)*(1.0+LOG(Tstak1/T(1))))
  EPS(1)=Wnet/(We(1)+We(2)+We(3)+Bia+Biw-Be)

```

```

EPS(2)=Wnet/(We(1)+We(2)+We(3)+Bia+Biw)
EPS(3)=(Wt1-Wc(1)-Wp+Bs1)/(We(1)+Wes(1)+Wes(2)+Wes(3)-Be1)
EPS(4)=(Wt1-Wc(1)-Wp+Bs1)/(We(1)+Wes(1)+Wes(2)+Wes(3))
EPS(5)=(Wt1-Wc(1)-Wp+Bs2)/(We(1)-Be1)
EPS(6)=(Wt1-Wc(1)-Wp+Bs2)/We(1)
ENDIF
C
RETURN
END
C
C
C
SUBROUTINE CWORK(T1,P1,Pr,ETAc,P2,T2,Wc)
C
C This subroutine finds the required compressor work input.
C
CHARACTER*4 TYPE
REAL T1,P1,Kao,Ka,Pr,P2,Ts2,ETAc,T2o,T2n,T2,Cpa,Ra,Tisen,Tact
C
DATA Kao/1.397/,Ra/.28700/
C
TYPE='COMP'
Ka=Kao
P2=P1*Pr
Ts2=Tisen(TYPE,T1,Pr,Ka)
T2o=Tact(TYPE,T1,Ts2,ETAc)
C
10 CALL CPAIR1(T1,T2o,Cpa)
C
Ka=Cpa/(Cpa-Ra)
Ts2=Tisen(TYPE,T1,Pr,Ka)
T2n=Tact(TYPE,T1,Ts2,ETAc)
IF(ABS(T2n-T2o).GE.0.1) THEN
    T2o=T2n
    GO TO 10
ENDIF
T2=T2n
Wc=Cpa*(T2-T1)
C
RETURN
END
C
C
C
SUBROUTINE TWORK(CYCLE,T1,P1,P2,Mr,ETAt,T2,Cpmix,Wt)
C
C This subroutine finds the turbine work output.
C
CHARACTER*1 CYCLE
CHARACTER*4 TYPE
REAL T1,P1,P2,Mr,Kao,Ka,Kso,Ks,ETAt,Ra,Rs,T2,Cpmix,Wt,Ts2,Tisen,
+T2o,T2n,Tact,Cpa,Cpao,Cps,Cps0,Kmix,Pr
C
DATA Kao/1.397/,Kso/1.327/,Cpao/1.0035/,Cps0/1.8723/,Ra/.28700/,
```

```

+Rs/.46152/
C
TYPE='TURB'
T2o=0.0
Ka=Kao
Ks=Kso
Cpa=Cpao
Cps=Cps0
Pr=P1/P2
IF(CYCLE.NE.'S') Kmix=Ka
IF(CYCLE.EQ.'S') Kmix=(Mr*Cps+.95*Cpa)/((Mr*Cps/Ks)+(.95*Cpa/Ka))
Ts2=Tisen(TYPE,T1,Pr,Kmix)
T2n=Tact(TYPE,T1,Ts2,ETAt)
IF(ABS(T2n-T2o).GE.0.1) THEN
  T2o=T2n
  CALL CPAIR1(T1,T2o,Cpa)
  CALL CPH2O(T1,T2o,Cps)
  Ka=Cpa/(Cpa-Ra)
  Ks=Cps/(Cps-Rs)
  GO TO 10
ENDIF
T2=T2n
IF(CYCLE.NE.'S') Cps=0.0
Cpmix=(Mr*Cps+0.95*Cpa)/(0.95+Mr)
Wt=Cpmix*(.95+Mr)*(T1-T2)
RETURN
END

C
C
C
SUBROUTINE HRSG1(T1,T6,T9,Mr,L,Cph,Qhex,T5s,Cpsc,Qhs,Tstack,K,
+Tsat1,Qsat)

C
C
C
This subroutine calculates the performance of the HRSG for the
STIG cycle. It finds the exiting steam temperature, the exhaust
gas stack temperature, and the heat required to raise the exiting
steam to the turbine inlet temperature. For this subroutine the
hot exhaust gas is a mixture of steam and air.

C
C
C
INTEGER K,L
REAL Tsat(5),Hfg(5),Cpw(5),Q1,Q2,Q3,Qhex,Qhex1,Qhs,Tpp,Tpp1,Tpp2,
+T1,T6,T9,Tstack,Tstak1,Tstak2,Tstak3,T5s,T5s1,T5s2,Cpmix,Cpmix1,
+Cpmix2,Cps,Cpsc,Cph,Ch1,Ch2,Mr,Tsat1,Qsat

C
DATA Tsat(1)/417.3/,Tsat(2)/444.1/,Tsat(3)/461.7/,Tsat(4)/475.2/,
+Tsat(5)/486.2/,Hfg(1)/2132.4/,Hfg(2)/2046.2/,Hfg(3)/1984.0/,
+Hfg(4)/1932.7/,Hfg(5)/1887.8/,Tpp1/0.0/,T5s1/0.0/,Tstak1/0.0/,
+Cpw(1)/4.205/,Cpw(2)/4.215/,Cpw(3)/4.225/,Cpw(4)/4.230/,
+Cpw(5)/4.245/

C
Tsat1=Tsat(L)

C
Check if water can reach saturation.

```

```

Tpp=T1+26.0
Q1=Mr*Cpw(L)*(Tsat(L)-T1)
CALL CPM(Tpp,T9,Mr,Cpmix)
Cpmix1=Cpmix
Qhex1=(Mr+0.95)*Cpmix*(T9-Tpp)
CALL CPH20(Tsat(L),T6,Cps)
Cpsc=Cps
IF(Qhex1.LT.Q1) THEN
  Qhs=Q1-Qhex1+Mr*(Hfg(L)+Cpsc*(T6-Tsat(L)))
  Tstack=Tpp
C
C An approximation (due to CpW value) of water temp entering
C combustor.
C
C      T5s=Qhex1/(Mr*Cpw(L))+T1
C      IF((T9-T5s).LT.26.0) THEN
C
C Pinch point is at approach temperatures.
C
C      T5s=T9-26.0
C      Tstak2=T1+50.0
C      Qhex=Mr*Cpw(L)*(T5s-T1)
C      IF(Qhex.GT.Q1) THEN
C        T5s=Qhex1/(Mr*Cpw(L))+T1
C        GO TO 15
C      ENDIF
10   CALL CPM(Tstak2,T9,Mr,Cpmix)
C      Tstak2=T9-Qhex/((Mr+0.95)*Cpmix)
C      IF(ABS(Tstak2-Tstak1).GE.0.1) THEN
C        Tstak1=Tstak2
C        GO TO 10
C      ENDIF
C      Tstack=Tstak2
C      Cph=Cpmix
C      Qhs=Mr*(Cpsc*(T6-Tsat(L))+Hfg(L)+Cpw(L)*
+ (Tsat(L)-T5s))
C      K=2
C
C The pinch point location is at the approach temperature
C location and the water exits the HRSG as a liquid.
C
C      GO TO 90
15   ENDIF
C      Qhex=Qhex1
C      Cph=Cpmix1
C      K=1
C
C The pinch point location is at the water entry point and
C the water exits the HRSG as a liquid.
C
C      GO TO 90
ENDIF
C
C Check if steam can reach superheat. First assume pinch point is

```

```

C at entry to saturation region.
C
17 Tpp=Tsat(L)+26.0
Tstak1=0.0
20 Tstak2=Tpp-Q1/((Mr+0.95)*Cpmix)
IF(ABS(Tstak2-Tstak1).GE.0.1) THEN
  CALL CPM(Tstak2,Tpp,Mr,Cpmix)
  Tstak1=Tstak2
  GO TO 20
ENDIF
Tstak3=Tstak2
CALL CPM(Tstak2,T9,Mr,Cpmix2)
Ch1=Cpmix1*(Mr+0.95)
Ch2=Cpmix2*(Mr+0.95)
Qhex=Ch2*(T9-Tstak2)
Q2=Mr*(Hfg(L)+Cpw(L)*(Tsat(L)-T1))
IF(Qhex.LT.Q2) THEN
  Cph=Cpmix2
  T5s=Tsat(L)
  Qhs=Q2-Qhex+Mr*Cpsc*(T6-Tsat(L))
  Tstack=Tstak2
  Qsat=Q2-Qhex
  K=3
C
C The pinch point location is at the beginning of the sat-
C uration region and the steam exits the HRSG in saturation.
C
C Check to see if pinch point is at water entry point.
C
  IF((Tstack-T1).LT.26.0) THEN
    Tstack=T1+26.0
C
C Check to see if Mode 3 is more applicable.
C
25 Tpp2=Tsat(L)+30.0
CALL CPM(Tstack,Tpp2,Mr,Cpmix)
Tpp2=Q1/((Mr+0.95)*Cpmix)+Tstack
IF(ABS(Tpp2-Tpp1).GE.0.1) THEN
  Tpp1=Tpp2
  GO TO 25
ENDIF
IF((Tpp2-Tsat(L)).LT.26.0) THEN
  GO TO 17
ENDIF
C
  Qhex=Ch1*(T9-Tstack)
  Cph=Cpmix1
  Qhs=Q2-Qhex+Mr*Cpsc*(T6-Tsat(L))
  Qsat=Q2-Qhex
  K=4
C
C The pinch point location is at the water entry point and the
C steam exits the HRSG in saturation.
C

```

```

ENDIF
GO TO 90
ENDIF
C
C Last choice, steam reaches superheat with pinch point at water
C entry point, entry to saturation region, or at steam exit
C (approach temperatures).
C
C With assumption pinch point is at approach temperatures check to
C see if temperature difference at other possible pinch point loca-
C tions is more than minimum limit.
C
T5s=T9-26.0
CALL CPH20(Tsat(L),T5s,Cps)
Q3=Mr*(Cps*(T5s-Tsat(L))+Hfg(L))
C
C Initial guess on Tpp2 to determine Cpmix.
C
Tpp1=0.0
Tpp2=Tsat(L)+100.0
30 CALL CPM(Tpp2,T9,Mr,Cpmix)
Tpp2=T9-Q3/((.95+Mr)*Cpmix)
IF(ABS(Tpp2-Tpp1).GE.0.1) THEN
    Tpp1=Tpp2
    GO TO 30
ENDIF
Tpp=Tpp2
C
Qhex=Q3+Q1
Tstak1=0.0
40 Tstak2=T9-Qhex/(Cpmix*(Mr+0.95))
IF(ABS(Tstak2-Tstak1).GE.0.1) THEN
    CALL CPM(Tstak2,T9,Mr,Cpmix)
    Tstak1=Tstak2
    GO TO 40
ENDIF
Tstack=Tstak2
Cph=Cpmix
CALL CPH20(T5s,T6,Cpsc)
Qhs=Mr*Cpsc*(T6-T5s)
K=5
C
C The pinch point location is at the approach point temperature
C location and the steam exits the HRSG as a superheated vapor.
C
C Check to see if Mode 6 or 7 are more applicable.
C
IF((Tstack-T1).LT.26.0.AND.(Tstack-T1).LT.(Tpp-Tsat(L))) GO TO 70
IF((Tpp-Tsat(L)).LT.26.0) THEN
50   Tpp=Tsat(L)+26.0
       Tstack=Tstak3
       Cph=Cpmix2
       Qhex=Ch2*(T9-Tstack)
       T5s2=Tsat(L)+100.0

```

```

60    CALL CPH20(Tsat(L),T5s2,Cps)
      T5s2=(Qhex-Q2)/(Mr*Cps)+Tsat(L)
      IF(ABS(T5s2-T5s1).GE.0.1) THEN
          T5s1=T5s2
          GO TO 60
      ENDIF
      T5s=T5s2
      CALL CPH20(T5s,T6,Cpsc)
      Qhs=Mr*Cpsc*(T6-T5s)
C
      IF((Tstack-T1).LT.26.0) THEN
          GO TO 70
      ENDIF
C
      K=6
C     The pinch point location is at the beginning of the saturation region and the steam exits as a superheated vapor.
C
      GO TO 90
ENDIF
C
      GO TO 90
C
70  Tstack=T1+26.0
C
C     Check to see if Mode 6 is more applicable.
C
      Tpp1=0.0
      Tpp2=Tsat(L)+30.0
75  CALL CPM(Tstack,Tpp2,Mr,Cpmix)
      Tpp2=Q1/((Mr+0.95)*Cpmix)+Tstack
      IF(ABS(Tpp2-Tpp1).GE.0.1) THEN
          Tpp1=Tpp2
          GO TO 75
      ENDIF
      IF((Tpp2-Tsat(L)).LT.26.0) THEN
          GO TO 50
      ENDIF
C
      CALL CPM(Tstack,T9,Mr,Cph)
      Qhex=(Mr+0.95)*Cph*(T9-Tstack)
      T5s1=0.0
      T5s2=T9-50.0
80  CALL CPH20(Tsat(L),T5s2,Cps)
      T5s2=(Qhex-Q2)/(Mr*Cps)+Tsat(L)
      IF(ABS(T5s2-T5s1).GE.0.1) THEN
          T5s1=T5s2
          GO TO 80
      ENDIF
      T5s=T5s2
      CALL CPH20(T5s,T6,Cpsc)
      Qhs=Mr*Cpsc*(T6-T5s)
      K=7
C

```

```

C The pinch point location is at the water entry point and the
C steam exits the HRSG as a superheated vapor.
C
90 RETURN
END
C
C
C
SUBROUTINE HRSG2(T1,T6,T9,Mr,L,T5s,Tstack,Wes,K1,Qhex Bs1,Bs2)
C
C This subroutine calculates the performance of a HRSG combined
C with a GT cycle to produce process steam. In this case the hot
C exhaust gas is air only as there is no steam injection. This
C subroutine does the same calculations as the HRSG1 subroutine.
C
INTEGER K1,L
REAL T1,T6,T9,Tpp,Tpp1,Tpp2,Tstack,Tstak1,Tstak2,Tstak3,T5s,
+T5s1,T5s2,Wes(3),Cpa,Cpa1,Cpa2,Cps,Cps1,Ch1,Ch2,Q1,Q2,Q3,Qhex,
+Qhex1,Tsat(5),Hfg(5),Cpw(5),Sfg(5),Mr,Bs1,Bs2,X
C
DATA Tstak1/0.0/,Tpp1/0.0/,T5s1/0.0/,Tsat(1)/417.3/,
+Tsat(2)/444.1/,Tsat(3)/461.7/,Tsat(4)/475.2/,Tsat(5)/486.2/,
+Hfg(1)/2132.4/,Hfg(2)/2046.2/,Hfg(3)/1984.0/,Hfg(4)/1932.7/,
+Hfg(5)/1887.8/,Cpw(1)/4.205/,Cpw(2)/4.215/,Cpw(3)/4.225/,
+Cpw(4)/4.230/,Cpw(5)/4.245/,Sfg(1)/5.1100/,Sfg(2)/4.6067/,
+Sfg(3)/4.2964/,Sfg(4)/4.0670/,Sfg(5)/3.8825/
C
CALL CPH20(Tsat(L),T6,Cps)
Bs1=Mr*(Cpw(L)*(Tsat(L)-T1*(1.0+LOG(Tsat(L)/T1)))+
+Hfg(L)-T1*Sfg(L)+Cps*(T6-Tsat(L)-T1*LOG(T6/Tsat(L))))
Tpp=T1+26.0
Q1=Mr*Cpw(L)*(Tsat(L)-T1)
CALL CPAIR1(Tpp,T9,Cpa)
Cpa1=Cpa
Qhex1=0.95*Cpa1*(T9-Tpp)
CALL CPH20(Tsat(L),T6,Cps1)
IF(Qhex1.LT.Q1) THEN
  Tstack=Tpp
  T5s=Qhex1/(Mr*Cpw(L))+T1
  Wes(1)=Mr*Cpw(L)*(Tsat(L)-T5s-T1*LOG(Tsat(L)/T5s))
  Wes(2)=Mr*(1.0-T1/Tsat(L))*Hfg(L)
  Wes(3)=Mr*Cps1*(T6-Tsat(L)-T1*LOG(T6/Tsat(L)))
  Bs2=Mr*Cpw(L)*(T5s-T1*(1.0+LOG(T5s/T1)))
  K1=1
  IF((T9-T5s).LT.26.0) THEN
    T5s=T9-26.0
    Qhex=Mr*Cpw(L)*(T5s-T1)
    IF(Qhex.GT.Q1) THEN
      T5s=Qhex1/(Mr*Cpw(L))+T1
      GO TO 20
    ENDIF
  Tstack2=T1+50.0
  CALL CPAIR1(Tstack2,T9,Cpa)
  Tstack2=T9-Qhex/(0.95*Cpa)
10

```

```

IF(ABS(Tstak2-Tstak1).GE.0.1) THEN
  Tstak1=Tstak2
  GO TO 10
ENDIF
Tstack=Tstack2
Wes(1)=Mr*Cpw(L)*(Tsat(L)-T5s-T1*LOG(Tsat(L)/T5s))
Wes(2)=Mr*(1.0-T1/Tsat(L))*Hfg(L)
Wes(3)=Mr*Cps1*(T6-Tsat(L)-T1*LOG(T6/Tsat(L)))
Bs2=Mr*Cpw(L)*(T5s-T1*(1.0+LOG(T5s/T1)))
K1=2
GO TO 130
ENDIF
20  Qhex=Qhex1
  GO TO 130
ENDIF
30  Tpp=Tsat(L)+26.0
  Tstak1=0.0
40  Tstak2=Tpp-Q1/(0.95*Cpa)
  IF(ABS(Tstak2-Tstak1).GE.0.1) THEN
    CALL CPAIR1(Tstak2,Tpp,Cpa)
    Tstak1=Tstak2
    GO TO 40
  ENDIF
  Tstak3=Tstak2
  CALL CPAIR1(Tstak2,T9,Cpa2)
  Ch1=Cpa1*0.95
  Ch2=Cpa2*0.95
  Qhex=Ch2*(T9-Tstak2)
  Q2=Mr*(Hfg(L)+Cpw(L)*(Tsat(L)-T1))
  IF(Qhex.LT.Q2.OR.Qhex1.LT.Q2) THEN
    T5s=Tsat(L)
    Tstack=Tstack2
    Wes(2)=(1.0-T1/Tsat(L))*(Q2-Qhex)
    Wes(3)=Mr*Cps1*(T6-T5s-T1*LOG(T6/T5s))
    X=(Qhex-Q1)/(Mr*Hfg(L))
    Bs2=Mr*(Cpw(L)*(Tsat(L)-T1*(1.0+LOG(Tsat(L)/T1)))-
    +T1*X*Sfg(L))+Qhex-Q1
    K1=3
    IF((Tstack-T1).LT.26.0) THEN
      Tstack=T1+26.0
      Tpp2=Tsat(L)+30.0
      CALL CPAIR1(Tstack,Tpp2,Cpa)
      Tpp2=Q1/(0.95*Cpa)+Tstack
      IF(ABS(Tpp2-Tpp1).GE.0.1) THEN
        Tpp1=Tpp2
        GO TO 50
      ENDIF
      IF((Tpp2-Tsat(L)).LT.26.0) GO TO 30
      Qhex=Ch1*(T9-Tstack)
      Wes(2)=(1.0-T1/Tsat(L))*(Q2-Qhex)
      Wes(3)=Mr*Cps1*(T6-T5s-T1*LOG(T6/T5s))
      X=(Qhex-Q1)/(Mr*Hfg(L))
      Bs2=Mr*(Cpw(L)*(Tsat(L)-T1*(1.0+LOG(Tsat(L)/T1)))-
      +T1*X*Sfg(L))+Qhex-Q1
    ENDIF
  ENDIF

```

```

      K1=4
      ENDIF
      GO TO 130
    ENDIF
    T5s=T9-26.0
    CALL CPH20(Tsat(L),T5s,Cps)
    Q3=Mr*(Cps*(T5s-Tsat(L))+Hfg(L))
    Tpp1=0.0
    Tpp2=Tsat(L)+100.0
60   CALL CPAIR1(Tpp2,T9,Cpa)
    Tpp2=T9-Q3/(0.95*Cpa)
    IF(ABS(Tpp2-Tpp1).GE.0.1) THEN
      Tpp1=Tpp2
      GO TO 60
    ENDIF
    Tpp=Tpp2
    Qhex=Q3+Q1
    Tstak1=0.0
70   Tstak2=T9-Qhex/(Cpa*0.95)
    IF(ABS(Tstak2-Tstak1).GE.0.1) THEN
      CALL CPAIR1(Tstak2,T9,Cpa)
      Tstak1=Tstak2
      GO TO 70
    ENDIF
    Tstack=Tstak2
    CALL CPH20(T5s,T6,Cps)
    Wes(3)=Mr*Cps*(T6-T5s-T1*LOG(T6/T5s))
    CALL CPH20(T5s,Tsat(L),Cps)
    Bs2=Mr*(Cpw(L)*(Tsat(L)-T1*(1.0+LOG(Tsat(L)/T1)))+
+Hfg(L)-T1*Sfg(L)+Cps*(T5s-Tsat(L)-T1*LOG(T5s/Tsat(L))))
    K1=5
    IF((Tstack-T1).LT.26.0.AND.(Tstack-T1).LT.(Tpp-Tsat(L)))
+GO TO 100
    IF((Tpp-Tsat(L)).LT.26.0) THEN
80   Tpp=Tsat(L)+26.0
    Tstack=Tstak3
    Qhex=Ch2*(T9-Tstack)
    T5s2=Tsat(L)+100.0
90   CALL CPH20(Tsat(L),T5s2,Cps)
    T5s2=(Qhex-Q2)/(Mr*Cps)+Tsat(L)
    IF(ABS(T5s2-T5s1).GE.0.1) THEN
      T5s1=T5s2
      GO TO 90
    ENDIF
    T5s=T5s2
    CALL CPH20(T5s,T6,Cps)
    Wes(3)=Mr*Cps*(T6-T5s-T1*LOG(T6/T5s))
    CALL CPH20(Tsat(L),T5s,Cps)
    Bs2=Mr*(Cpw(L)*(Tsat(L)-T1*(1.0+LOG(Tsat(L)/T1)))+
+Hfg(L)-T1*Sfg(L)+Cps*(T5s-Tsat(L)-T1*LOG(T5s/Tsat(L))))
    K1=6
    IF((Tstack-T1).LT.26.0) GO TO 100
    GO TO 130
  ENDIF

```

```

      GO TO 130
100   Tstack=T1+26.0
      Tpp1=0.0
      Tpp2=Tsat(L)+30.0
110   CALL CPAIR1(Tstack,Tpp2,Cpa)
      Tpp2=Q1/(0.95*Cpa)+Tstack
      IF(ABS(Tpp2-Tpp1).GE.0.1) THEN
          Tpp1=Tpp2
          GO TO 110
      ENDIF
      IF((Tpp2-Tsat(L)).LT.26.0) GO TO 80
      Qhex=Ch1*(T9-Tstack)
      T5s1=0.0
      T5s2=T9-50.0
120   CALL CPH20(Tsat(L),T5s2,Cps)
      T5s2=(Qhex-Q2)/(Mr*Cps)+Tsat(L)
      IF(ABS(T5s2-T5s1).GE.0.1) THEN
          T5s1=T5s2
          GO TO 120
      ENDIF
      T5s=T5s2
      CALL CPH20(T5s,T6,Cps)
      Wes(3)=Mr*Cps*(T6-T5s-T1*LOG(T6/T5s))
      CALL CPH20(Tsat(L),T5s,Cps)
      Bs2=Mr*(Cpw(L)*(Tsat(L)-T1*(1.0+LOG(Tsat(L)/T1)))+
      +Hfg(L)-T1*Sfg(L)+Cps*(T5s-Tsat(L)-T1*LOG(T5s/Tsat(L))))+
      K1=7
130   RETURN
      END
C
C
C
      SUBROUTINE CPAIR1(T1,T2,Cpa)
C
C This subroutine finds the specific heat at constant pressure
C of air as a function of average temperature of the process.
C It is based on a relation by Irvine and Liley, STEAM AND GAS
C TABLES WITH COMPUTER EQUATIONS, Academic Press, Inc., Orlando,
C FL, 1984.
C
      INTEGER I
      REAL T1,T2,Tavg,A(5),Cpa
C
      DATA A(1)/0.103409E1/,A(2)/-0.2848870E-3/,A(3)/0.7816818E-6/,
      +A(4)/-0.4970786E-9/,A(5)/0.1077024E-12/
C
      Cpa=0.0
      Tavg=(T1+T2)/2.0
      DO 10 I=1,5
          Cpa=Cpa+A(I)*(Tavg**(I-1))
10     CONTINUE
      RETURN
      END
C

```

```

C
C
C      SUBROUTINE CPH20(T1,T2,Cps)
C
C      This subroutine finds the specific heat at constant pressure
C      of steam (ideal gas) as a function of average temperature of
C      the process. It is based on a relation by Reynolds, THERMO-
C      DYNAMIC PROPERTIES IN SI, Stanford University, Stanford, CA,
C      1979.
C
C      INTEGER I
C      REAL T1,T2,Tavg,G(6),Rs,Cvs,Cps
C
C      DATA G(1)/4.6E+04/,G(2)/1.011249E+03/,G(3)/8.3893E-01/,
C      +G(4)/-2.19989E-04/,G(5)/2.46619E-07/,G(6)/-9.7047E-11/,
C      +Rs/.46152/
C
C      Cvs=0.0
C      Tavg=(T1+T2)/2.0
C      DO 10 I=1,6
C          Cvs=Cvs+G(I)*(Tavg**(I-2))
10    CONTINUE
C      Cps=(Cvs/1000.)+Rs
C      RETURN
C      END
C
C
C
C      SUBROUTINE CPM(T1,T2,Mr,Cpmix)
C
C      This subroutine finds the specific heat at constant pressure
C      of the steam/air mixture of the STIG cycle using the two
C      subroutines listed above.
C
C      REAL T1,T2,Mr,Cpa,Cps,Cpmix
C
C      CALL CPAIR1(T1,T2,Cpa)
C      CALL CPH20(T1,T2,Cps)
C      Cpmix=(Mr*Cps+0.95*Cpa)/(0.95+Mr)
C
C      RETURN
C      END
C
C      -----
C      REAL FUNCTIONS
C
C      REAL FUNCTION Tisen(TYPE,T1,Pr,Ka)
C
C      This function finds the end state temperature for an isentropic
C      compression or expansion process.
C
C      CHARACTER*4 TYPE
C      REAL T1,Pr,Ka
C
C      IF(TYPE.EQ.'COMP') THEN

```

```
Tisen=T1*(Pr**((Ka-1.0)/Ka))
ELSE
  Tisen=T1/(Pr**((Ka-1.0)/Ka))
ENDIF
RETURN
END

C
C
C
REAL FUNCTION Tact(TYPE,T1,Ts2,ETA)
C
C This function finds the actual end state temperature for a
C compression or expansion process using the isentropic
C process end temperature and the component's isentropic
C efficiency.
C
CHARACTER*4 TYPE
REAL T1,Ts2,ETA
C
IF(TYPE.EQ.'COMP') THEN
  Tact=T1+(Ts2-T1)/ETA
ELSE
  Tact=T1-ETA*(T1-Ts2)
ENDIF
RETURN
END
```

APPENDIX B

FORTRAN PROGRAM CONDEN

PROGRAM CONDEN

```

C
C This program modifies data files to insure no steam condenses
C inside the components of the STIG cycle. It checks the output
C files of max First Law efficiency and corresponding steam/air
C mass ratio versus turbine inlet temperature. If the stack temp
C at max efficiency is below the dewpoint temp then the mass ratio
C is decreased until the stack temp is above dewpoint. This program
C must be linked with the subroutines of PROGRAM GT.
C

CHARACTER*1 CYCLE
CHARACTER*13 FNAME
INTEGER I,J,K,K1,L,NN,SIZE
REAL MAX(1334,5),T(9),Tstack,Tstack1,T5s,T5s1,Tdp,T9a,P(9),PL,
+ETA,EPS(6),Wc(2),Wt(2),Wp,Wnet,Cph,Cpsc,Cpmix,Qha(2),Qhs,Qhex,
+Qhexa,Be,We(3),Wt1,Bia,Biw,Be1,Wes(3),Bs1,Bs2,Mr
C
CYCLE='S'
C
WRITE(*,10)
10 FORMAT('0','What is the file to be reviewed (FOR _____.DAT;_)?')
READ(*,20) FNAME
20 FORMAT(A13)
C
OPEN(UNIT=10,NAME=FNAME,STATUS='UNKNOWN')
C
NN=1
30 READ (10,*,END=40) (MAX(NN,J), J=1,5),L
NN=NN+1
GO TO 30
40 CONTINUE
C
CLOSE(UNIT=10,STATUS='SAVE')
C
SIZE=NN-1
DO 80 I=1,SIZE
  T6=MAX(I,1)
  Mr=MAX(I,2)
  Tstack=MAX(I,5)
  CALL DEWPT(Mr,Tdp)
C
IF(Tstack.LT.Tdp) THEN
C
  DO 50 J=1,500
    Mr=Mr-0.001
    CALL DEWPT(Mr,Tdp)
    CALL CYCLE2(T6,L,Mr,CYCLE,T,P,PL,ETA,EPS,Wc,Wt,Wp,
+Wnet,Cph,Cpsc,Cpmix,Qha,Qhs,Qhex,Tstack,T5s,K,Be,We,Wt1,Bia,
+Biw,Be1,Wes,K1,T5s1,Tstack1,Qhexa,T9a,Bs1,Bs2)
    IF(Tstack.GT.Tdp) GO TO 60
  CONTINUE
C
  MAX(I,2)=Mr
  MAX(I,3)=ETA
50
60

```

```
      MAX(I,4)=Wnet
      MAX(I,5)=Tstack
      ENDIF
C
      WRITE(19,70) (MAX(I,J), J=1,5)
70      FORMAT(' ',F6.1,2X,F7.3,2X,F6.4,2X,F8.3,2X,F9.5)
80      CONTINUE
C
      STOP
      END
C
C-----SUBROUTINE-----
C
C      SUBROUTINE DEWPT(Mr,Tdp)
C
C      This subroutine determines steam saturation temperature as a
C      function of saturation pressure. It is based on a relation
C      by Irvine and Liley, STEAM AND GAS TABLES WITH COMPUTER
C      EQUATIONS, Academic Press, Inc., Orlando, FL, 1984.
C
C      REAL Mr,Psat,Ys,Tdp
C
C      DATA MWa/28.97/,MWs/18.1015/,A/42.6776/,B/-3892.70/,C/-9.48654/
C
C      Ys=(Mr*MWa)/(0.95*MWs+Mr*MWa)
C      Psat=Ys*101.325
C      Tdp=A+B/( ALOG(Psat/1000.0)+C)
C
C      RETURN
      END
```

REFERENCES

1. Boyce, M.P., Gas Turbine Engineering Handbook, Gulf Publishing Co., Houston, TX, 1982.
2. Bathie, W.W., Fundamentals of Gas Turbines, John Wiley and Sons, New York, 1984.
3. Wilson, D.G., The Design of High-Efficiency Turbomachinery and Gas Turbines, the MIT Press, Cambridge, MA, 1984.
4. Stochl, R.J., "Assessment of Steam-Injected Gas Turbine Systems and Their Potential Application," NASA-TM-82735, February 1982.
5. Fraize, W. and Kinney, C., "Coal-Fired Gas Turbine Power Cycles with Steam Injection," Society of Automotive Engineers, Inc., 1978, pp. 300-308.
6. Day, W.H. and Kidd, P.H., "Maximum Steam Injection in Gas Turbines," ASME Paper 72-JPC-GT-1, 1972.
7. Borat, O., "Efficiency Improvement and Superiority of Steam Injection in Gas Turbines," Energy Conversion Management, Vol. 22, 1982, pp. 13-18.
8. Gasparovic, I.N. and Hellemans, J.G., "Gas Turbines with Heat Exchangers and Water Injection in the Compressed Air," Combustion, December 1972, pp. 32-40.
9. Bhutani, J., Fraizer, W., and Lenard, M., "Effects of Steam Injection on the Performance of Open Cycle Gas Turbine Power Cycles," Report No. MTR-7274, The MITRE Corporation, July 1976.
10. Boyce, M.P., Vyas, Y.K., and Trevillion, W.L., "The External Combustion Steam Injected Gas Turbine for Cogeneration," Society of Automotive Engineers, Inc., 1978, pp. 860-865.
11. Boyle, R.J., "Effect of Steam Addition on Cycle Performance of Simple and Recuperated Gas Turbines," NASA -TP-1440, 1979.
12. Gigumarthi, R. and Chang, C., "Cheng-Cycle Implementation on a Small Gas Turbine Engine," Journal of Engineering for Gas Turbines and Power, Vol. 106, July 1984, pp. 699-702.
13. Larson, E.D. and Williams, R.H., "Steam-Injected Gas-Turbines," ASME Paper for presentation at Gas Turbine Conference, Dusseldorf, FRG, June 1986.
14. Koloseus, C. and Shepherd, S., "The Cheng-Cycle Offers Flexible Cogeneration Options," Modern Power Systems, March 1985, pp. 39-43.

15. Featherston, C.H., "Retrofit Steam Injection for Increased Output," Gas Turbine Int., Vol. 16, No. 3, May-June 1975, pp. 34-35.
16. Brown, D.H. and Cohn, A., "An Evaluation of Steam Injected Combustion Turbine Systems," Journal of Engineering for Power, Vol. 13, January 1981, pp. 13-19.
17. Messerlie, R.L., and Tischler, A.O., "Test Results of a Steam Injected Gas Turbine to Increase Power and Thermal Efficiency," 18th IECEC, Vol. 2, 1983, pp. 615-625.
18. Boehm, R.F., Design Analysis of Thermal Systems, to be published by John Wiley and Sons, New York.
19. Moran, M.J., Availability Analysis: A Guide to Efficient Energy Use, Prentice-Hall, Englewood Cliffs, New Jersey, 1982.
20. Kotas, T.J., The Exergy Method of Thermal Plant Analysis, Butterworths, London, 1985.
21. Van Wylen, G.J. and Sonntag, R.E., Fundamentals of Classical Thermodynamics, 3rd Edition, SI Version, John Wiley and Sons, New York, 1985.
22. Reynolds, W.C., Thermodynamic Properties in SI, Stanford University, Stanford, CA, 1979.
23. Irvine, T.F. and Liley, P.E., Steam and Gas Tables with Computer Equations, Academic Press Inc., New York, 1984.
24. Incropera, F.P. and DeWitt, D.P., Fundamentals of Heat Transfer, John Wiley and Sons, New York, 1981.
25. Kreith, F. and Black, W.Z., Basic Heat Transfer, Harper & Row, New York, 1980.
26. Rice, I.G., "The Combined Reheat Gas Turbine/Steam Turbine Cycle," Journal of Engineering for Power, Vol. 102, January 1980, pp. 42-49.
27. Keenan, J.H., Keyes, F.G., Hill, P.G., and Moore, J.G., Steam Tables, John Wiley & Sons, New York, 1978.
28. El-Masri, M.A., "On Thermodynamics of Gas Turbine Cycles: Part 1 - Second Law Analysis of Combined Cycles," Journal of Engineering for Gas Turbines and Power, Vol. 107, October 1985, pp. 880-889.
29. Fraas, A P., Engineering Evaluation of Energy Systems, McGraw-Hill, New York, 1982.



D T T C

7 - 86